Fate and Transformation of Metal-(Oxide) Nanoparticles in Wastewater Treatment

by

Lauren Elizabeth Barton

Department of Civil and Environmental Engineering
Duke University

Date:_____

Approved:

_____
Mark R. Wiesner, Supervisor

_____
Jean-Yves Bottero

_____
Mélanie Auffan

_____
Claudia K. Gunsch

_____
Heileen Hsu-Kim

Dissertation submitted in partial fulfillment of
the requirements for the degree of Doctor
of Philosophy in the Department of
Civil and Environmental Engineering in the Graduate School
of Duke University

2014

ABSTRACT

Fate and Transformation of Metal-(Oxide) Nanoparticles in Wastewater Treatment

by

Lauren Elizabeth Barton

Department of Civil and Environmental Engineering
Duke University

Date:_____

Approved:

_____
Mark R. Wiesner, Supervisor

_____
Jean-Yves Bottero

_____
Mélanie Auffan

_____
Claudia K. Gunsch

_____
Heileen Hsu-Kim

An abstract of a dissertation submitted in partial
fulfillment of the requirements for the degree
Doctor of Philosophy in the Department of
Civil and Environmental Engineering in the Graduate School of
Duke University

2014

Abstract

The study and application of materials possessing size dimensions in the nano scale range and, as a result, unique properties have led to the birth of a new field; nanotechnology. Scientists and engineers have discovered and are exploiting the novel physicochemical characteristics of nanoparticles (NPs) to enhance consumer products and technologies in ways superior to their bulk counterparts. Escalating production and use of NPs will unavoidably lead to release and exposure to environmental systems. This introduction of emerging potential contaminant NPs will provide new and interesting challenges for exposure and risk forecasting as well as environmental endurance.

The ultimate goal of this research is to develop a framework that incorporates experimental and computational efforts to assess and better understand the exposure of metal and metal-oxide NPs released to wastewater treatment plants (WWTPs) and further implications on land application units (LAUs) where biosolids can be applied. The foundation of the computational effort is comprised of Monte Carlo mass balance models that account for the unique processes affecting NP fate and transport through the different technical compartments of a WWTP and LAU. Functional assay and bioreactor experiments in environmental media were used to determine parameters capable of describing the critical processes that impact the fate of NPs in wastewater.

The results of this research indicate that a simplified, but still environmentally relevant nano-specific exposure assessment is possible through experimentation to parameterize adapted models. Black box modeling efforts, which have been shown in previous studies, show no disadvantage relative to discretization of technical compartments as long as all key transport and fate mechanisms are considered. The distribution coefficient (γ), an experimentally determined, time-dependent parameter, can be used to predict the distribution of NPs between the liquid and solid phase in WWTPs. In addition, this parameter can be utilized a step further for the estimation of the more fundamental, time independent attachment efficiency between the NPs and the solids in wastewater. The NP core, size, and surface coating will influence the value of these parameters in addition to the background particle characteristics as the parameters are specific to the environmental system of study. For the metal and metal-oxide NPs studied, preferential overall association of approximately 90% or greater with the solid phase of wastewater was observed and predicted.

Furthermore, NP transformations including dissolution, redox reactions, and adsorption can potentially impact exposure. For example, experimental results showed that nano-CeO_2 is reduced from Ce(IV) to Ce(III) when in contact with wastewater bacteria where Ce_2S_3 will likely govern the Ce(III) phase in biosolids. From the literature, similar transformations have been observed with Ag and ZnO NPs to Ag_2S and ZnS. With respect to TiO_2 NPs, studies indicated that due to high insolubility, these

NPs would not undergo transformation in WWTPs. The distribution and transformation rate coefficients can then be used in fate models to predict the NP species exposed to aquatic and terrestrial systems and environmentally relevant concentrations released from WWTPs.

Upon completion of the WWTP model, the predicted concentrations of NPs and NP transformation byproducts released in effluent and biosolids were attainable. A simple mass balance model for NP fate in LAUs was then developed to use this output. Results indicate that NP loading on LAUs would be very low but that build up over time to steady state could result in mass concentrations on the order of the typical level for the background metal in soil. Transport processes of plant uptake and leaching were expected to greatly impact the solid phase concentration of the NPs remaining in the LAU, while rainfall did not impart a significant influence upon variation between low and high annual amounts. The significance of this research is the introduction of a method for NP exposure assessment in WWTPs and subsequently in LAUs. This work describes and quantifies the key processes that will impact Ag, TiO_2, CeO_2 and ZnO NP fate and transport, which can inform future studies, the modeling community and regulatory agencies.

Dedication

This dissertation for the degree of Ph.D. in Environmental Engineering from Duke University is dedicated to the author's fiancé, Kendall Fitzgerald and her parents, Kenneth and Anne Barton for their unwavering enthusiasm and support without which this work would not have come to fruition.

Contents

List of Tables

List of Figures

Acknowledgements

I am most grateful to my advisors Mark Wiesner and Jean-Yves Bottero and my co-supervisor Melanie Auffan for their indispensible support, enthusiasm and patience over the course of my doctoral studies. They have taught me in different ways the importance of creativity and excitement in research. I am also grateful for the insights and encouragement of Claudia Gunsch and Heileen Hsu-Kim, my other committee members in addition to Nicolas Roche, Catherine Santaella, Jason Unrine, Greg Lowry and Liz Casman in supporting this work.

I am also extremely thankful for my funding sources including the Chateaubriand fellowship, which allowed for continued collaboration and an incredible scientific and personal experience in France. This work was also funded by the United States Environmental Protection Agency (EPA-G2008-Star-R1) Joint US – UK Research Program, the National Science Foundation Cooperative Agreement EF-0830093, Center for the Environmental Implications of NanoTechnology (CEINT), and the CNRS through the International Consortium for the Environmental Implications of Nanotechnology (GDRi iCEINT), Labex SERENADE (11-LABX-0064), and the FR-ECCOREV.

Finally, this degree was also made possible only with the constant support of family and friends. I am forever grateful to my fiancé, Kendall Fitzgerald for being an unwavering source of encouragement and enthusiasm and for teaching me to always see

the light at the end of the tunnel, regardless of how dim it may be. I would also like to deeply thank my parents for their inspiration and for helping me realize the personal and professional rewards in hard work and determination. In addition to my parents, I would like to thank my three younger sisters and the remainder of the Wiesner team for keeping my spirits high and helping me to laugh often over the course of this journey.

1. Introduction

1.1 Motivation

Numerous advancements in analytical techniques over the past few decades have resulted in the exploration and development of novel materials at the nano scale (Maynard, 2006). The design and production of such materials has paved the way for the birth of a new scientific field known as nanotechnology, which encompasses research and application in all facets of the life cycle of a nanoparticle (NP) from inception to impact. While these materials possess potentially incredible benefits to a vast array of disciplines and consumer products, they could also have significant negative impacts on humans, organisms and ecosystems. The mounting growth of NP incorporation in technology will inevitably result in increasing release to the environment (Gottschalk & Nowack, 2011, Wiesner et al., 2009). Introduction of never before seen materials such as these could pose important new challenges with respect to ecosystem adaptation and survival and the associated exposure and risk assessments. At present, methods for assessing exposure and hazards of traditional environmental contaminants are not adequate for use with NPs because they do not account for the inherent differences experienced in the nano size regime, as examples, changes in mobility, surface area, reactivity, optical, electronic, and thermal properties. Thus, there is a void that must be filled by the modification of current experimental and

computational methods to be appropriate for use with NPs that are released to the environment.

Intentional and unintentional release scenarios need to be studied such that a more comprehensive understanding concerning the potential exposure routes of NPs can be established. In 2011, Gottschalk and Nowack published a review covering the possibilities of NP liberation from products and use patterns. They indicated that a critical piece of information for NP exposure assessment is the nature of the NP within its nano-modified product. For example, nanomaterials can be embedded in a matrix as a solid form, can be present in suspension in liquid form, or utilized as aerosols in the gas phase. Discharge of nanoparticles in any form across the life cycle of production, product incorporation, use, disposal and recycling is possible. The highest amounts of NP liberation were anticipated to occur during product use and disposal.

The release of NPs from products to the waste stream serves as a critically important exposure route for many common metal and metal-oxide NPs, which are the focus of this doctoral work due to prevalence in consumer technologies (Blaser et al., 2008). Figure 1, adapted from Kiser, (2011), illustrates the cyclic nature of NP exposure through wastewater. Nanoparticles will be released from consumers and industries during manufacturing, use and disposal (Mueller and Nowack, 2008). From these life cycle stages, NPs can be released to influent wastewater, where the fate and transport will be impacted by interactions with wastewater constituents in the varying

environmental conditions of the technical WWTP compartments (Keller et al., 2013). The subsequent discharge of NPs from the technical compartments of WWTPs will be predominantly into landfills, land application units, and surface water.

NPs in WWTPs will exist in two phases, either suspended or dissolved in the aqueous phase or sorbed to the solid matrix. NPs that remain in the liquid phase of sludge will be discharged directly to surface water resulting in environmental exposure and potentially organismal and human level exposure. Those particles not present in the liquid will either undergo absorption into solid flocs or adsorption by physical or chemical interactions onto solids (Metcalf & Eddy, 2003, Lowry et al., 2012). Wastewater solids are composed of primary and secondary solids, which are processed through anaerobic digestion into biosolids. From here, biosolids can be used or removed by means of application to agricultural lands, incineration or disposal in landfills (Blaser et al., 2008). Biosolids will contain NPs that have not been biotransformed and the transformation by products. When biosolids are applied to land, the NPs present can either remain in the contaminated soil, be removed through biouptake or transport mechanisms including runoff and leaching that can relocate the NPs to other environmental compartments such as surface water and ground water, respectively. Finally, from here NPs can be cycled back to consumers and industry due to surface water treatment and use or plant consumption. The research of Blaser et al., (2008), indicated that the most imminent exposure of NPs to the environment would be through

wastewater effluent and land applied biosolids. Therefore, it is imperative to gain a better understanding of the processes that can impact NP fate and transport in WWTPs and LAUs in order to predict environmentally relevant exposure.

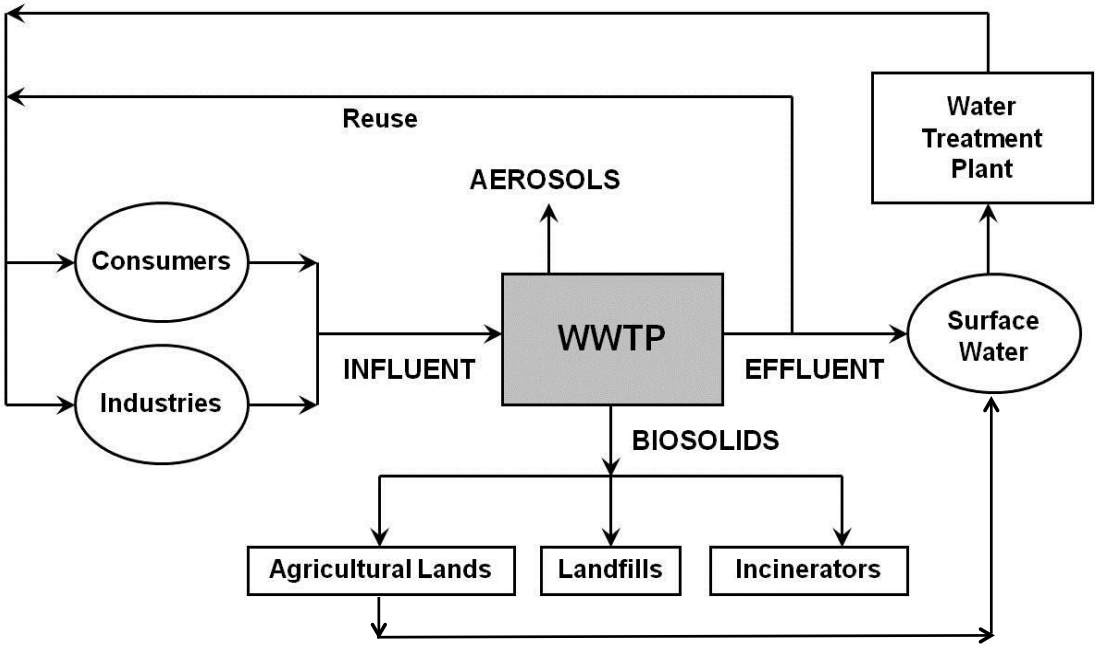

Figure 1: The cycle of NP release from consumers and industries to WWTPs. The majority of NPs are discharged from WWTPs in effluent and biosolids, from which they can be transported through surface water and back to consumers.

1.2 Background and Technical Need

1.2.1 Production, Application and Unique Properties of Metal and Metal-Oxide NPs

Nanotechnology is the design, production, and application of materials having a dimension between 1 and 100 nm (Auffan et al., 2009). Currently, the field of engineered nanotechnology is considered in its infancy, however, there are still over 1,600 nano-enabled products on the global market (Consumer Products Inventory, 2013). Global

and US production estimates of the most commonly utilized metal and metal-oxide NPs are listed in Table 1. The methods by which these estimates were made largely involved surveying production companies and extrapolating from collected data in addition to projections based on market studies (Hendren et al., 2011, Piccinno et al., 2012, Keller et al., 2013). Much of the information concerning production quantities of NPs is proprietary. However, understanding realistic magnitudes of NPs produced that could be released to the environment is critical to predict environmentally relevant concentrations. The results of research in this field have indicated that SiO_2 NPs are one of if not the most highly produced NP followed by TiO_2, Fe, Al_2O_3, ZnO, CeO_2, Ag, and Cu NPs (Keller et al., 2013). Still, production volumes of NPs pose a great challenge due to the lack of consistent, available data. Improved knowledge of NP manufacturing would greatly improve the data and simulation quality in the field.

Table 1 also identifies the common applications that involve nano modifications. Many of the metal and metal-oxide NPs are incorporated into applications, which have significant releases to wastewater including cosmetics, coatings, paints and pigments (Keller et al., 2013). In tons/year, the greatest quantity of NPs (80,500) would be incorporated into coatings, paints and pigments. Additionally, 48,700 tons/year are estimated to be used in electronics and optics applications, 48,000 tons/year are used in cosmetics, 43, 700 tons/year are incorporated into energy applications, and 37,500 tons/year are employed in catalysts. Further, 23,500 tons/year are predicted to be used

in the automotive industry and 13,400 tons/year are incorporated into medical applications (Keller et al., 2013). The greatest majority of the NPs released over the life cycle of the material were estimated to ultimately accumulate in landfills and soils. The predicted compartment eventually containing the lowest concentration of released NPs was air (Keller et al., 2013). This suggests that the chronic effects and behaviors of NPs in terrestrial environments should be a main focus of future research efforts.

Table 1. Common metal and metal-oxide NPs with associated applications, production estimates and environmental compartment where accumulation is most likely.

NP Type	Core	Application	Global Production (t/y) Keller et al., 2013	Global Production median (t/y) Piccinno et al., 2012	US Production Range (t/y) Hendren et al., 2011	Environmental compartment accumulation
Metal	Fe	Coatings, paints and pigments, electronics and optics, catalysts, medical drug delivery and imaging, cosmetics	42,000	55		Landfill > soil > water > air
	Cu	Catalysts, microelectronics, capacitors, conductive coatings, lubricant additives	200			Landfill > soil > water > air
	Ag	Antimicrobial, medical, paint, coatings, food packaging, cosmetics, textiles, electronics and optics	452	55	2.8 – 20	Landfill > soil > water > air
Metal Oxide	ZnO	Electronics and optics, medical, catalysts, cosmetics, plastics, energy, textiles, coatings, paints and pigments	34,000	550		Landfill > soil > water > air
	TiO_2	Coatings, paints and pigments, cosmetics, plastics, photocatalysts, energy	88,000	3,000	7,800 – 38,000	Soil > landfill > water > air
	SiO_2	Automotive, catalysts, electronics and optics, energy, sensors, coatings, paints and pigments	95,000	5,500		Landfill > soil > water > air
	Al_2O_3	Catalysts, coatings, paints and pigments, electronics and optics, cosmetics, energy	35,000	55		Landfill > soil > water > air
	CeO_2	Electronics and optics, catalysts, coatings, ceramics, polishing agents, energy	10,000	55	35 – 700	Landfill > soil > water > air

The use of NPs to enhance consumer products and technologies stems from the unique properties experienced in the nanoscale. These novel properties may be intrinsic to the material or extrinsic and therefore influenced by the environment where the NP will accumulate. Unique intrinsic properties of NPs include a large surface area to

volume ratio as a result of their physical dimensions and this can lead to novel electronic, compositional and optical properties relative to bulk counterparts (Brar et al., 2010). Size and crystallinity will impact the electric, magnetic, optical and thermal properties of NPs. For example, an order of magnitude decrease in diameter from 100 to 10 nm can reduce the melting point values of two metallic nanoparticles, tin and indium, by 80°C and 120°C, respectively (Auffan et al., 2009, 2010). The solubility of inorganic NPs is also affected by size such that the solubility products of the metals increase with decreasing diameter, which can correspond to increased release of toxic metal ions such as Ag^{+} and Zn^{2+}. The solubility product, k_{sp}, is typically understood to equal k_b, the effective solubility product of the crystal, when describing bulk phase materials. However, these two coefficients values begin to deviate as the particles enter the nanoscale because the relative number of atoms present at the surface of the material and thus, the surface tension become more significant in NPs (Auffan et al., 2009).

Furthermore, the catalytic properties of NPs can be altered as a function of size. The two key factors that make NPs prime for catalytic reactions are their large surface area to volume ratio and their unique and highly reactive binding environments on the surface. TIO_2 and fullerenes are among the most common nano-scale catalysts. For example, nano TiO_2 in an optimum size range of 11 – 25 nm, in the presence of sunlight can generate a redox active surface for sorbed molecules (Auffan et al., 2009). Photocatalysis with C_{60} can result in the efficient production of reactive oxygen species

(ROS) like singlet oxygen, which leads to hydroxylation of the fullerene surface (Bottero & Wiesner, 2010).

Materials in the nanoscale are also distinguished by excess surface energy, thermodynamic instability, and a majority of present atoms are localized on the surface of the material (Navrotsky, 2003). For example, a 10 nm particle will be have 35-40% of its constituent atoms on the surface and this amount decreases to approximately 20% for particles larger than 30 nm. This structural alteration and instability can lead to rearrangements or morphological changes, and can greatly impact chemical reactivity and a need for stabilization. Modifications and defects of the surface atoms lead to stronger affinity of solute molecules because the thermodynamic drive to reduce surface energy allows for an increased capacity for adsorption (Bottero & Wiesner 2010). In addition to colloid stabilization by adsorption of counter ions on the surface with the induced repulsion between particles because of the layer of like charge, another means of stabilization is achieved sterically. For steric stabilization to occur, a long molecule, with a high affinity for the solvent, interacts with the NP surface and serves as a barrier to aggregation. In order for two NPs to interact in this system, they must exclude the solvent present between the particles. However, this is difficult and thermodynamically unfavorable because the long molecules tethered to the NP surface have the highest relative affinity for the solvent. Thus, this alteration provides another means of stabilization for nanoparticle colloids (Christian et al., 2008).

Another important NP characteristic is mobility, which departs from the typical mobility experienced in bulk phase material. NP mobility by diffusion is greatly affected by the particle diameter and is governed by gravity, buoyancy, and Brownian motion. The diffusion coefficient (D) as a function of particle radius (a) can be determined by combining Einstein's law of diffusion and Stokes law into Equation 1.1,

Equation 1.1

$$D = \frac{kT}{6\pi\eta a}$$

where k is the Boltzmann constant, T is temperature and η is the viscosity. This equation indicates an inverse relationship between size and the diffusion coefficient, which means that smaller particle radii will lead to larger diffusion coefficient and thus, increased particle mobility (Christian et al., 2008).

These unique properties of NPs can impact the transformations undergone when the NP is released into the waste stream or directly into the environment. NP transformations are any processes that lead to changes in the native NP that is released upon introduction to the environment. The transformations of NPs can be classified into four main groups including chemical transformations, physical transformations, biological transformations and interactions with macromolecules, illustrated in Figure 2 from Lowry et al., (2012). Chemical transformations concern redox processes, dissolution and adsorption. A number of inorganic NPs are likely to undergo redox modifications because of the redox activity of the metal core (ex. Ce, Ag, Zn and Fe).

Oxidizing and reducing environments in addition to interactions with bacteria can lead to changes in the oxidation states of NPs. These reactions can lead to the release of ions or surface functional groups due to changes in charge and result in the precipitation of new phases (Auffan et al., 2009, Bottero & Wiesner, 2010). Redox reactions can also change the persistence of the material in the environment and lead to the generation of ROS (Lowry et al., 2012). Another key chemical change for NPs in the environment is dissolution and then the possibility of complexation processes with ligands including sulfide and phosphate acting on the available ions. These reactions will affect the surface structure, reactivity, toxicity, bioavailability, and persistence of the NP (Lowry et al., 2012).

The final chemical transformation illustrated is adsorption and desorption. Adsorption can occur via three processes, physisorption where particles interact by van der waals attraction, ion exchange that involved electrostatic interactions and chemisorption through chemical bonding. Physisorption is a much weaker means of association relative to ion exchange and chemisorption. Similar to aggregation, adsorption between nanoparticles and other constituents can result in either stabilization or destabilization of the NP. For example, if the surface coverage of adsorbed material is only partial, the matrix can be destabilized and aggregation through bridging can occur. However if surface coverage is complete, the NPs may be stabilized and resist aggregation forces. Desorption is less common in the environment

with respect to NPs (Lowry et al., 2012). However, it is possible that changes in solution chemistry and other environmental conditions can alter the equilibrium and reduce the chemical potential of the adsorbed substance (Nowack et al., 2012). Adsorption and desorption can modify surface charge, surface chemistry and, as a result, the reactive and toxic characteristics of the materials in the environment.

The key physical transformation experienced by NPs is aggregation, both homoaggregation with other nanoparticles and heteroaggregation with background particles present in the ecosystem. The process of aggregation reverses the high reactivity of nanomaterials by diminishing the high surface area to volume ratio effects through reduction of the surface available for chemical reactions to occur. The extent of this available surface reduction will be a function of nanoparticle concentration, particle size distribution and fractal dimension or morphological arrangement of the aggregates. The generation of aggregates of larger size will have significant impacts on the fate, transport, toxicity, uptake potential and reactivity of the NPs. Aggregation has been observed to decrease the toxicity of NPs because of the limitations on chemical transformations such as ROS generation and dissolution into ions. Also, aggregates can easily become too large for transport in aqueous environments and settle out. Again, because of the highly dynamic nature of this system, environmental conditions and particle characteristics can affect the type and extent of aggregation experienced by NPs (Christian et al., 2008, Nowack et al., 2012, Lowry et al., 2012). For example, it has been

shown that not only do pH, ionic strength, and presence of natural organic matter (NOM) influence aggregation but aggregation is also concentration dependent. Phenrat et al., (2007), discovered that the rate of aggregation and the size of the individual aggregates increased with higher concentrations of the primary nanoparticles. Further research concerning the complex interactions between particles and the environment will lead to a better understanding and better predictions of NP interactions within environmental systems.

The third possible transformation of NPs is biologically stimulated. Transformations mediated by microorganisms can alter the core nanoparticle and the coating, which can result in surface compositional changes or changes to aggregation state, reactivity, transport, and toxicity potential. Redox reactions are possible on the surface of the microbes and within bacterial flocs. For example, the metabolic processes of biomass produce a reducing environment in the vicinity of the bacterial surface, which can lead to reduction of redox active NPs (Law et al., 2008). One example of a redox active couple is CeO_2 nanoparticles. CeO_2 NPs are used in applications because of the antioxidant and UV absorbing properties they possess and the fast exchange between Ce(III) and Ce(IV) that can be exploited for O_2 storage. The redox potential for this couple in water is characterized by Eh (Ce^{4+}/Ce^{3+}) = +1.15V, however this potential is higher than what is measured when the nanoparticles are placed in biological media because reduction of CeO_2 in the presence of microbes is highly favorable (Thill et al.,

2006). There are also redox couples that experience oxidation when in contact with microorganisms, an example being magnetite oxidation to maghemite (Auffan et al., 2008). These redox reactions can lead to differential toxic effects. CeO_2 reduction on bacterial surfaces produces high cytotoxicity whereas the oxidized maghemite is stable and does not lead to significant toxicity (Thill et al., 2006 and Auffan et al., 2008).

The final transformation experienced by NPs is interaction with macromolecules, the most environmentally important being NOM with concentrations much higher than any NP present in most environments. NOM has a high affinity for NP surfaces and can result in modification of the surface through adsorption processes. This adsorption is typically considered irreversible and impacts all other environmental processes that dictate the fate and transport of the NP including aggregation and surficial attachment. NOM coating can either decrease aggregation by charge or steric stabilization or it can enhance aggregation by charge neutralization or bridging mechanisms. In addition, biomolecular surface coatings alter the toxicity, uptake and bioaccumulation of NPs (Christian et al., 2008 and Lowry et al., 2012).

Further research will be needed to accurately predict transformations of NPs in the environment that will impact exposure potential, hazards and ultimately risk. Environmental systems exposed to NPs are inherently dynamic and complex and can greatly affect NP properties. Understanding the ecological settings that promote or limit

such transformations will be necessary to predict release, transport, toxicity and NP persistence in the environment (Nowack et al., 2012, Lowry et al., 2012).

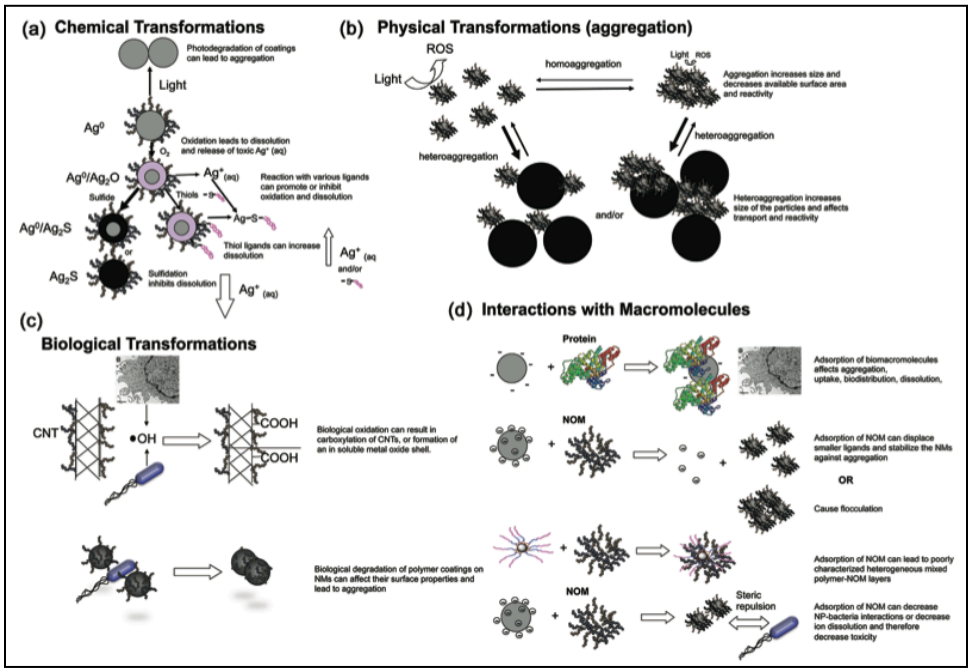

Figure 2: Schematic of the main processes that can lead to the transformation of NPs (From Lowry et al. 2012).

1.2.2 NPs in Wastewater Treatment

Research indicates that a critical exposure pathway by which NPs can be introduced to water, soil and air will be through contaminated wastewater effluent and land applied biosolids from municipal WWTPs (Blaser et al., 2008, Handy et al., 2008, Limbach et al., 2008, Mueller & Nowack, 2008). NP release to WWTPs has been measured and subsequent transport to environmental compartments would be expected (Westerhoff et al., 2011). Despite the widespread use and therefore release of NPs, there

is little knowledge concerning the environmental fate of these potential emerging contaminants once in the waste stream.

Recent years, in an attempt to fill the void of research concerning NP exposure, have seen an increase in studies examining NPs transport through the waste stream, a likely first route of NP exposure and risk (Blaser et al., 2008). Experimentation has focused on a wide range of NPs that are predicted to enter the waste stream as a result of their applications in consumer products and technologies (Keller et al., 2013). Much of this research has explored NP removal and stability in wastewater and the impacts of NP core and coating. Many studies have found that many metal and metal-oxide NPs appear to preferentially associate (> 70%) with the solid phase of wastewater including TiO_2, Ag, CeO_2, ZnO, and Cu (Kiser et al., 2010, Ganesh et al., 2010, Limbach et al., 2008, Westerhoff et al., 2011). The magnitude of this association with the solid phase will depend on different NP densities, surface functionalization and charge, and size. For example, Kiser et al., (2010), showed that surface functionalized NPs remained in higher degree in effluent due to charge stabilization of the present functional groups on the surface while pristine NP counterparts, without surface coatings, typically had higher association with solid phase. In addition to surface functionalization leading to greater persistence in effluent, higher concentrations of non-biodegradable stabilizing surfactants in wastewater resulted in greater release of NPs through the liquid phase (Limbach et al., 2008). For example, adsorption of small peptides was observed onto the

surface of CeO_2 nanoparticles, which caused a shift in the ζ potential in wastewater, increasing stability.

A number of proposed mechanisms exist for the high removal of NPs to the solid phase of wastewater. Activated sludge units can remove aggregates and suspended NPs in the influent waste stream by size-dependent electrostatic interactions with the bacteria in sludge, precipitation of mineral phases such as silver sulfide, interaction with organic matter, aggregation and subsequent settling, and physical removal via entrapment within solid material (Tiede et al., 2009, Kim et al., 2010). The conclusions from previous studies were removal and stability of NPs in wastewater will be greatly impacted by particle concentration, dispersivity, dissolution rate, aggregate formation, surface area and other surface characteristics (Rottman et al., 2012, Kim et al., 2010). In addition, it can also be concluded that there is a high possibility for NP accumulation in biosolids, which could be applied to land. Land application of biosolids was thought to be a sustainable exercise because of the high nutrient load they possess. However, they could potentially also contain high concentrations of contaminants. Therefore, more research in NP interactions in biosolids and agricultural soils must be completed.

Another important fate predictor of NPs in the environment is the potential for transformations. Research has found that Ag nanoparticles undergo transformation via sulfidation (> 90%) in environments like activated sludge (Levard et al., 2011, 2012, Kaegi et al., 2011). This transformation impacts the ultimate fate of the NP by affecting

the aggregation state, surface chemistry and charge, and ion release. This high magnitude of reduction to Ag_2S was observed to occur independently of surface functionalization. Sulfidation is not the only key transformation of Ag, nano-Ag can also form complexes with chloride species, dominant in many aquatic environments. Another transformation of Ag that could impact exposure was found to be dissolution. Ma et al., (2012), found that size was the most critical determinant in nanoparticle dissolution with smaller particles having higher solubility and subsequently increased mobility. Transformations such as these will be dependent on environmental conditions. For example, sulfidation of Ag was enhanced in the anaerobic environment likely because of the higher amounts of reduced sulfur, neither limited by kinetics, residence time or available sulfide (Kaegi et al., 2011).

Another important redox-active NP is ZnO. Following incubation with activated sludge, 90% of the added ZnO was observed to undergo transformation to predominantly sulfide species but some associated with phosphates or cysteine. This was proposed to be due to dissolution and subsequent complexation and precipitation. Following aerobic treatment, Zn speciation was investigated in anaerobic digestion. Results indicated that Zn complexed by cysteine decreased and the concentration of Zn sulfides continued to increase. Finally, Lombi et al., (2012), observed Zn transformations during composting, a process conducted prior to land application of biosolids. Dramatic

shifts in the Zn species were detected as the majority of the ZnS was oxidized to $Zn_3(PO_4)_2$ and Zn-FeOOH.

The implications of transformation studies in WWTPs are the illustration of how different environmental conditions can lead to drastically different and potentially non-nano species that are exposed to the environment through effluent and biosolids. Future research should focus on determining the stability of nanoparticle complexes in activated sludge treatment and anaerobic digestion and their further transformations during biosolid composting and land application.

1.2.3 NP Exposure Assessment and Risk Forecasting

Currently, investigative exposure methods that account for how the uniqueness of the NP affects transport and toxicity are lacking (Wiesner et al., 2009, Arvidsson et al., 2011, Hendren et al., 2013). Thus, there is a pressing need for a method that can effectively and efficiently provide an accurate idea of the exposure potential and risk of emerging nano-contaminants already in use by the public and, as a result, entering the environment (Gottschalk & Nowack, 2011, Nowack et al., 2012). This method must incorporate those novel physicochemical properties of NPs that have the potential to influence the fate and transport of the particles in the environment, while taking into account how those properties are affected by environmental conditions. In order to achieve this, NP-specific functional assays must be designed examining mobility and transformations of NPs likely in representative environments to provide preliminary

information for model parameterization. While this method will not be sufficient in fully capturing all environmental complexities, adequate information can be gleaned to improve our limited understanding of NP exposure and risk (Wiesner et al., 2009).

The foundation of typical risk assessments for environmental contaminants hinges on the idea of tracking the release, fate and transport of the material across its complete life cycle. This type of analysis looks at potential releases of the material from the time of raw extraction and production, through testing and assimilation into products, until the time it is recycled or disposed in order to obtain a more complete understanding of the exposure and hazard potential (Theis et al., 2011). Life cycle principles were embedded in a risk strategy developed recently by the United States Environmental Protection Agency (US EPA) known as a Comprehensive Environmental Assessment (CEA) (Hendren, 2010). The CEA would be the most inclusive method for predicting the risk of a material to individuals, populations and ecosystems. Shown in Figure 3 is a CEA modified for an NP that is transported through the waste stream, a likely first route of exposure (Blaser et al., 2008) and the focus of this research. There are limitations, however, because in order to utilize the CEA, a vast knowledge of the material physicochemical properties, environmental interactions, and toxic potential at any point from inception to impact must be well characterized. Unfortunately, for many novel environmental contaminants, in particular NPs, risk forecasting methods cannot be strictly based on traditional risk assessment approaches due to the myriad of data

gaps, high amount of intrinsic uncertainties and forward-looking nature of the problem. Modification or theoretical adaptation of current experimental and modeling frameworks in conjunction with probabilistic approaches designed to deal with large uncertainty will provide the best design for considering the problem of environmental and human exposure to NPs and the associated risk (Blaser et al., 2008, Arvidsson et al., 2011, Gottschalk et al., 2010, Grieger et al., 2011, Wiesner et al., 2006, Hendren et al., 2013).

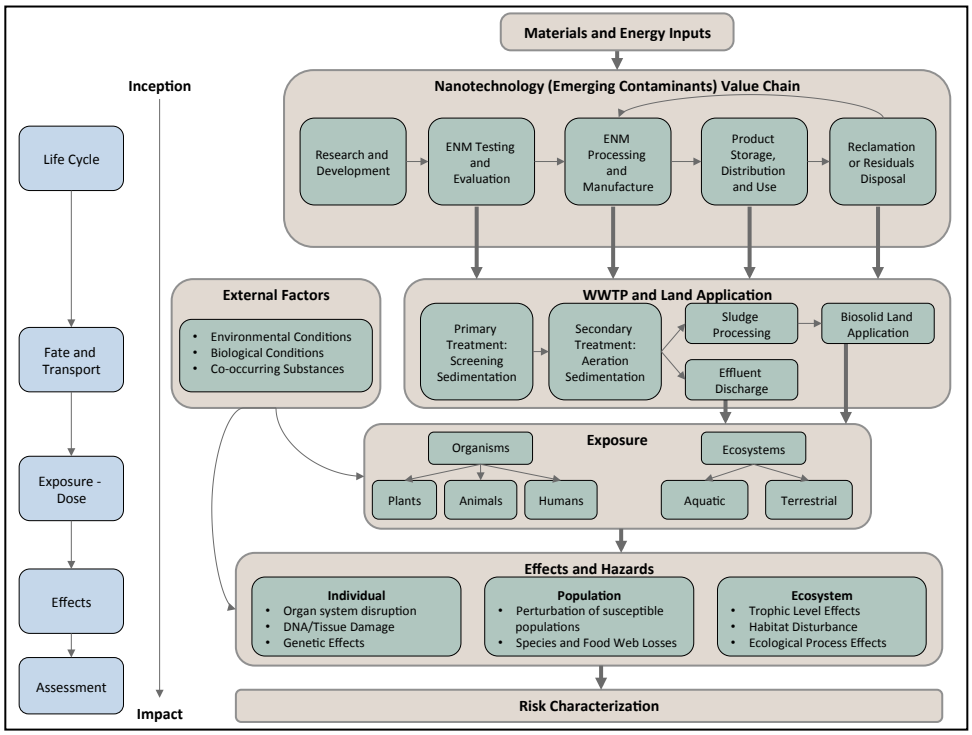

Figure 3: Framework for a Life-Cycle – Inspired, Comprehensive Environmental Assessment of Exposure and Forecast of Risk for NPs (an Emerging Environmental Contaminant) transported through a WWTP and LAU (adapted from Hendren, 2010).

The risk of NPs on the environment is a function of an innumerable number of parameters including NP physicochemical properties, fate and transport, reactivity, and

toxicity. The challenges in characterization of these risks are not that inherently different from the challenges faced with other novel emerging contaminants but while a number of these "traditional" contaminants, like organic pollutants have pre-determined hazard and exposure identification methods, the field of nanotechnology is less developed. Another difficulty is that NPs are characterized by intrinsically mutable behavior that is highly dependent on the particle of interest and the environmental conditions. For example, sorption, distribution and transformations differ from bulk counterparts as a result of size and/or modifications on the surface, which can be further influenced by the pH, redox potential, and ionic composition, for example, of the environmental compartment where the NP exists. In addition, mechanisms of toxicity can vary because of increased availability to cells or generation of ROS due to high surface area to volume ratios. Thus, there is an important gap that must be made priority with respect to the determination of appropriate measurements and properties that may influence exposure, hazard and ultimately risk (Shatkin & Barry, 2010).

As a result of the fundamentally dynamic nature of NP systems, the nanotechnology community has widely established that the most appropriate means of risk analysis should incorporate a life cycle approach. It should involve the determination of key material applications and forms, exposure pathways, and hazard potentials at various stages from "cradle to grave (Shatkin & Barry, 2010)." NP risk analysis is the product of the hazards associated with the materials and the exposure

potential. Traditional environmental risk assessment begins with characterization of the impending hazards of the contaminant, determination of the likelihood that these hazards are environmentally relevant, assessment of the exposure pathways and probability of such exposures with respect to the identified hazards, and finally risk determination. Unfortunately, this series of analysis will be impossible because NPs are already employed in research and development and consequently released to the environment with little to no knowledge of persistence and hazard potential. In addition, methods for determining the quantities of nanomaterials released are not sufficient. Therefore, the most rational start is to try and identify the release pathways, estimate the magnitude of release, and predict fate and transport in the environment with simplified methods that do not require extensive characterization of intrinsic and dynamic NP properties.

Environmental exposures to NPs can come from intentional or unintentional releases with a major pathway being exposure through the waste stream. These will likely lead to contamination of NPs in soils and sediments, plants, water, microorganisms and the atmosphere. One immediate issue is that quantitative measurement of exposure and hazard will be difficult because of changes experienced when NPs interact with the environment including surface modifications, morphological deviations and changes in size. This renders a dose-response like relationship unreasonable to define for NPs. Distribution of NPs in aqueous and

terrestrial environments will also vary due to particle properties, surface charge, solubility, aggregation potential, diffusion, deposition and settling likelihood making it exceedingly problematic to estimate the concentrations of NPs in various environmental compartments. Challenges in predicting exposure potential and concentrations can then lead to an inaccurate understanding of the possible hazards for ecosystems (Hannah & Thompson, 2008).

The ideal method for addressing NP risk would be the application of multi-media modeling methods through various environmental compartments, which necessitates extensive data on the compounds of interest and their environmental interactions as a result (Mackay et al., 1996, Wania et al., 1998). In the case of NPs however, data on novel characteristics that could impact transport is scarce and the fate predictors conventionally used to assess exposure may be inappropriate (Auffan et al., 2009). This lack of knowledge regarding the relationships between NP properties, exposure, and toxicological endpoints renders most (if not all) currently available risk models incapable of providing reliable estimates of risk (Grieger et al., 2010). Still, scientific development forges ahead with an increasing use of NPs in consumer products, therefore it will be indispensible to be able to foresee and manage negative impacts. In order to accomplish this, new methods must be established to not only use the available information in a predictive fashion but also to prioritize future research efforts (Wiesner et al., 2009).

To achieve an understanding of NP risk through WWTPs, it is essential to assess exposure potential and characterize the release of NPs to the environment. Gottschalk and Nowack, (2011), combined efforts in a review focused on nanoparticle releases and subsequent exposure in the environment. There were a number of different release scenarios possible for NPs throughout the life cycle. They could be released during production, manufacturing, and product applications, from technical compartments including WWTP and during use and disposal of products. An important factor for being able to model exposure would be the quantity and nature of the NP that was released. For example, NPs could be released as nanoparticulates, embedded in a matrix, or as aggregated particles. With respect to the quantities of release, much of the NP incorporation in products data is proprietary preventing adequate estimations of use and magnitude of potential NP release. The authors proposed that future experimentation must focus on a single release process and determine the reproducibility of obtaining the same release. Due to the fact that data on NPs was so limited, Gottschalk and Nowack maintained that mathematical modeling of NP exposure and risk was an important tool for estimation and prediction. However, the main shortcomings of the available models were denoted as simplification by assuming steady state and coalescing NPs based on core instead of differentiating by coating.

Once NP production and environmental releases can be estimated, exposure assessment models could be developed to track NPs along the major exposure routes.

Following is a review of the major works in NP exposure and risk assessment over the past decade. Morgan et al., completed one of the initial studies in the field in 2005 where expert elicitation was employed to compile potential risk factors and assemble a network of NP properties that would likely influence the material fate and transport. Morgan's influence diagram was composed of nine nodes from the product to risk end points on a time index including product development, use/disposal of products, particle-related characteristics, presence of nanoparticles, uptake capacity, transport and fate, toxic effects, ecological risk, and human health risk. This served as a preliminary effort because, at the time of conception, there was insufficient data to populate this framework. However, one of the key things presented was an outline of the integral relationships between physicochemical NP properties and exposure and hazard potential. This study helped to broaden the scope of research concerning NPs and their ecological and organismal impacts. It was one of the first indications that future efforts must be expanded to understand exposure probabilities in addition to the toxicological effects rendered by NPs. Finally, the author's illustration revealed the cross-disciplinary nature of the problem and necessitated collaborative efforts. The ultimate purpose of the tool Morgan developed was therefore not to produce quantitative answers but rather to provide a utility to focus research on the parameters that would be necessary to conduct a complete risk assessment.

Two years later, Boxall et al., (2007), published a technical report, looking further at the issues with exposure of NPs and proposed equations by which to model exposure. While the authors indicated that the limitations of NP information were extraordinary, they still developed a predictive tool for fate and transport in WWTPs, water and soil through extrapolation from data for metals and viruses of similar size. No definitive conclusions could be reported but they provided considerations that would be key for these environmental systems including removal mechanisms and processes impacting fate and transport. The following year, Blaser et al., (2008), explored a more specific scenario, the release of nano-Ag from plastics and textiles, attempting to compare the estimated water concentration with a predicted no-effect level (PNEC) to provide a preliminary forecast of risk in a specific system. The authors developed a flow model that began with the use of the products and release to a sewage treatment plant (STP). From the STP, the Ag could be transported to aquatic or terrestrial environments. Assuming emission scenarios for minimum, intermediate and maximum release completed parameterization of the model. Once the Ag was released into aquatic environments, the processes of diffusion, sedimentation, resuspension, and burial were analyzed to determine water and sediment concentrations. It was observed that the highest concentration of the Ag was predicted in the sediments, however there was no distinction made with respect to the type of silver (i.e. nanoparticulate, silver ions or silver sulfides) in the environmental compartments, which will be important

information to predict risk. The results indicated that 15% of the total Ag emissions in water originated in biocidal plastics and textiles but that rigorous exposure and risk assessment was impossible due to extreme uncertainty in the data. The ultimate conclusions indicated that rigorous exposure and risk assessment was impossible due to extreme uncertainty in the data. In another study completed in 2008, Mueller and Nowack aimed to incorporate a life-cycle perspective into a model that attempted to capture the flow of NPs (TiO_2, Ag and CNTs) through environmental compartments. Their model was based on an approach developed to assess environmental exposure of chemicals. With respect to risk, the model outputs suggested that there might be risk of TiO_2 in aqueous environments, which the authors indicated as strictly a rough approximation to aid in research prioritization. Based on the current state of the data used in their model, the authors found that nano-Ag and CNTs would likely pose little risk, however it was critical to note that this was for strictly nanoparticulates and not transformation products. In fact, one key process that must be considered in the future to accurately model exposure is to account for nano-specific transformations.

In 2009 and 2010, Gottschalk et al., building on the work of Mueller and Nowack, (2008), suggested that an NP exposure analysis would require broad assumptions concerning the material production, the products use patterns, and the environmental releases drawing on the principles of material flow analysis (MFA). In these works, the authors applied probabilistic methods to assess the fate and transport in the

environment of five common NPs, Ag, ZnO, TiO_2, CNTs and fullerenes. The simulation included the following compartments: production, manufacturing, and use, which could lead to release to sewage treatment and then on to waste incineration, landfill, or the environmental compartments of soil, surface water, sediments, ground water and the atmosphere with connecting flow lines. After calculating environmental exposure, the authors combined the information with toxicity data to determine risk. Risk characterization was found to be only significant for inorganic NPs present in WWTP effluent. Also in 2010, Musee explored the risk of a specific location to NPs in cosmetics. The risk values calculated using this model indicated potential risk of Ag and TiO_2 in aquatic environments and relatively little risk for terrestrial systems. A further publication in 2010 examined the current state of NP exposure assessment. Abbott and Maynard, (2010), reiterated the urgency of the need for predictive exposure measurements for NPs in addition to relevant toxicological metrics. They suggested mass concentration would no longer be sufficient (i.e. a small mass concentration of single nanometer particles that can innervate and deposit in alveolar regions would be high risk); shape, specific surface area, surface composition and charge, crystalline composition, aggregation state and fractal dimension would all be more important NP properties to report. A final remark from the authors recommended that monitoring of NPs in the environment would be a necessary next step. The fate of NPs do not follow fate of traditional contaminants as they can be influenced by NOM and other

environmental conditions that can impact stability. Monitoring techniques would allow for a more comprehensive idea of fate and transport in different environments, which would ultimately inform exposure and risk predictions.

Another important example of an NP-specific environmental multimedia model proposed by Praetorius et al., (2012), explored the fate and transport of nano-TiO_2 in river systems and was adapted from the model completed by Blaser et al. (2008). The goal of this research was to predict PEC values for TiO_2 while accounting for NP specific fate and transport induced by novel physical and chemical properties. The schematic of their model is shown in Figure 4. Figure 4 provides a context that indicates differences in fate for "traditional" organic contaminants relative to NPs. While transformations for organic chemicals are simply degradation or volatilization, NPs can undergo homoaggregation, dissolution or surface transformations. With respect to contact with surrounding matter, chemicals can be adsorbed on the surface while NPs interactions are described by heteroaggregation. Finally the transport mechanisms are slightly different. Organic chemicals can be moved in advective flow as suspended molecules or they can sediment out of solution associated with other particulate matter. Once in the sediments, chemicals can be buried, resuspended in association with other particles or diffuse back into the water column. NPs can be transported by advective flow or they can homoaggregate or heteroaggregate and settle. From the sediments, they can either be resuspended or buried.

The model generated by Praetorius et al., is composed mass balance equations that were coupled between compartments with parameterization by coefficients that best describe NP fate and transport. The results from this study showed that the concentration of TiO_2 NPs decreased as the contaminant was transported away from the emission site. As the NPs moved, they associated with suspended particulates and settled out. The concentrations were seen to be very sensitive to the attachment efficiency between the nanoparticles and the background material, which indicated that NP fate and transport will depend on the other particulate matter and their associated characteristics in the system. A strength of this model is that it can be adapted to a variety of environmental conditions and different NPs easily to produce time dependent PEC values for NPs in aqueous environmental compartments.

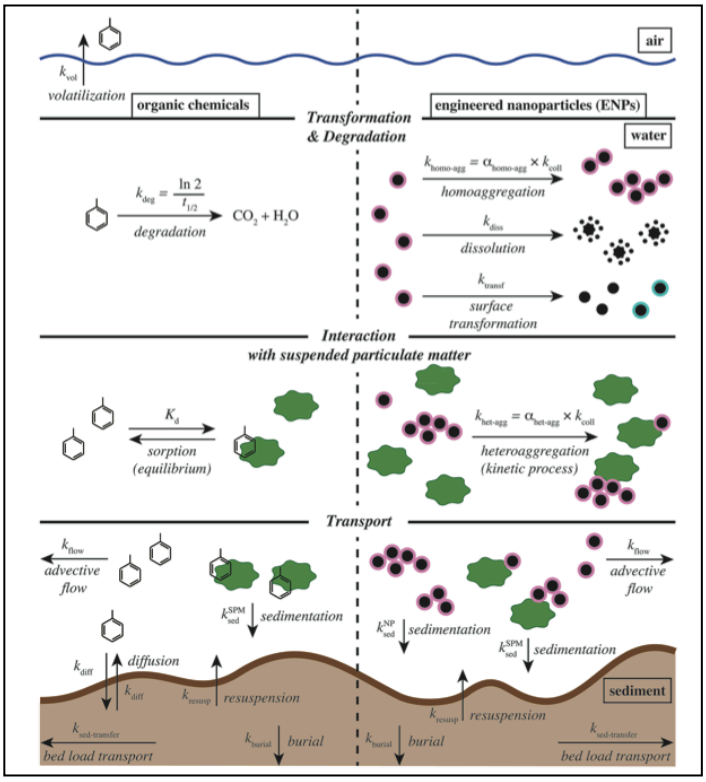

Figure 4. The schematic of the multi-media model proposed by Praetorius et al. (2012) for the exposure and risk assessment of TiO_2 in a river system.

Finally, in 2013, a simplified but more environmentally relevant model was proposed analyzing only transport of Ag in WWTPs to predict concentrations in effluent and sludge. Hendren et al., employed a model parsimony approach to develop a mass balance based model that could accurately predict concentrations with a limited number of input parameters introduced as distributions to account for the inherent uncertainty of the system. Sensitivity analyses implied that the model was most altered by the fraction of NPs released to wastewater and the production volume and least sensitive to plant operational parameters like residence times. The conclusions of this research pointed to further investigation needed for the determination of production quantities

and release rates. The study highlighted the importance of accounting for surface modifications of NPs in exposure assessment. However, it was still unable to account for key transformation processes that could highly impact the nature of the exposed material.

One of the major issues, illustrated by all exposure studies is the lack in reliable data. The limitations in data robustness in conjunction with the complexities of real systems result in enormous uncertainty when trying to predict the fate of emerging contaminants. Probabilistic methods have been developed to deal with some of the uncertainty by describing model parameters with distributions and reporting simulation results using a range with associated probability (Gilks et al., 1996). While a number of researchers have incorporated these methods into their models, unfortunately, the ability to accurately predict environmental concentrations is still severely hindered by the numerous assumptions and sources of uncertainty from data gaps (Gottschalk et al., 2010). In 2009, Lowry and Casman detailed those areas where our knowledge of NP interactions and exposure must be improved. The authors suggested that the fundamental areas where data was limiting included aggregation, deposition, and distribution of NPs in the environment. In addition, competence in the areas of surface coatings and their effects on transport and toxicity, transformations, and processes impacting NP persistence could greatly improve the field. Only after this information has been elucidated do Lowry and Casman suggest that accurate exposure and risk

assessment can be completed. However, they did indicate that intermediate assessments employing available information could provide an idea of environmental implications.

In addition to Lowry and Casman, (2009), other studies have attempted to illustrate some of the main uncertainties and complexities that will impact risk forecasting for NPs (Wiesner et al., 2009). First, there are widespread gaps in data concerning how physical and chemical properties of NPs combined with changing environmental conditions impact the localization and nature of NPs in the environment. Methods and protocols must be improved for determination of NP production, in order to understand the effects of novel NP properties on aggregation and deposition and to elucidate the impact of biological and chemical transformations. Ultimately, Wiesner et al., called for a "mechanistic understanding of the forms in which NPs are transported through and retained within ecosystem compartments" and the impacts of their presence. Due to the current, highly speculative nature of NP risk assessment; Wiesner et al., suggested that simple models were still capable of providing insights into the hazards and exposures of NPs. Mass balance models based on distribution of NPs between environmental compartments were deemed appropriate for this problem, but the information that they provide is still limited.

Perhaps, an important step on the way to filling the voids where NP information is unavailable could be the reprioritization of research efforts and standardization of measurements. Grieger et al., (2009), noted areas of significant concern that result in

knowledge gaps: lack of standardization of methods and availability, lack of study on environmental fate and reactivity, lack of quantitative research in exposure and nanotoxicology for humans and environmental species, lack of life cycle analysis and difficulty in detection and quantification of NPs in environmental matrices. In addition, the work addressed those immediate research needs that would reduce uncertainty including: testing methods and instrumentation and characterization techniques within environmental and biological matrices. The final conclusion of this work was that a risk assessment framework adopted from those used for chemicals should be appropriate for NP risk forecasting with methodological modifications and increased reduction of data gaps.

1.3 Scope of Research and Project Objectives

1.3.1 Research Need

As indicated in the above review of the state of the science, there is a critical need to predict the exposure of NPs being utilized in products and subsequently released to the waste stream. Traditional methods for organics in their current formulation will be impossible due to the expansive limitations on available data concerning NP characterization, fate and transport in the environment and potential affects. Thus, the next logical step would be adaptation of current methods to a simplified, yet still environmentally relevant model driven by parameters experimentally determined through NP-specific functional assays that can describe fate and transport. A number of

studies have attempted this simplification by describing WWTPs as black box models where distribution between effluent and solids is the only key fate predictor. In this work, advantages due to discretization of the WWTP into individual technical compartments are investigated. In addition, experimental literature and additional experimentation were utilized to provide information on transformations and colloidal stability that will be important for fate and transport in WWTPs and have been ignored previously.

The following commentary on model development and proposed parameterization allows this work to incorporate our current knowledge of NP – environmental interactions in order to gain an understanding of exposure potential. It will provide the most realistic prediction of environmental concentrations of NPs and their transformation byproducts. In addition, this research can help focus and prioritize future research efforts by indicating the most probable compartments of accumulation and the nature of the NP species present in that compartment while also informing regulatory bodies examining the impacts of NPs released to the environment through wastewater treatment.

1.3.2 Objectives and Dissertation Formulation

The incorporation of NPs in various technologies and consumer products is increasing and release to environmental compartments has already been observed without full understanding of the fate, transport and harmful potential associated with

them. There is a need to predict the relevant concentrations of these materials discharged to the environmental and the unavoidable effects. The ultimate goal of this research is to develop a framework based on functional assay experimentation and updated modeling efforts for the environmental exposure assessment of metal and metal-oxide NPs released to the waste stream. There are four main objectives for this research:

1. Distribution Functional Assays
    a. Identify the transport and distribution of metal and metal-oxide NPs (Ag, TiO_2, ZnO, and CeO_2) in the unit operations of a WWTP.
        i. Determine the distribution coefficient of NPs in the primary and secondary clarifiers.
        ii. Relate the distribution coefficient to the more fundamental attachment efficiency through a mathematical relationship and justify with a rigorous heteroaggregation model.
    b. Dissertation Chapter 3
    c. Accepted Publication: Barton, L. E., Therezien, M., Auffan, M., Bottero, J-Y., Wiesner, M. R., *Theory and Methodology for Determining Nanoparticle Affinity for Heteroaggregation in Environmental Matrices Using Batch Measurements*. Environmental Engineering Science, 2014.
2. Transformation Bioreactor Scale Study and Functional Assays
    a. Characterize the transformations of pristine and citrate-functionalized CeO_2 in an activated sludge bioreactor.
    b. Determine the rate coefficient of transformation in the presence of aerobic and anaerobic sludge through batch experiments.
    c. Dissertation Chapter 2
    d. Accepted for Publication: Barton, L. E., Auffan, M., Bertrand, M., Barakat, M., Santaella, C., Mason, A., Borschneck, D., Olivi, L., Roche, N., Wiesner, M. R., Bottero, J-Y., *The Transformation of Pristine and Citrate-Functionalized CeO_2 Nanoparticles in a Laboratory Scale Activated Sludge Reactor*. Environmental Science and Technology, 2014.
3. Develop a nano-specific Monte Carlo model to assess the exposure of NPs through WWTPs.
    a. Incorporate distribution and transformation parameters to describe the fate and transport of Ag, TiO_2, ZnO, and CeO_2 through the compartments of a WWTP.

b. Compare the discretized modeling effort with black box studies to provide justification for one form of simplified simulation.
c. Dissertation Chapters 4 and 5
d. Submitted for Publication: Barton, L. E., Auffan, M., Bottero, J-Y., Wiesner, M. R., *Monte Carlo Simulations of the Transformations and Removal of Ag, TiO_2, and ZnO Nanoparticles in Wastewater Treatment*. Science of the Total Environment, 2014.
e. Submitted for Publication: Barton, L. E., Auffan, M., Olivi, L., Bottero, J-Y., Wiesner, M. R., *Heteroaggregation, Transformation, and Fate of CeO_2 Nanoparticles (NPs) in Wastewater Treatment*. Environmental Pollution, 2014.

4. Discuss the development of a nano-specific Monte Carlo model to assess the implications of NP exposure through LAUs.
    a. Develop of a particulate LAU model that includes fate and transport parameters to predict terrestrial and aqueous concentrations of Ag, TiO_2, and ZnO. (In collaboration with RTI and TINE)
    b. Dissertation Chapter 6

This dissertation is compiled into chapters, which aim to address the overarching need of methods for exposure assessment of NPs released to the waste stream during production, use, and disposal. The discussion begins by addressing the key processes that impact NP fate in WWTPs, transformation and distribution. From the determination of the distribution coefficient, further commentary is provided on the relationship between it and α, the attachment efficiency or a measure of the affinity of NPs for a background material, which in this case would be wastewater solids. This bridges the gap between a time dependent operational parameter and a more fundamental NP property. Following experimental parameterization, this dissertation will review the WWTP model development and results. It will discuss these results and the relationship with results generated using black box modeling. In addition, it will introduce the LAU model development. The complete experimental results for the LAU

model are currently unavailable, as collaborators whose work is ongoing will provide the model parameters. However, assumptions have been made to provide an initial assessment of LAU implications following application of NP contaminated biosolids. Finally, this dissertation will conclude with a summary and interpretation of the results, in addition to future research perspectives.

2. The Transformation of Pristine and Citrate-Functionalized CeO_2 Nanoparticles in a Laboratory Scale Activated Sludge Reactor.

2.1 Abstract

Engineered nanoparticles (ENPs) are used to enhance the properties of many manufactured products and technologies. Increased use of nanoparticles (NPs) will inevitably lead to environmental release. An important route of exposure is through the waste stream where NPs will enter wastewater treatment plants (WWTPs), undergo transformations, and be discharged with treated effluent or biosolids. To better understand the fate of a common NP in WWTPs, experiments with laboratory scale activated sludge reactors and pristine and citrate-functionalized CeO_2 nanoparticles were conducted. Greater than 90% of the CeO_2 introduced was observed to associate with biosolids. This association was accompanied by reduction of the Ce(IV) NP to Ce(III). After 5 weeks in the reactor, 44 ± 4% reduction was observed for the pristine NPs and 31 ± 3% for the citrate functionalized NPs, illustrating surface functionality dependence. Thermodynamic arguments suggest that the likely Ce(III) phase generated would be governed by CeO_2, $Ce_2(SO_4)_3$-$8H_2O$, and $CePO_4$ in the aerobic compartments of the WWTP and Ce_2S_3 in anaerobic digestion. This study indicates that the majority of CeO_2 nanoparticles (> 90%) entering WWTPs will be released in the solid phase and a significant portion will be Ce(III). At maximum, 10% of the CeO_2 will remain in the effluent and be discharged as Ce(IV).

2.2 Introduction

The unique properties of NPs are exploited to enhance or enable a variety of technologies and consumer products (Maynard, 2006). The mounting growth of NP use will inevitably result in their release to the environment (Gottschalk & Nowack, 2011, Wiesner et al., 2009). One of the primary routes of environmental exposure of many metal and metal oxide nanoparticles is through wastewater treatment plants (WWTPs) (Blaser et al., 2008). To understand the possible impacts and fate of NPs, distribution and transformations during wastewater treatment must be considered. NPs may undergo multiple transformations and the kinetics of these reactions can be altered over the course of time (Christian et al., 2008, Lowry et al., 2012). Transformations of metal-containing nanoparticles may include redox reactions, dissolution, adsorption (*i.e.*. physisorption, ion exchange, chemisorption), desorption, precipitation of new phases, and aggregation (homoaggregation with other nanoparticles or heteroaggregation with background particles). Environmental factors that may affect NP transformations include pH, redox potential and the quantity and composition of natural organic matter (NOM) (Lowry et al., 2012). Moreover, many NP transformations are irreversible and will be the primary determinants of NP fate, transport and toxicity (Auffan et al., 2009). Transformations mediated by microorganisms can alter the core NP as well as surface functionality, the latter leading to possible changes in surface composition, aggregation

state, reactivity, and toxicity potential (Lowry et al., 2012, Bottero & Wiesner, 2010, Auffan et al., 2010).

For the case of silver nanoparticles (AgNPs) entering WWTPs, it has been shown that AgNPs primarily associate with the biosolids and, regardless of surface functionality, undergo oxysulfidation prior to release in effluent and biosolids (Kaegi et al., 2011, Liu et al., 2011, Doolette et al., 2013, Ma et al., 2012). This sulfidation results in changes in reactivity with respect to dissolution potential, in addition to changes in mobility and bioavailability of the nanoparticles, ultimately impacting their environmental risks (Ma et al., 2012, Levard et al., 2011, 2012).

ZnO nanoparticles also undergo critical transformations in wastewater treatment and subsequent sludge composting (Lombi et al., 2012). Speciation data indicated that ZnO NPs were transformed rapidly into ZnS during wastewater treatment. However, the ZnS was lost during composting and most of the Zn was actually found associated with phosphates and iron hydroxides during aerobic composting. It is these final transformation products that will likely be present in biosolids entering landfills, incinerators or applied to land, while ZnS is anticipated to be the dominant species of Zn in wastewater effluents. As with Ag, these transformations of Zn will greatly impact exposure and hazard potential in the environment.

The current work considers the transformation of another common metal-oxide NP that will likely be released to WWTPs, CeO_2. Transformations of two varieties of

CeO_2 NPs, pristine and citrate-functionalized, were followed in an aerobic bioreactor simulating wastewater treatment by conventional activated sludge. CeO_2 is a NP used in a variety of consumer, industrial and medical applications. It is commonly used as a fuel catalyst in vehicle exhaust systems and a fuel additive to promote complete combustion (Cornelis et al., 2010). CeO_2 can be utilized as a chemical and mechanical polishing agent in the semiconductor industry, a UV light absorber, a fuel cell electrolyte and it has also been found to possess antioxidant properties, which could lead to applications in the medical field for cell protection against radiation, oxidative stress, and inflammation (Pelletier et al., 2010). Environmental exposure to CeO_2 NPs is anticipated from several possible pathways. In addition to direct discharge to wastewater, atmospheric releases of cerium oxide have been documented by Park et al., (2008), in the form of particulate matter generated from nano-CeO_2 enhanced fuel additives for diesel engines. They observed that the release resulted in slightly increased concentrations of CeO_2 in the soils immediately surrounding major roadways in the UK. As in wastewater treatment, there is the possibility for redox transformation in soils. Further transformation and subsequent exposure to aquatic environments via erosion and runoff are likely. The complex redox chemistry of CeO_2 combined with small size and associated reactivity are anticipated to affect the fate and transport of CeO_2 NPs (Gomez-Rivera et al., 2012).

Furthermore, previous studies have shown CeO_2 toxicity to some microbial communities associated with the reduction of cerium from Ce(IV) to Ce(III). Pristine CeO_2 nanoparticles are characterized at neutral pH by a near neutral net surface charge, which allows for favorable interaction with the negatively charged surface of bacteria. Direct contact between pristine CeO_2 nanoparticles and bacterial membranes is thought to favor Ce reduction and oxidation of the cell membrane (Thill et al., 2006, Zeyons et al., 2009). Thus, in addition to changing the subsequent toxicity of the CeO_2 NPs, reductive transformation of CeO_2 NPs in the presence of activated sludge bacteria, might be anticipated to provoke changes in the microbial community within activated sludge units. However, in the current work we focus uniquely on possible transformations to the CeO_2 NPs that may occur in the presence of aerobic bacteria under highly aerated conditions representative of those present in activated sludge basins.

2.3 Experimental

2.3.1 Materials

The pristine CeO_2 nanoparticle used in this work were commercially available crystallites of cerianite with diameter of 3 – 4 nm as viewed by transmission electron microscopy (TEM) (Appendix A1) where the Ce exists in the +4 oxidation state. TEM images were obtained using a JEOL 2010F operating at 200 kV and are shown in Appendix A. Sample preparation involved the placing of a droplet of the stock suspensions on a carbon-coated copper grid and allowing for evaporation at room

temperature. The average hydrodynamic diameter in their stock suspension as measured by DLS for pristine CeO_2 approximately 8 nm ± 2nm. The aqueous point of zero charge (PZC) was reported between 7 – 7.5 (Diot, 2012). Citrate-functionalized CeO_2 NPs were provided by Byk-Gardner GMBH (Geretsried, Germany). They were also made of 3 – 4 nm crystallites of cerianite with an average hydrodynamic diameter reported to be 10 nm by the supplier. The zeta (ζ) potential calculated from electrophoretic mobility measures (Zetasizer, Malvern, UK) was found to be relatively constant with a value of -45 ± 5 mV over a range of pH values of 3 to 10 due to the negatively charged citrate coating (Diot, 2012). Citrate-functionalized CeO_2 NPs are used for UV absorbance in applications of floor and furniture wood coatings for long-term protection with high transparency. The differences in surface functionalization and ζ potential between these two variants were hypothesized to affect the colloidal stability of these particles in environmental media, thus impacting NP fate, transport and affinity for attachment to bacterial surfaces.

Activated sludge was sampled from the aeration basin of an urban WWTP in Aix-en-Provence, France (165,000 inh eq.). The sludge was concentrated to 10 g/L, which was maintained over the six-week life of each of the two reactors. Aeration within the 10 L reactor was maintained at 200 L/h with daily denitrification for an hour. Recycle was simulated by pumping 9% of the sludge matrix from the base of the reactor through external tubing and reintroducing it at the top of the reactor. The solids residence time

was maintained at 20 days by withdrawing 500 mL of the homogeneous suspension daily. The sludge was fed with a synthetic substrate at a constant mass loading rate equal to 0.25 g COD (Chemical Oxygen Demand) g^{-1} TSS day^{-1}, which was comprised of 77% sucrose and 23% liquid meat extract (Viandox™, Knorr-Unilever, Rueil-Malmaison, France) in order to maintain the TSS concentration (Akkache et al., 2013). One gram of sucrose was equivalent to one gram of COD and one gram of Viandox was equivalent to 0.25 g of COD. Viandox addition was adjusted, as necessary, to decrease the nitrogen input and maintain the filamentous bacterial communities at a minimum level.

A concentration of 104 μg/L of pristine or citrate-functionalized CeO_2 nanoparticles were added in the separate reactors three times weekly to achieve a final concentration of approximately 1.5 mg/L after 6 weeks. This rate of addition was chosen to mimic CeO_2 maximum concentrations expected in wastewater influents based on estimates of production amounts of 35 to 700 tons per year for CeO_2 published by Hendren et al., (2011). A worst-case scenario (maximum concentration) of 100 μg/L was determined assuming that approximately half of the CeO_2 nanoparticles produced would be incorporated into products that would be exposed to wastewaters. Due to weekly sampling and the inherent loss of CeO_2 during that process, 104 μg/L of the NPs was the actual concentration added to maintain the desired concentration in the reactor. The semi-chronic addition method was employed in an effort to better resemble realistic scenarios of CeO_2 NPs release to the waste stream.

2.3.2 Analysis

The initial state (after a start-up period but prior to CeO_2 NP addition) of the reactors was analyzed to confirm that both reactors were compositionally similar prior to amendment with CeO_2 nanoparticles. Sludge was sampled, freeze-dried, and analyzed by powder X-ray Diffraction (XRD) and micro-X-ray Fluorescence (μXRF) to determine the mineralogical and elemental composition. The X-ray diffractometer (Panalytical X'Pert Pro MPD) was equipped with Co Kα radiation (1.79 Å) and operated at 40 kV and 40 mA current. A counting time of 400 seconds per 0.03° step was used for the 2θ range from 10 - 70°. The X-ray fluorescence microscope (XGT 7000, Horiba Jobin Yvon) was equipped with an X-ray guide tube producing a finely focused beam with a 100 μm spot size (Rh X-ray tube, 30 kV, 1 mA equipped with an EDX detector).

^{13}C Nuclear Magnetic Resonance (NMR) was employed for compositional analysis of bacterially generated extracellular polymeric substances (EPS). EPS is known to exist in two major phases, freely suspended in solution and more tightly associated with the surface of the bacterial floc. The separation method of free EPS and bound EPS from the bacteria was detailed in Akkache et al., (2013). Following this separation, the two samples from both reactors were freeze-dried for ^{13}C NMR analysis. Solid-state ^{13}C – ^{1}H cross-polarization magic angle spinning nuclear magnetic resonance (^{13}C CP-MAS NMR) analyses were carried out at a frequency of 101.6 MHz on a Bruker AvanceWB 400-MHz Spectrometer. Samples were packed into a 4-mm zirconia rotor and spun at 10

kHz in a MAS probe. Cross-polarization was performed with a ramped 1H pulse to circumvent the Hartmann-Hahn mismatches. All spectra were obtained with a 2 ms contact time and 2 s recycling time. To improve the resolution, dipolar decoupling was applied on protons during acquisition. Chemical shifts were referenced to tetramethylsilane.

Finally, microbial community structure was investigated to ensure that the starting communities between the two reactors matched. 1 mL of the bioreactor sludge was centrifuged at 16,110 G for 15 min. DNA was extracted from the solid phase using the Fast DNA spin kit for soil and a MP Bio, FastPrep®, according to the protocol of the manufacturer. Extracted DNA (100 µl) was quantified using a Nanovue™ spectrophotometer. SSU rRNA gene amplification was performed with barcoded-primers for the V1 – V3 regions. The 16S universal Eubacterial primers 27Fmod (5'-AGRGTTTGATCMTGGCTCAG) and 519R (5'- GTNTTACNGCGGCKGCTG) were used for amplifying the ~500 bp region of the 16S rRNA genes. The 454 Titanium sequencing run was performed on a 70675 GS PicoTiterPlate by using a Genome Sequencer FLX System (Roche, Nutley, NJ). Sequences were depleted of barcodes and primers, short sequences < 200 bp were removed, sequences with ambiguous base calls removed, and sequences with homopolymer runs exceeding 6 bp removed. Sequences were then denoised and chimeras removed. Operational taxonomic units were defined after removal of singleton sequences, clustering at 3% divergence (97% similarity) (Dowd et

al., 2011). Operational taxonomic units (OTUs) were then taxonomically classified using RPD Classifier (Ribosomal Database Project, http://rdp.cme.msu.edu/classifier.jsp) and compiled into each taxonomic level into both "counts" and "percentage" files. R (http://www.r-project.org) was used to calculate the α-diversity indices (Shannon-Wiener index) and β-diversity index (Bray-Curtis similarity index). Statgraphics Centurion XVI was used to perform statistical analyses.

The time-dependent affinity of CeO_2 NPs for the liquid and solid phases of the sludge within the aerobic reactors was monitored by ICP-OES. Weekly sampled sludge was centrifuged at 4,000G for 15 minutes to separate the phases. The liquid phase was subsequently acidified with 5% trace metal grade HNO_3 and the solids were oven dried. In most cases, the concentration of CeO_2 associated with the solid phase was determined by mass balance. However, to confirm the mass balance, a few of the solid samples were digested using EPA Method 200.7 (US EPA, 1994). Following measurement of Ce in the supernatant or associated with free EPS, Ce was measured in association with bound EPS upon separation (Akkache et al., 2013). In this study, the more strongly linked EPS or the "bound" phase of EPS is more specifically defined as those small molecular weight proteins and substances that are liberated through short sonication of the centrifuged solids resuspended in nanopure water (Akkache et al., 2013). The measured Ce concentration in each phase was then normalized by the total organic carbon (TOC)

in the "free" and "bound" phases respectively. TOC was measured on a Shimadzu, TOC-L for each phase after sample dilution.

In addition, colloidal stability of the NPs was assessed in the environmental matrix of WWTP effluent. The effluent was separated using gravity settling. The particle size distribution of the effluent was monitored using a Malvern Mastersizer 3000 and the refractive index of carbon. Size measurements were conducted on 10-second intervals. Pristine and functionalized CeO_2 NPs were spiked into the effluent and the evolution of the diameter of suspended solids was tracked.

Transformations of CeO_2 NPs in wastewater were monitored by following the Cerium L_3-edge XANES spectra collected on the XAFS bending magnet beamline (11.1) at the Elettra-Trieste Synchrotron light source (Italy) using a Si(111) monochromator. Samples were collected from each bioreactor after five weeks of incubation. The liquid and solid phases were separated via centrifugation at 4,000 G for 15 min, freeze dried, pressed into 13 mm pellets, and analyzed at room temperature in fluorescence mode. Potential beam damage due to the analysis at room temperature was checked. XANES spectra acquired at 15 to 20 °C or in liquid nitrogen cryostat were then compared. No change in the position or shape of the spectra was observed evidencing the absence of beam damage. In addition to measurement of the bioreactor samples, Ce(IV) and Ce(III) references powders were diluted in PVP, pressed into 13 mm pellets and measured in transmission mode. The Ce(IV) references included the nanoparticles, pristine and

citrate-functionalized along with Ce(III) Carbonate, Ce(III) Sulfate, and Ce(III) Oxalate. The spectra presented were the summation of 3 to 5 scans. The energy was calibrated using a macroscopic CeO_2 reference compounds. XANES spectra were pre-edge subtracted and normalized using IFEFFIT software (Ravel & Newville, 2005). Least-squares optimization of Linear Combination Fitting (LCF) was also performed using IFEFFIT. The precision of LCF is estimated to be ± 10%.

For assessment of the kinetics of the CeO_2 transformations, a spike experiment was performed with 0.4 mg Ce / 30 mg sludge to optimize the $\Delta\mu$ during XANES analysis at the Ce L_3-edge analysis. Wastewater sludge not yet contaminated with CeO_2 was sampled from the bioreactor and mixed with either pristine or citrate-functionalized NPs for multiple time points between 1 hour and 1 day. Samples were prepared in the same manner. The samples were then measured in transmission mode and LCF was completed for data analysis with the same reference compounds.

2.4 Results and Discussion

2.4.1 Bioreactor Initial Analysis

Initial characterization of the sludge from the two reactors by XRD and μXRF indicated the presence of three dominant mineral phases; quartz, halite, and calcite and a number of dominant elements, all listed in Appendix A2. The diffractograms and elemental composition for the two reactors were in good agreement suggesting similar mineral and chemical composition of the sludge prior to spiking with CeO_2 NPs.

The ^{13}C NMR spectra (Appendix A3) for the bound and free phases of EPS were observed to be similar. The majority of the EPS molecules consisted of proteins and polysaccharides (45 – 65 ppm and > 110 ppm as shown in Appendix A3), which is in agreement with previous studies (Jorand et al., 1995, Cadoret et al., 2002, Martin-Cereceda et al., 2001). At the initial time point, the bound EPS was compositionally different from the free EPS meaning the types of proteins and carbohydrates varied depending on the phase of EPS analyzed. However, the two phases, bound and free EPS, from reactor 1 (prior to pristine CeO_2 NPs addition) matched the same respective fractions in reactor 2 (prior to citrate-functionalized CeO_2 NPs addition). Major peaks corresponding to carbohydrates and proteins are detailed in Appendix A4. The spectra measured for the EPS generated by the sampled wastewater sludge in these reactors suggested strong similarities in the different regions with spectra from other isolated EPS fractions (Metzger et al., 2009)

Finally, the similarity of the two reactors before ENM addition was assessed in terms of microbial community composition by 16S rRNA gene pyrosequencing. Appendix A5 shows the different indices characterizing the α-diversity (Richness and Shannon-Wiener indices) and β-diversity (Bray-Curtis dissimilarity) of samples. From Appendix A5, minor variations in the α-diversity (Richness and Shannon-Wiener indices) of microbial communities present in each sludge were observed. Bray-Curtis dissimilarity between two samples varies in the 0 - 1 range. Two communities that share

no OTU have a maximum Bray-Curtis dissimilarity of 1, while 0 means the samples are exactly the same. A dissimilarity of 0.32 thus indicated good agreement between the compositions in the two reactors.

As shown in Figure 5, the microbial community structures on phylum level were alike in terms of dominant phyla and in the content of each phylum (Hu et al., 2012). Based on the sign and signed rank test, comparison of microbial populations in the two reactors (paired samples) at the phylum level showed no significant differences between the two data samples ($p > 0.05$). The most predominant phyla *Proteobacteria*, *Bacteroidetes* and *Actinobacteria* have been previously identified as major phyla in activated sludges (Hu et al., 2012). In summary, these data show that the elemental, mineralogical, EPS, and microbial composition are similar in the two bioreactors prior to NPs addition (t_0).

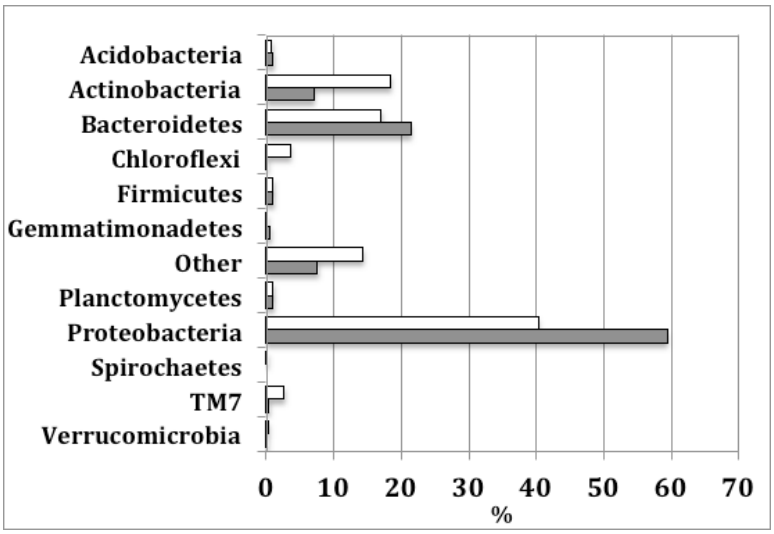

Figure 5. Bacterial community structures in the two bioreactors prior to addition of pristine CeO_2 (Reactor 1, white bars) or citrate-functionalized CeO_2 (Reactor 2, dark bars) NPs.

2.4.2 Ce Distribution

Distribution experiments indicated a high affinity of the CeO_2 NPs for the solids relative to the liquid phase regardless of surface treatment with greater than 90% of the particles retained in the solid matrix. As seen in Figure 6a, after 6 weeks in the bioreactors and addition of 1.5 mg/L NPs, ~23 μg/L of pristine CeO_2 remained in the effluent relative to ~27 μg/L of the functionalized NPs. Other inorganic NPs including Ag and TiO_2 have been shown to behave similarly with strong affinities for the solids (Kiser et al., 2010, Hendren et al., 2013). It has been reported that NPs in complex matrices like sludge will interact with a variety of surface functional groups like acids and hydroxyls, which can improve the affinity with the solid phase leading to high removal (Levard et al., 2011). Figure 6b shows the concentration of NPs associated with the solid phase relative to the added concentration to the experiment. These results

confirm that the majority (~ 90%) of the CeO_2 NPs interact with the solids. Similar findings were reported where CeO_2 effluent concentrations ranged from 6 – 11% of the total introduced to wastewater (Gomez-Rivera et al., 2012, Limbach et al., 2008).

To investigate differences in colloidal stability imparted by surface functionalization, the effective size of suspended solids in wastewater effluent was analyzed before and after NPs addition. It was observed that citrate-functionalized particles did not alter the size distribution of effluent suspended material, which remained constant with a dv_{50} of 50 μm. However, upon addition of the pristine CeO_2 NPs, the hydrodynamic diameter was observed to rapidly increase from 50 μm to 130 μm. This suggested that the pristine NPs acted as a coagulant and caused the suspended solids to aggregate. The increased colloidal stability of the citrate-functionalized NPs in the supernatant can explain the decreased removal to the sludge matrix.

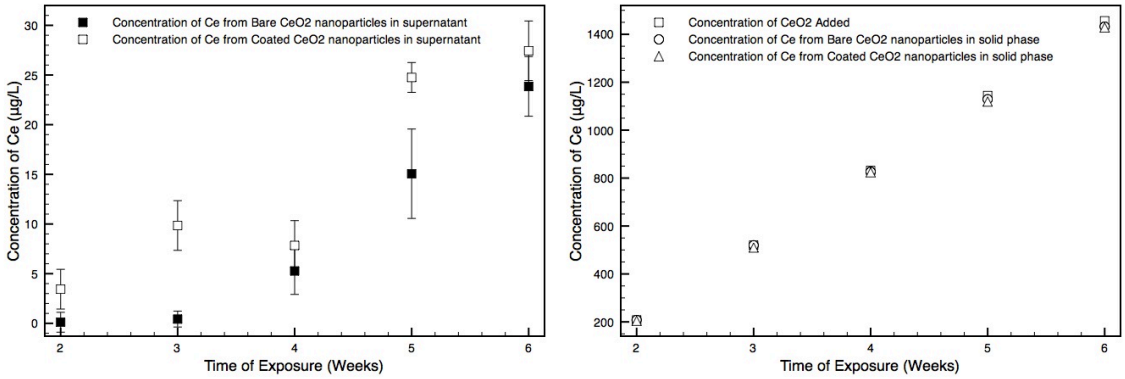

Figure 6. (A) Supernatant phase Ce concentration (µg/L) over the lifetime of the reactors. (B) Solid phase concentration of Ce measured in the reactor relative to the added concentration.

The Ce associated with the free and bound EPS phases was also analyzed. It was observed (Figure 7) after normalization by the mass of total organic carbon that a higher amount of the functionalized CeO_2 NPs associated with both fractions of EPS. It is important to note that the concentration of Ce measured in the EPS did not exceed 15% of the added amount, meaning that the highest portion of the CeO_2 added remained well associated with the in tact solids. These results do suggest though, that the functionalized CeO_2 may be associated with those polymeric substances that are more loosely arranged in the matrix and therefore liberated, while the pristine CeO_2 may have a higher affinity for the bacterial surface.

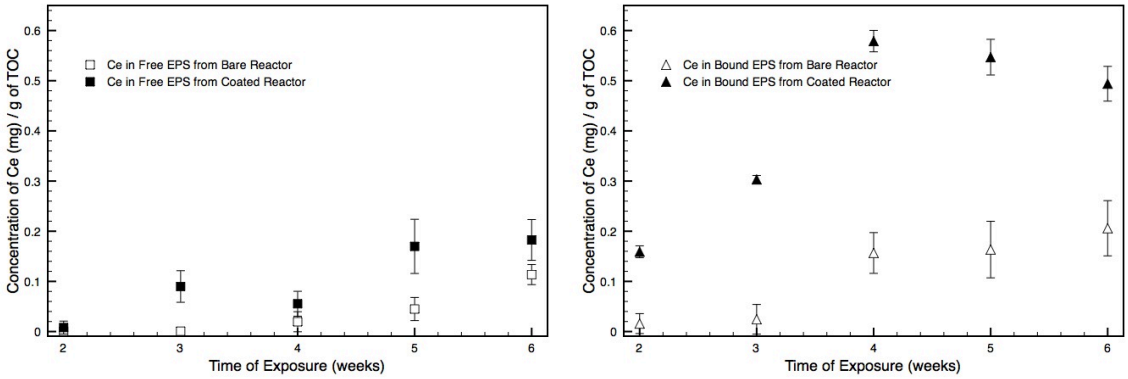

Figure 7. (A) Concentration of Ce associated with the bound fraction of EPS. (B) Concentration of Ce associated with the free fraction of EPS.

2.4.3 Transformations of CeO_2 NPs in Activated Sludge Bioreactors

The speciation of Ce within the solid phase of each bioreactor after 5 weeks was analyzed using XANES to determine transformations (Figure 8). The difference in XANES spectra for Ce(IV) versus Ce(III) is easily distinguishable as Ce(IV) has two absorption peaks at 5733 eV and 5740 eV, while the Ce(III) has one absorption peak at 5729 eV. LCF of the XANES spectra of the initial nanoparticle and Ce(III) references (Ce(III) carbonate, oxalate and sulfate) were used to estimate the percentage of Ce(IV) and Ce(III) in our experimental spectra. The most appropriate Ce(III) reference was determined to be Ce(III) oxalate, which generated the lowest R factors.

The XANES analysis of the Ce in the bioreactors indicated reduction of the Ce(IV) NPs to a Ce(III) phase. Comparing the two bioreactors, the pristine CeO_2 was reduced to a greater extent (44 ± 4% of Ce(III)) relative to the citrate-functionalized CeO_2 (31 ± 3% of Ce(III)) after a period of 5 weeks (Figure 8). The limited reduction of functionalized CeO_2 was likely due to differences in affinity for the bacterial surface,

which research indicates is necessary for reduction (Zeyons et al., 2009). The citrate functionalization likely acted as a barrier against interaction with the bacterial surface, limiting the magnitude of reduction.

In this experiment, the reduction occurred in an aerobic or oxidizing system. Therefore, CeO_2 NPs must come into contact with micro-reducing zones generated by bacterial sludge flocs for Ce reduction to occur. Within microbial flocs, these reducing environments occur as the result of microbial metabolism that depletes the oxygen present allowing for reduction mechanisms to take place (Li & Bishop, 2004). Such a reduction of CeO_2 NPs to Ce(III) was observed by Thill et al., (2006), and Zeyons et al., (2009) in contact with the membranes of gram-negative *E. coli* and *Synechocystis* bacteria.

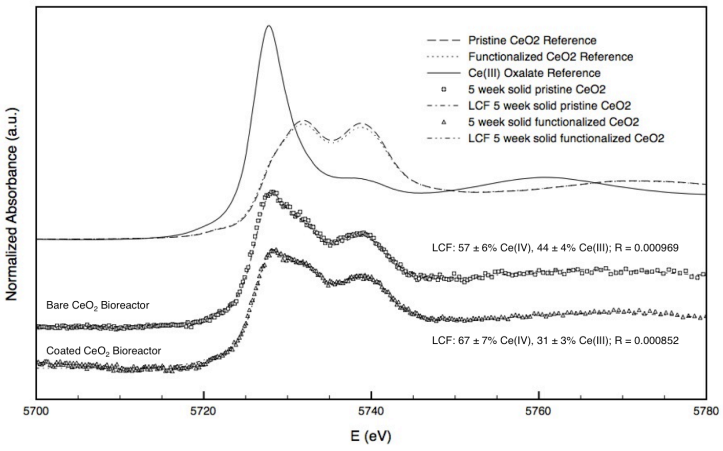

Figure 8. Experimental XANES spectra at the Ce L_3-edge after a 5 week incubation of pristine and citrate-functionalized in a bioreactor.

2.4.4 Kinetics of CeO_2 NPs Transformation

The kinetics of the Ce(IV) reduction were more closely analyzed by XANES following a spike addition of CeO_2 NPs at a higher concentration (~ 100 mg/L) added in batch and mixed with sludge (90 mL) for 1 hour, 8 hours, and 1 day. Figure 9 illustrates the increased reduction of Ce(IV) to Ce(III) as a function of mixing time for pristine and functionalized CeO_2 NPs in contact with the solid phase of activated sludge. Within the first hour, significant reduction (27 ± 3% of Ce(III)) was observed for pristine CeO_2. With mixing times between 1 hour and 1 day, the reduction of the pristine CeO_2 did not significantly increase. Comparing the pristine to the citrate-functionalized NPs, the results suggested slowed transformation kinetics with only about half as much reduction (12 ± 1% of Ce(III)) measured at 8 hours and 1 day for the citrate-functionalized CeO_2. Consequently at 8 hours (typical solids residence time in an

activated sludge reactor), the functionalized CeO_2 is anticipated to be more chemically stable than the pristine CeO_2 (Figure 9 and Table 2). It has been shown that direct contact with the bacterial membrane was necessary for the reduction to occur and that organics on the surface of microorganisms could limit this reduction either by a protective barrier or reducing the affinity for interaction (Zeyons et al., 2009). It can thus be concluded that the citrate treatment reduces nanoparticle-bacteria contacts and therefore prevents the reduction of the citrate CeO_2 NPs. The transformations of CeO_2 NPs were also investigated in the liquid phase of the spiked samples (Figure 9, Table 2). Both pristine and functionalized CeO_2 NPs after 8 h and 1 d in contact with the liquid phase were present in the Ce(IV) phase at greater than 90% of the total. It is possible that either those NPs were never reduced or that reoxidation from Ce(III) to Ce(IV) occurred in the oxidizing supernatant.

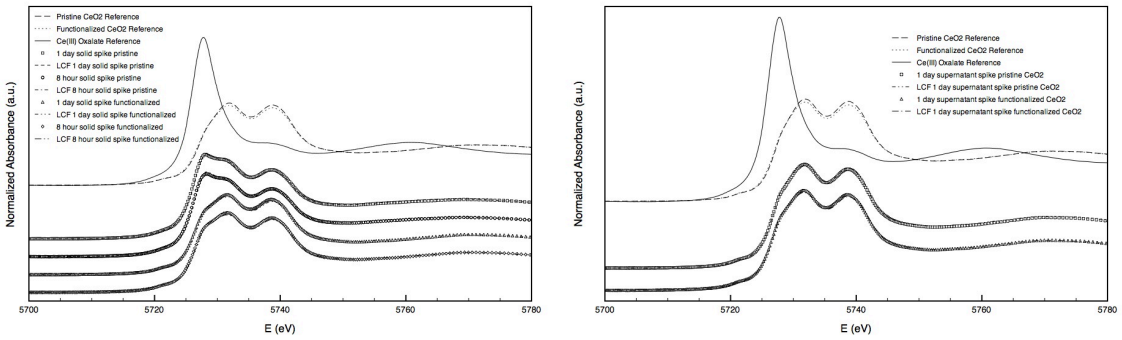

Figure 9. (A) Solid phase XANES spectra from the spike experiment. (B) Supernatant phase XANES spectra from the spike experiment.

Table 2. Summary of LCF results of XANES spectra from solid and liquid phase spike experiments.

Sample	Duration	% Ce(IV)	% Ce(III)	R factor	Sample	Duration	% Ce(IV)	% Ce(III)	R factor
Pristine CeO_2 in solid phase of the spike experiment	1 hour	73	27	0.000270	Functionalized CeO_2 in solid phase of the spike experiment				
	8 hour	67	33	0.000281		8 hour	89	11	0.000249
	1 day	68	33	0.000317		1 day	89	12	0.000139
Pristine CeO_2 in liquid phase of the spike experiment	1 hour	> 90	< 10	0.000123	Functionalized CeO_2 in liquid phase of the spike experiment				
	8 hour	> 90	< 10	0.000106		8 hour	> 90	< 10	0.000268
	1 day	> 90	< 10	0.000067		1 day	> 90	< 10	0.000149

2.4.5 Transformation Products of CeO_2 Reduction in a WWTP

Upon reduction by bacteria in the activated sludge, the Ce(III) is most likely complexed in the solid phase given the large concentrations of ligands available. If the Ce(III) distributes back to the supernatant, reoxidation likely occurs because Ce(III) is not observed in the supernatant and oxidation is favorable due to the aerobic environment. The formation of a Ce(III) complex can only be hypothesized thermodynamically because the L_2-edge XANES of Ce interrupts the EXAFS region,

which provides binding environment information. The thermodynamic argument for the Ce(III) complexes formed in this system required the investigation of the solid phase speciation and mineral activity of cerium minerals in wastewater sludge provided in Figure 10. Essington and Mattigod (1985) used mineral activity ratios to analyze the stability of cerium minerals in oxidizing and reducing sludge environments. The results indicated that in the oxidizing environment of sewage sludge where the concentration of sulfur is high, that $Ce_2(SO_4)_3$-$8H_2O$ would control Ce^{3+} activity. With increasingly oxidizing conditions, cerianite (CeO_2) would be expected to control Ce speciation. In addition, the authors found that under reducing conditions, similar to what is observed in anaerobic digesters, Ce_2S_3 would be the stable solid phase. This would suggest that CeO_2 NPs that undergo reduction in activated sludge result in the formation of $Ce_2(SO_4)_3$-$8H_2O$ that is later transformed to Ce_2S_3 in anaerobic digestion. Another possible metastable phase of cerium is monazite ($CePO_4$), which has been observed in soil environments (Cornelis et al., 2011). This could suggest that further transformation of reduced Ce_2S_3 upon removal from the anaerobic digester to aerobic compositing prior to recycling or disposal of biosolids would be possible.

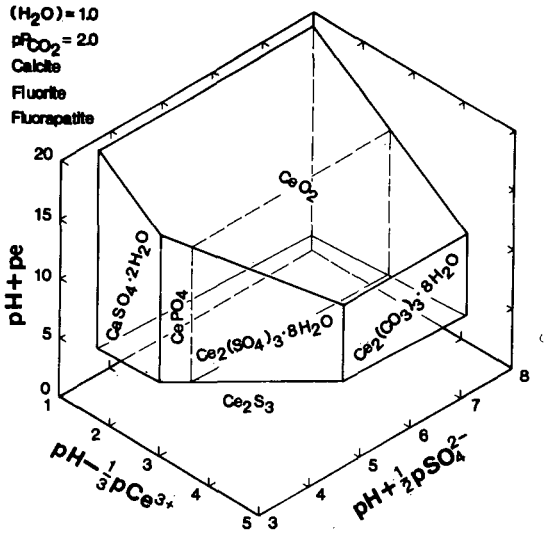

Figure 10. Solid phase activity diagram for cerium minerals in aerobic and anaerobic sludge matrices (Essington & Mattigod, 1985).

The results of this work suggested that a significant portion of the CeO_2 released to WWTPs would associate with the solids and approximately half would be reduced in the activated sludge tank. In addition, the presence of an organic coating was observed to slow the kinetics of this reduction. The remaining (< 10%) CeO_2 NPs in the liquid phase would be discharged in effluent as CeO_2, which is the mineral phase that governs cerium speciation in aerobic environments. These results are of critical importance for predicting concentrations of CeO_2 in the environment following release to the waste stream and indicate that Ce(III) complexes could be of importance to analyze further.

3. Theory and Methodology for Determining Nanoparticle Affinity for Heteroaggregation in Environmental Matrices Using Batch Measurements

3.1 Abstract

In this study, we present a method for determining the relative affinity of nanoparticles (NPs) for an ensemble of other particles in a complex, heterogeneous suspension. We evaluate this method for the case of NPs heteroaggregating with suspended solids present in activated sludge. A relationship is derived between the heterogeneous affinity coefficient, α, and measurements over time of the distribution coefficient , γ, of NPs measured in supernatant versus those removed by heteroaggregation and subsequent settling. Application of this method to a series of metal and metal oxide NPs, heteroaggregated with activated sludge, indicated a relative affinity in the order of pristine CeO_2 TiO_2 NPs, and ZnO NPs > Ag(0) NPs surface modified with polyvinylpyrrolidone (PVP) > citrate-functionalized CeO_2 NP > Ag(0) NPs surface modified with gum arabic (GA). This trend in relative affinity followed the observed trend in removal such that higher affinity corresponded to higher removals of NPs.

Values of α were calculated from the measured relative affinities using the number average diameter and concentration of the activated sludge particles. The value calculated for PVP-stabilized Ag(0) NPs was comparable to a value previously reported for the attachment of these same NPs to a biofilm. Calculations also yielded a size

dependence of α in the case of the two Ag(0) evaluated that may be linked to nanoparticle dissolution.

3.2 Introduction

The growing use of engineered nanoparticles (ENPs) in consumer products and technology will result in unavoidable human and environmental exposures (Gottschalk and Nowack, 2011, Wiesner et al., 2009). Methods to evaluate nanoparticles (NP) fate, transformation and transport, as a basis for estimating exposure and potential risk, remain limited (Wiesner et al., 2006, Hendren et al., 2013). In particular, simple functional assays are needed to predict the environmental mobility and fate of NPs, analogous to the use of the octanol-water partition coefficient used for synthetic organic chemicals. Previous investigators have analyzed the association of NPs with bacteria (Kiser et al., 2010), quantifying this association using a Freundlich isotherm.

It has been previously proposed that processes controlling nanoparticle transport and attachment to environmentally relevant surfaces can be used as the basis for a functional assay (Lecoanet et al., 2004). Aggregation and deposition are analogous processes involving particle-particle or particle-surface interactions occurring in sequential steps of transport and attachment. Physical-chemical processes controlling nanoparticle attachment or "affinity" for abiotic or biotic surfaces such as bacteria, algae, clays, and the tissues of higher organisms, will play a key role in determining whether NPs associate with larger "background" particles that accumulate in sediments, whether

NPs adhere to gills or skin, or whether they stick to the media in ground water aquifers. Such processes of heteroaggregation and deposition are therefore likely to impact transport, bioavailability and bio-uptake of NPs (Lin et al., 2011). Measurement of surface affinity may therefore provide a means for predicting important dimensions of the environmental behavior of NPs.

Many NPs used in consumer products will be modified by surface functionalization designed to impede aggregation through charge or steric stabilization (Napper and Netschey, 1971). Stabilization of colloids can enhance transport in environmental media due to decreased removal, which is typically achieved via aggregation processes (Espinasse et al., 2007, Chen et al., 2008). Environmental conditions such as ionic strength, the presence of naturally occurring macromolecules, redox conditions, and the pH of the media will further influence or modify the affinity of NPs for each other and for other surfaces (Lin et al., 2012).

The attachment efficiency (α) describes the likelihood of attachment for each collision between two surfaces. The surface affinity between NPs in homoaggregation can be estimated by normalizing the aggregation rate in a given system to the rate of aggregation observed when chemical conditions favor the process (where α is assumed to be unity) such as when stability is due to particle charge and salt concentrations that are above the critical coagulation concentration (CCC). These rates of aggregation are determined from the slope of the linear zone of the plot of changing hydrodynamic

radius as a function of time (Petosa et al., 2010). As an example, when using analytical techniques to monitor hydrodynamic radius, α_{homo} can be calculated using the slope of the rate of changing radius shown in Equation 3.1:

Equation 3.1

$$\alpha_{homo} = \frac{\frac{1}{C_0}\left(\frac{dr_h}{dt}\right)}{\frac{1}{C_{0,fav}}\left(\frac{dr_h}{dt}\right)}$$

where r_h is the hydrodynamic radius, C_0 is the initial concentration and *fav* denotes the aggregation reaction under favorable conditions. This method is however limited to determination of attachment efficiency in homoaggregation alone and requires advanced instrumentation.

Nanoparticle deposition in a porous medium of spheres of known composition can be used to obtain information on the affinity coefficient between NPs and a model reference surface such as glass beads. Removal of NPs across the column containing a packed bed of the reference porous medium "collectors" (after the first two to three pore volumes have been eluted) is related to the affinity coefficient, α_{hetero} as:

Equation 2.2

$$\alpha_{hetero} = -\frac{2d_c}{3(1-\varepsilon)\eta_0 L} ln\left(\frac{C}{C_0}\right)$$

where d_c is the diameter of the collectors, ε is the porosity of the packed bed, L is the length of the column, C and C_0 are the concentration of the particles in the effluent and influent respectively, and η_0 is the single collector efficiency which describes particle

transport and can be calculated from theory. In addition to limitations on the type of surfaces that can be represented as spherical collectors, this method requires equipment providing for accurate flow control, injection, and sample collection.

Environmentally relevant systems will often present a heterogeneous ensemble of surfaces of complex geometries that render traditional experimental determination of the attachment efficiency challenging. In this work, we present a method for obtaining estimates of the overall affinity of NPs for surfaces in such systems that is both experimentally simple and easily interpreted in a theoretical context.

3.3 Theory

Due to their small size, the settling rate of individual NPs is negligible. Homo- or hetero-aggregation can produce objects that are sufficiently large to settle from suspension over times scales of seconds to days. In systems where NPs are present in small concentrations, typical of those predicted from production estimates of NPs (e.g., Gottschalk and Nowack, 2011, Hendren et al., 2011) particle collisions in a suspension will likely be dominated by heteroaggregation with larger "background" particles (clays, bacteria, etc.). Settling of the resulting aggregates (and further aggregation during settling) will therefore result in the removal of many of the products of heteroaggregation. The distribution of NPs between those that are not associated with background particles (not heteroaggregated) and those that have heteroaggregated at any time is an instantaneous picture of the extent of heteroaggregation that has

occurred. If settling is assumed to remove the majority of heteroaggregates from the suspension, then the distribution coefficient, γ, can be approximated as the distribution of NPs between the suspended and settled (heteroaggregated) compartments. This distribution coefficient would ideally be taken as the ratio of measurement of mass or number of NPs per mass of solids that have settled from suspension to the mass or number concentration of NPs remaining in suspension at any time:

Equation 3.3

$$\gamma = \frac{\frac{M_S}{M_B}}{C_L}$$

where M_S is the mass of the NP associated with the settled material, M_B is the mass of the background particles removed by settling, and C_L is the concentration of the NPs that remains in the supernatant. Thus, γ has units of $m^3\ kg^{-1}$. In practice, if the concentrations of particles native to a given system (background particles) and NPs are followed over time, γ at any time during heteroaggregation can be calculated from measurements of the supernatant alone calculating the amounts removed with the settled heteroaggregates by difference from the initial amounts present.

Consider the products of heteroaggregation, before settling occurs, as representing a balance between the forward reaction of heteroaggregation and a reverse break-up reaction that returns particles that have previously aggregated to a state of free suspension due to erosion or fracturing. Modifying the Smoluchowski equation (Smoluchowski, 1917) the forward reaction is described by the product of the second

order collision rate constant, β, the concentration of un-heteroaggregated NPs, n, the concentration of background particles, B (which remains constant), and the affinity coefficient between nano- and background- particles, α. The reverse reaction (break-up of larger aggregates into the primary particle sizes) can be assumed to be proportional (by the rate constant k_B) to the number of NPs that have heteroaggregated (n_0-n) such that:

Equation 3.4

$$\frac{dn}{dt} = -\alpha\beta(n,B)nB + k_B(n_o - n)$$

The collision rate constant, β(n,B) is the sum of transport interactions induced by Brownian motion, differential settling and shear, and varies as function of the diameters of nano- and background particles, mixing conditions, temperature, fluid viscosity and particle densities. If the forward and reverse reactions come to steady state and all of background particles (including the heteroaggregation products) were removed from suspension without disturbing the remaining un-aggregated NPs, measurement of the distribution coefficient γ would be expected to yield a value equal to the ratio of the forward and reverse reaction rate constants:

Equation 3.5

$$\gamma(steady\ state) = \frac{\frac{(n_o - n)}{C_B}}{n} \approx \frac{\alpha\beta}{k_B M_B}$$

where C_B is the mass concentration of background particles (number concentration, B, multiplied by the mass of a single background particle). In other words, at steady state,

the distribution coefficient should be proportional to the affinity coefficient by a factor $\beta/k_B M_B$.

The time-variable solution to Equation 3.4 yields:

Equation 3.6

$$n = n_0 e^{-(\alpha\beta B + k_B)t} + \frac{k_B n_0}{\alpha\beta B + k_B}\left(1 - e^{-(\alpha\beta B + k_B)t}\right)$$

Subtracting n from n_0 and dividing by $n^* C_B$ yields an expression for the instantaneous distribution coefficient, $\gamma(t)$:

Equation 3.7

$$\gamma(t) = \frac{1}{C_B}\left(\frac{1}{\left(e^{-(\alpha\beta B + k_B)t} + \frac{k_B}{(\alpha\beta B + k_B)}\left(1 - e^{-(\alpha\beta B + k_B)t}\right)\right)} - 1\right)$$

During the early stages of heteroaggregation breakup can be assumed to be negligible, and Equation 3.7 can be simplified and rearranged to yield the following equation relating the affinity coefficient and $\gamma(t)$:

Equation 3.8

$$\ln(\gamma(t) C_B + 1) = \alpha\beta(n, B) B t$$

Thus, a plot of $\ln(\gamma(t) C_B + 1)$ versus the heteroaggregation time is predicted to yield a linear relationship where the slope of this plot, $\alpha\beta B$ is a measure of the relative affinity of the NPs for the background particles.

By performing experiments in which a known quantity of NPs is introduced to a suspension of background particles, and allowing heteroaggregation to proceed with

mixing for a series of programmed times, values for the instantaneous distribution coefficient can be calculated by measuring the NPs remaining in solution after mixing is halted and background particles are allowed to settle from the suspension. Plotting the resulting data versus heteroaggregation (mixing) time as described by Equation 3.8 allows for the calculation of the relative affinity of NPs for the background particles. Absolute values of α can be obtained by dividing the value of the slope by the mass concentration of the background particles and a calculated collision frequency. Alternatively, the product βB for a given system (background particles, mixing conditions, etc.) can be obtained by altering the chemical conditions (such as ionic strength) to favor aggregation analogous to Equation 3.2:

Equation 3.9

$$\alpha_{hetero} = \frac{\beta B}{\beta B_{fav}}$$

or by calibrating the system to a known value of α_{hetero} determined, for example, from column experiments.

3.4 Computational verification

Equation 3.4, and the subsequent solution presented above, approximates the heteroaggregating suspension as consisting of only two particles classes, monodisperse NPs and background particles. A more complete description of heteroaggregation accounts for all possible combinations of nanoparticle and background particle aggregates and must be solved numerically. This more precise description of

heteroaggregation was coded in Matlab (Matlab R2010a, the MathWorks Inc., Natick, MA, USA) and is expressed as a system of "m" differential equations, each of which describes the change in number concentration of particle aggregates in one size class k, such that k = 1 to m. If NPs of radius r_{NP} occupy the smallest size class (the subscript NP indicating k = 1), the rate of change of the number concentration of NPs, n_{NP}, (assuming no breakup) is equal to the rate at which they aggregate with themselves and with particles in all other size classes such that:

Equation 3.10

$$\frac{dn_{NP}}{dt} = -n_{NP} \sum_{k} \alpha_{NP}(f_{Sk}) \cdot \beta(r_{NP}, r_k, f_{Sk}) \cdot n_k$$

where n_k is the number concentration of size k aggregates, $\beta(r_{NP}, r_k, f_{Sk})$is the collision rate kernel describing the rate at which a NP comes in contact with a particle or aggregate in size class k accounting for porosity of the aggregates based on their fractal dimension (Wiesner, 1992), and α_{NP} is the attachment efficiency between a nanoparticle and a size k aggregate with an average fraction of NPs (f_{Sk}) on its surface. In these simulations, attachment efficiencies between size classes evolve as a function of f_{Sk} in each size class, modifying the initial affinity coefficient between nano- and background-particles, α_{BN} as the average surface of background particles is modified by the heteroaggregated NPs. For k > 1, the remaining m - 1 differential equations include a term describing gains in aggregate number concentration due to aggregation from

smaller size classes, as well as the losses to larger size classes such as that shown for NPs in Equation 3.10.

The numerical solution of the system of "m" differential equations over time yields an aggregation between NPs and an evolving distribution of background particles and aggregates distributed through these "m" size classes. These simulations were performed to test the validity of the approximating the heteroaggregation process as occurring between just two size classes as described by Equation 3.4. The simulation parameters covered ranges similar to those of the experimental measurements described further, with a fixed initial concentration of background particles (C_B = 4 gL^{-1}), initial concentrations of NPs of 10 and 50 mgL^{-1}, initial background particles diameters ranging from 2 to 15 μm, initial NP diameters ranging from 5 to 20 nm, and attachment efficiencies between background particles and NP ranging from 0.001 to 1. By varying simulation time for heteroaggregation and following the total amount of NPs associated with background particles over time, simulated values of $\gamma(t)$ were generated. The results of these simulations confirm the linear relationship between $\ln(\gamma(t)C_B + 1)$ and time for the more complex, multi-size class system as described by Equation 3.10. Figure 11 shows one such plot from simulations where the heteroaggregation affinity constant, α_{BN}, was fixed at a value of 0.1. Affinity coefficients calculated from the slopes of such plots were within 0.58%, 1.2%, 2.2%, and 3.4% of the values of 0.001, 0.01, 0.1, and 1 applied respectively to α_{BN} in the simulations, and R^2 values were all larger than 0.99,

confirming the validity of assumptions when break up is ignored such as is likely to occur in the initial stages of heteroaggregation.

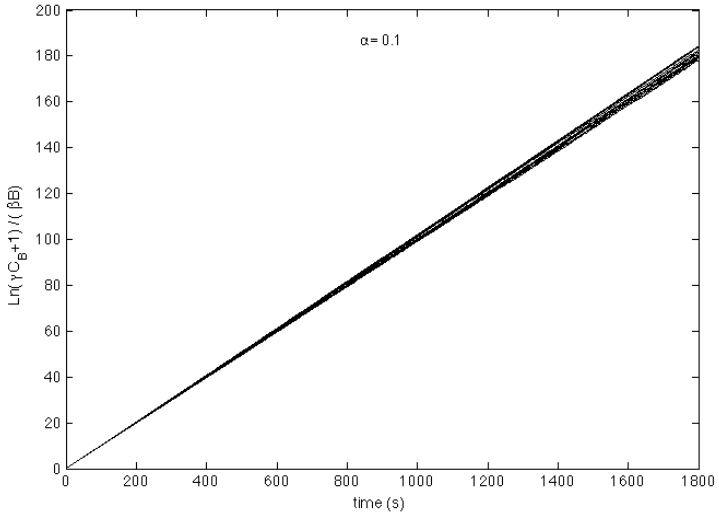

Figure 11. Confirmation of linearity using numerical simulations of heteroaggregation for a system of many interacting particle size classes.

3.5 Experimental

3.5.1 Materials

Metal and metal-oxide NPs with core compositions of Ag, CeO_2, ZnO, and TiO_2 were employed in this study due to their prevalence in consumer products and technologies and their likelihood of release to the wastewaters (Blaser et al., 2008). Table 3 indicates the NPs used and the associated characteristics including size and coating. The nano-Ag particles used were all synthesized in-house at CEINT (the Center for the Environmental Implication of Nanotechnology, Duke University, Durham, NC) and differed in size and surface functionalization. Pristine CeO_2 NPs were provided by Rhodia (LIONS, Saclay, France) while the citrate functionalized CeO_2 was purchased

from Byk Additives (Altana, Wesel, Germany). The ZnO NPs (Nanosun P99/30) were donated by Micronisers (Dandenong, Australia) and the TiO_2 NPs were purchased from Evonik Industries (Essen, Germany), neither possessed surface macromolecule functionalizations. The dispersions were all made in nanopure water with an average pH of 5.6. Zeta potential was measured at 100 mgL^{-1} on a Malvern Zeta-Sizer (Malvern Instruments, Malvern, UK) and is reported in Table 3.

Table 3. The eight NPs used in this study with associated physical/chemical characteristics and manufacturing information.

NP	Manufacturer	Surface Functionalization	Size (nm)	Zeta Potential in Nanopure Water (pH = 5.6) (mV)
GA Ag	CEINT	GA	25	-27.5 ± 0.2
	CEINT	GA	6	-38.8 ± 0.9
PVP Ag	CEINT	PVP	40	-12.0 ± 0.6
	CEINT	PVP	8	-8.2 ± 0.6
Pristine CeO_2	Rhodia	None	8	32.2 ± 4.1
Citrate CeO_2	Byk Additives	Citrate	10	-17.9 ± 4.5
TiO_2	Aeroxide P25	None	20	32.7 ± 0.5
ZnO	Nanosun	None	30	16.0 ± 0.3

3.5.2 Distribution Experiments

Time-dependent distribution coefficients (γ) were measured in 25 mL batch experiments. Secondary wastewater sludge was sampled from the activated sludge basin of the Durham County Wastewater Treatment Plant (WWTP) in Durham, NC. The average pH and chemical oxygen demand (COD, as measured by HACH test kits) of the activated sludge were approximately 7.2 and 350 – 550 mgL^{-1}, respectively. The

total suspended solids (TSS) was approximately 3.81 gL^{-1}. Sludge was stored at 4 °C for less than one week prior to experimental completion (Hendren et al., 2013). In the batch tests, NPs were added at concentrations of either 10 or 50 mgL^{-1} to the activated sludge suspension and mixing ensued for a programmed period of 0 minutes to 1 hour with data collected at 6 time points overall. After programmed mixing, the heteroaggregated suspension was gravity separated for approximately 30 minutes. The supernatant was decanted and acidified with 2% HNO_3 prior to analysis on the ICP-OES. The solid concentration was determined via mass balance for most samples and confirmed by solid digestion (US EPA 1994) on a subset of samples. Removal was assessed and the distribution coefficient was then calculated according to Equation 3.5.

3.6 Results

The removal, r, of NPs from suspension (as measured by initial and final metal concentrations, $r = (n_0-n)/n_0$) after mixing for one hour followed by settling indicated high levels of removal (> 70%) for all of the inorganic NPs assessed in this study. Unfunctionalized CeO_2 and TiO_2 NPs were removed to the greatest extent, (95 – 100%) followed by ZnO and PVP functionalized Ag NPs (~ 90%), citrate functionalized CeO_2 NPs (85%) and GA-functionalized Ag NP (~ 70%). Percent removals were similar at the two concentrations evaluated. Removal increased up to mixing times of 10 minutes, after which point removals tended to stabilize.

Removal differed based on surface functionalization. For example, in the case of CeO_2, the citrate surface modification exhibited a lower ζ potential (-17.9 ± 4.5 mV) as prepared in nanopure water at pH 5.6 compared with the pristine NPs (32.2 ± 4.1 mV), thereby increasing the stability of the functionalized NPs. However, it is not clear that changes in removal (85% vs. 98%) can be directly attributed to changes in the zeta potential since the complex mixture of solutes present in the wastewater would be expected to alter NP surface charge. Similarly, for the case of PVP- and GA- stabilized Ag NPs of similar size (6 vs. 8 nm in mean diameter), these two surface treatments imparted different surface charges as well as possibly different steric properties. The ζ potential of 6 nm GA functionalized Ag was measured at neutral pH to be -38.3 ± 0.9 mV while the ζ of the 8 nm PVP-Ag NPs was -8.19 ± 0.6 mV. As with the CeO_2 NPs, a higher (negative) electrophoretic mobility (from which the ζ is calculated) was associated with less removal to the settled material. These data were in agreement with trends of removal reported by Hendren et al. (2013) in batch studies, where the authors found that PVP coated NPs were removed to a greater extent compared to GA-Ag NPs. Other researchers have reported high levels of removal of Ag NPs (99%) after 2 hours of mixing without any impact of size (Kaegi et al., 2011, Kaegi et al., 2013, Kiser et al., 2010).

From Equation 3.5 (for any arbitrary time, rather than at steady state), the relationship between the time variable distribution coefficient (values presented in Appendix B1) and removal following a mixing period "t" is given by:

Equation 3.11

$$\gamma = r(t)\frac{C_0}{C(t)\cdot C_B}$$

assuming that all background particles are removed by settling (an assumption which was verified to hold within at least 1%). Distribution coefficients calculated from removal by settling, observed following programmed mixing at various times, "t" and plotted as ln (γC_B+1) plotted versus time (or equivalently, ln (rC_0/C + 1) versus time) yield a trend line with a slope of $\alpha\beta B$.

An example of one such plot is shown in Figure 12 for 50 mgL^{-1} of TiO_2 and GA-Ag NPs mixed with activated sludge. The linear portion of this plot, consistent with Equation 3.8, is apparent for mixing times between approximately zero and ten minutes. At longer periods of time, the plot reaches a plateau due to an increasing importance of breakup, modifications to heteroaggregate chemistry, or both. This linear range between zero and ten minutes of mixing was observed for all of the NPs investigated with R^2 values ranging from 0.85 – 0.98. The values of the slopes are presented in Table 4. The trend in the magnitude of the slope matches the trend in removals after one hour of mixing.

Estimates for the heteroaggregation affinity coefficient, α, for these combinations of NPs and activated sludge were obtained by dividing the measured slope, $\alpha\beta B$, by βB, obtained from measurements of the activated sludge (B) and calculated from theory (β). The mass and concentrations of background particles were from measurements of the

suspended solids concentration and particle size distribution of the activated sludge. The mass concentration of the sampled wastewater was measured to be approximately 4 gL^{-1} and a value for the density of the activated sludge of 1050 kgm^{-3} was assumed (Sears et al., 2006). The number average diameter of the background particles was determined to be 2.3 μm as obtained from static light scattering measurements (Malvern Mastersizer 3000, Malvern Instruments, Malvern, UK) of which similar to values reported by others (Schmid et al., 2003, Snidaro et al., 1997).

The collision frequency, β, describes particle collisions resulting from Brownian motion, differential settling and velocity gradients and was calculated using theory describing these interactions between porous aggregates (Veerapaneni and Wiesner, 1994, Thill et al., 2001). For the calculation of β, a value for the velocity gradient, G, of 20 s^{-1} was assumed and the density of the NPs was assumed to be the density of the metal core (Ag = 10500 kgm^{-3}, Ce = 7650 kgm^{-3}, Ti = 4230 kgm^{-3}, and Zn = 5610 kgm^{-3}). At the beginning of heteroaggregation experiments, there exists a dominant β associated with a single type of interaction, which corresponds to the interaction between an average size NP and an average size background particle. The experimental conditions for this study inspected the initial, fast stage of heteroaggregation, where changes in β and break up could be assumed negligible.

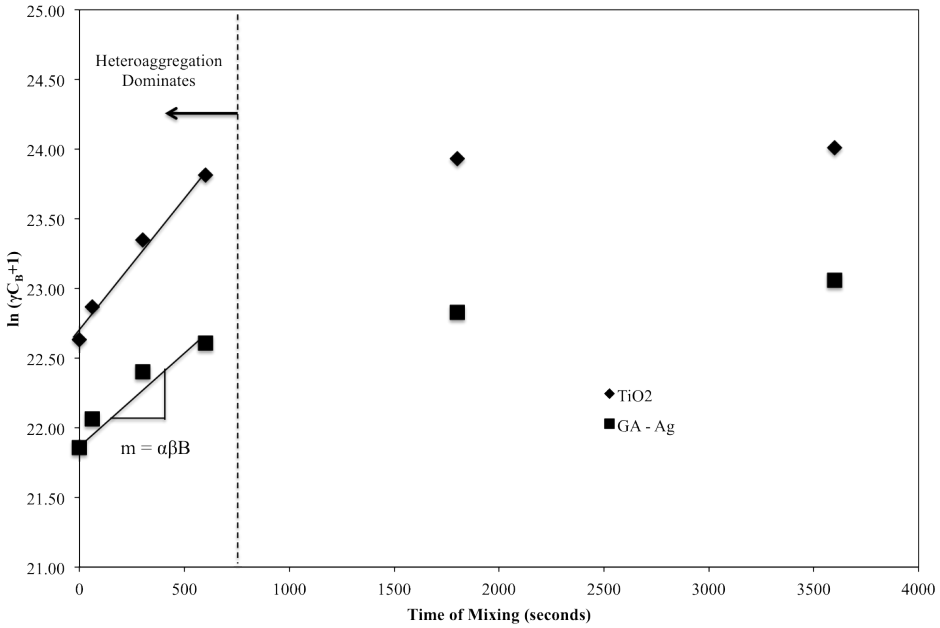

Figure 12. Representative plot for TiO_2 and GA-Ag NPs interacting with secondary sludge to illustrate the initial linear behavior that is used to determine αβB.

Table 4. The percent removal dictated by γ, the determined values for the slope (αβB), and the simulated α for the NPs studied.

NP	d_p (nm)	C_p (mg/L)	Final Removal (%)	αβB	Porous α_{calc} (2.3μm)
GA Ag	25	10	71.1 ± 0.4	2.55E-4	0.0017
		50	72.8 ± 1.8	3.07E-4	0.0020
	6	10	70.8 ± 2.1	1.86E-4	0.0003
		50	65.2 ± 3.8	1.60E-4	0.0003
PVP Ag	40	10	94.8 ± 2.2	1.16E-3	0.0120
		50	93.8 ± 0.8	1.15E-3	0.0119
	8	10	88.1 ± 1.7	9.63E-4	0.0020
		50	89.6 ± 1.2	1.02E-3	0.0022
Pristine CeO_2	8	10	90.8 ± 1.7	1.11E-3	0.0064
		50	98.8 ± 1.6	1.78E-3	0.0088
Citrate CeO_2	10	10	86.4 ±1.3	8.55E-4	0.0023
		50	83.4 ± 0.9	6.87E-4	0.0018
TiO_2	20	10	95.1 ± 1.7	1.53E-3	0.0080
		50	98.9 ± 1.0	1.80E-3	0.0094
ZnO	30	10	91.2 ± 0.3	1.13E-3	0.0088
		50	94.2 ±1.7	1.16E-3	0.0090

3.7 Discussion

Trends in calculated estimates of the affinity coefficients, α, were similar to those observed for both the relative affinities ($\alpha\beta$B) and settled removal of NPs following 60 minutes of mixing with 40 nm PVP-Ag > TiO_2 ≈ ZnO > Pristine CeO_2 > 8 nm PVP-Ag ≈ Citrate-functionalized CeO_2 ≈ 25nm GA-Ag > 6 nm GA-Ag. The calculation of α was found to be sensitive to the assumed properties of the background particles and the

mixing conditions. However, the value of ~ 0.01 calculated for the affinity coefficient for the 40 nm PVP Ag NPs by this method is close to the value of α previously reported by Xiao and Wiesner (2013) of 0.01 for a biofilm determined from column studies using the same PVP functionalized Ag NPs used in this work.

In the case of Ag NPs, where size was also a variable, the data suggested a possible size-dependence for α. While the mechanism that accounts for this phenomenon is unknown, we speculate that differences in α with size may be an artifact of silver dissolution. Dissolution kinetics in pure water have been shown to be size controlled such that smaller particles result in increased dissolution of Ag (Ma et al., 2012). If the smaller Ag NPs dissolved to a greater extent, more silver would have remained in the supernatant. Since only total silver was measured (as opposed to particulate and dissolved fractionation), this would give the appearance of less heteroaggregation, and therefore a smaller value for α. Size dependent changes in surface charge density and complexation of ligands in the wastewater as well as different initial values in the ζ potential may have also played a role. This method allows for the determination of a fundamental NP property in wastewater from a time dependent parameter that dictates removal. Both α and removal are useful for indicating NP behavior in environmental systems.

3.8 Summary

A simple method for quantifying the relative affinity of NPs with a complex mixture of larger particles has been shown to yield results that are consistent with theory and with observed trends in NP removal. The method serves as a functional assay for NP behavior in aquatic systems that are sensitive to differences in NP composition, including different surface functionalizations. Improvements to research would be an analysis of the impact of background sludge sampled from different locations due to the high variability of the wastewater matrix. In addition, further application of this work to other NPs and aged samples can provide important information on NP behavior in the environmental matrix of wastewater sludge. Estimates of surface affinity obtained by this method should be useful in predicting heteroaggregation and deposition of NPs and enable calculations of NP transport, bioavailability and bio-uptake.

4. Monte Carlo Simulations of the Transformations and Removal of Ag, TiO_2, and ZnO Nanoparticles in Wastewater Treatment.

4.1 Abstract

As more nano-enabled materials are used in research and development, the more imperative it becomes to understand the consequences of such materials entering the environment during production, use or disposal. The novel properties of nanomaterials that make them desirable for commercial applications also present the possibility of impacting aquatic and terrestrial environments in ways that may differ from materials in bulk format. Modeling techniques are needed to proactively predict the environmental fate and transport of nanomaterials.

A model for nanoparticle (NP) separation and transformation in water treatment is parameterized for three metal and metal-oxide NPs. Functional assays to determine NP specific distribution and transformation were used to parameterize the model and obtain environmentally relevant concentrations of NPs leaving WWTPs in effluent and biosolids. All three NPs were predicted to associate > 90% with the solid phase indicating significant accumulation in the biosolids. High rates of transformation for ZnO and Ag NPs resulted in ~ 97% transformation of the NPs that enter the plant despite differences in transformation rate in aerobic versus anaerobic environments. Due to high insolubility and negligible redox transformation, the only process predicted to impact TiO_2 NP fate and transport in WWTPs was distribution between the solid and

liquid phases. Predicted concentrations in the present study were in good agreement with previous literature values overall. However, none of the past work included and quantified transformation byproducts, which were shown to be critically important species in this study. In addition, this work provides justification for the use of black box relative to compartmentalized models. No significant advantage was obtained through discretization overall due to high distribution of NPs. However, this effort does identify the importance of accounting for transformations of NPs, which can aid in future research prioritization.

4.2 Introduction

The unique properties associated with novel nanoparticles (NPs) are exploited to improve and enrich many common manufactured goods. In addition to the benefits derived from these NPs, there is also concern about the potential risks of NPs when released into the environment. There is a need for tools that can effectively and efficiently provide accurate estimates of the environmental exposure potential of NPs already in commerce (Gottschalk & Nowack 2011, Nowack et al. 2012). Multi-media modeling methods for conventional compounds typically rely on physical chemical characterization of the compounds of interest and their environmental interactions (Mackay et al. 1996, Wania et al. 1998). However, the physicochemical properties of NPs that may be predictive of environmental exposure and resulting hazards have not been

elucidated and the fate predictors used to assess exposure of conventional compounds may be inappropriate (Auffan et al., 2009).

In addition, methods for estimating exposure that explicitly consider the unique properties of NPs and their effects on transport and toxicity are limited at best (Wiesner et al. 2009, Arvidsson et al. 2011, Hendren et al. 2013). Evaluation of NP exposure must consider how the properties of NP may be transformed as they transit through various environmental conditions. A lack of knowledge regarding the relationships between NP properties, exposure, and toxicological endpoints renders most (if not all) currently available models incapable of providing reliable estimates of exposure (Grieger et al., 2010). As an alternative, NP-specific functional assays, designed to allow laboratory predictions of large-scale system behavior, can help to address these shortcomings. While such functional assays cannot fully capture all environmental complexities, information can be gleaned to improve our limited understanding of NP exposure in relevant environmental scenarios under conditions of considerable uncertainty (Wiesner et al. 2009). Indeed, a number of researchers have incorporated these methods into their models, unfortunately, the ability to accurately predict environmental concentrations is still severely hindered by the numerous assumptions and sources of uncertainty from data gaps (Gottschalk et al., 2010).

Monte Carlo methods provide one means of capturing uncertainty in parameter estimation when performing simulations (Gilks et al. 1996). There is considerable

uncertainty regarding rates of aggregation, deposition, transformation and distribution of NPs in the environment. There is additional uncertainty regarding the effects of surface coatings on transport and toxicity, transformations, and processes impacting NP persistence could greatly improve the field (Lowry and Casman 2009). Monte Carlo parameter description to attempt to account for inherent error provides the best means of NP modeling due to these expansive uncertainties.

The current effort builds on a modeling effort in which Monte Carlo methods were applied to a simple model for aerobic wastewater treatment (Hendren et al., 2013) and nanoparticle removal in secondary clarifiers was estimated from experimentally-determined distributions of Ag NPs between the solid and the liquid phases. We expand on the previous study by incorporating experimental data from functional assays in environmentally relevant media into a WWTP model that considers both aerobic and anaerobic treatment and redox transformations of NPs that may occur during treatment. Values of parameters were determined in part from experiments conducted with primary and secondary wastewater to assess distribution between the solid and liquid phases of sludge. Rate constants for the pertinent redox reactions were obtained from laboratory studies in aerobic and anaerobic conditions.

4.3 Methods

4.3.1 Model Formulation

The WWTP model consists of a series of connected uniform compartments corresponding to the initial sewer system, primary and secondary clarification, in addition to activated sludge and anaerobic digestion (Figure 13). NP transformations may occur in all compartments, while separation (distribution between supernatant and sludge) is followed only in the primary and secondary clarifiers.

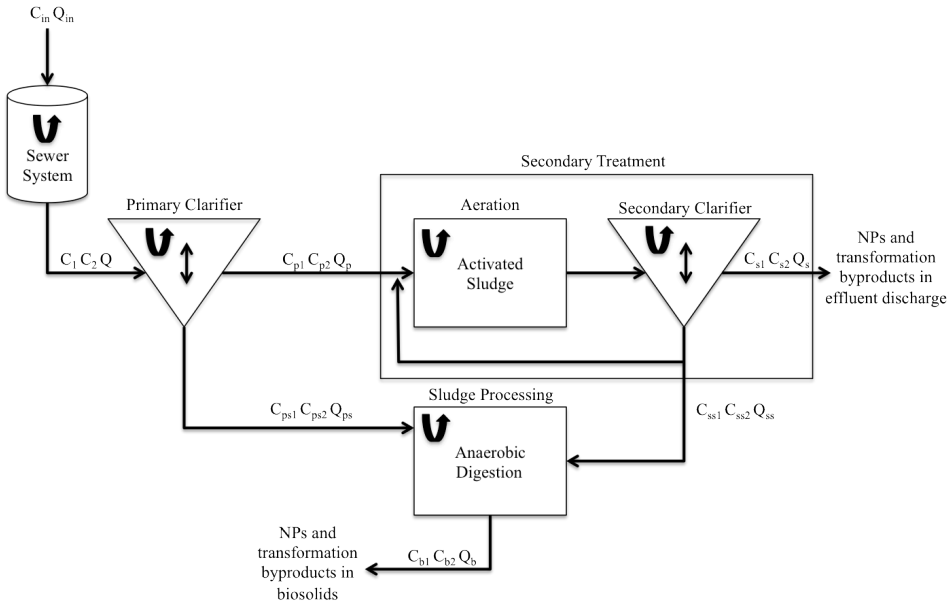

Figure 13. Conceptual model of the waste stream from the sewer system into the compartments of a wastewater treatment plant (WWTP).

Redox transformations may occur within the sewer system due to interactions with bacteria and other constituents. Deposition to biofilms lining the sewers is ignored as it has been shown that in the case of Ag NPs such deposition is likely negligible

(Kaegi et al. 2013). While there is also likely to be considerable spatial variation in transit through the sewer system, data are lacking and the sewers are simply described as single mixed compartment in which anaerobic transformations dominate. Assuming that the initial NP is transformed anaerobically, the mass balance on NPs (subscript 1) and a single by-product (subscript 2) can be written as:

Equation 4.1

$$V\frac{dC_1}{dt} = Q_{in}C_{in} - QC_1 - k_{t-anaerobic}C_1V$$

Equation 4.2

$$V\frac{dC_2}{dt} = -QC_2 + k_{t-anaerobic}C_1V$$

where model parameters are as described in Appendix C1. From the sewer system, all of the wastewater enters the treatment plant in the primary clarifier where settleable solids are removed. Equations 4.3 through 4.6 describe the change in NP concentration within this compartment.

Equation 4.3

$$V\frac{dC_{p1}}{dt} = QC_1 - Q_pC_{p1} - Q_{ps}C_{ps1} - k_{t-aerobic}C_{p1}V$$

Equation 4.4

$$V\frac{dC_{p2}}{dt} = QC_2 - Q_pC_{p2} - Q_{ps}C_{ps2} + k_{t-aerobic}C_{p1}V$$

Equation 4.5

$$V\frac{dC_{ps1}}{dt} = QC_1 - Q_pC_{p1} - Q_{ps}C_{ps1} - k_{t-aerobic}C_{ps1}V$$

Equation 4.6

$$V\frac{dC_{ps2}}{dt} = QC_2 - Q_pC_{p2} - Q_{ps}C_{ps2} + k_{t-aerobic}C_{ps1}V$$

From primary settling, the wastewater stream moves through secondary treatment, which incorporates both activated sludge treatment and secondary settling. Aerobic transformation and solids removal are assumed to be important in this compartment as described by Equations 4.7 and 4.10:

Equation 4.7

$$V\frac{dC_{s1}}{dt} = Q_pC_{p1} - Q_sC_{s1} - Q_{ss}C_{ss1} - k_{t-aerobic}C_{s1}V$$

Equation 4.8

$$V\frac{dC_{s2}}{dt} = Q_pC_{p2} - Q_sC_{s2} - Q_{ss}C_{ss2} + k_{t-aerobic}C_{s1}V$$

Equation 4.9

$$V\frac{dC_{ss1}}{dt} = Q_pC_{p1} - Q_sC_{s1} - Q_{ss}C_{ss1} - k_{t-aerobic}C_{ss1}V$$

Equation 4.10

$$V\frac{dC_{ss2}}{dt} = Q_pC_{p2} - Q_sC_{s2} - Q_{ss}C_{ss2} + k_{t-aerobic}C_{ss1}V$$

The final WWTP compartment considered in this model is anaerobic digestion where only transformation is assumed to be important. Equations 4.11 and 4.12 describe the change in NP concentration as a function of time in the digester.

Equation 4.11

$$V\frac{dC_{b1}}{dt} = Q_{ps}C_{ps1} + Q_{ss}C_{ss1} - Q_bC_{b1} - k_{t-anaerobic}C_{b1}V$$

Equation 4.12

$$V\frac{dC_{b2}}{dt} = Q_{ps}C_{ps2} + Q_{ss}Cs_{s2} - Q_bC_{b2} + k_{t-anaerobic}C_{b1}V$$

Steady state solutions to the aforementioned differential equations were solved using R, an open source modeling software package (R Development Core Team 2008). C_1 and C_2 represent the NP and transformation byproduct concentrations, respectively, exiting the sewer system and therefore serving as inputs to the WWTP. C_{in} values for the NPs released from the product life cycle to the waste stream were obtained from literature analysis of market studies concerning NP production and use patterns (Keller et al., 2013).

Transformations in primary settling were assumed to be aerobic with the possibility of removal of both the initial NPs and byproducts. C_{p1} and C_{p2} represent the concentrations of the native NP and transformation byproduct that remain in the liquid phase and are transported to secondary treatment, while C_{ps1} and C_{ps2} describe the concentrations of the native NP and transformation byproduct that distribute to the solid phase and are transported directly to anaerobic solids digestion. Similarly, C_{s1} and C_{s2} represent the concentrations of the NP and transformation by product released as effluent from the WWTP, likely discharged directly into surface water. C_{ss1} and C_{ss2}

indicate the concentrations of the NP and byproduct that associate with the solids and are transported to digestion.

Sludge removed from the clarifiers is routed to anaerobic digestion where anaerobic conditions allow for further transformations of NPs. All NPs entering the digester are assumed to exit with the biosolids produced either as the native NP (C_{b1}) and the transformation byproduct (C_{b2}) that may then be reused as fertilizers for agricultural lands or disposed of in landfills or by incineration (Metcalf and Eddy 2003).

The parameters for the model are listed in Appendix C1 to determine environmentally relevant estimates of the effluent and biosolids concentrations of PVP functionalized Ag, GA functionalized Ag, TiO_2, and ZnO NPs. WWTP parameters identified in Appendix C1 were gathered from Metcalf & Eddy (2003) and their associated distributions were taken from Hendren et al. (2013). The outputs of this Monte Carlo model are sensitive to the input distribution chosen to describe the simulation variables. Populations and additive processes were represented by normal distributions while physicochemical processes like distribution and transformation were represented by lognormal distributions. Finally those parameters described by a range with a likely value used a triangle distribution and the parameters where only a range was available were represented in the model by a uniform distribution (Lipton et al., 1995). For the model, probabilistic variables were sampled 10,000 times (Hendren et al., 2013).

4.3.2 Nanoparticles

The metal and metal oxide NPs investigated in this work were chosen due to their prevalence in consumer products and technologies (Blaser et al. 2008) and to their different physicochemical properties in aqueous media. The Ag, ZnO, and TiO_2 NPs employed were outlined in the Transatlantic Initiative for Nanotechnology and the Environment (TINE) to be critical materials to study further. The nano-Ag particles used were all synthesized in-house at CEINT (the Center for the Environmental Implication of Nanotechnology, Duke University, Durham, NC) and differed in size and surface functionalization. The ZnO NPs (Nanosun P99/30) were donated by Micronisers (Dandenong, Australia) and the TiO_2 NPs were purchased from Evonik Industries (Essen, Germany), neither possessed surface macromolecule functionalization. The dispersions were all made in nanopure water with an average pH of 5.6. NP suspensions were prepared on the day of experimentation from stocks and used immediately to avoid problems with dissolution or other particle changes.

4.3.3 Estimation of the Input Sources

Previous research indicated that exposure models are highly sensitive to the uncertainty associated with production and release to waste stream estimate of NPs (Hendren et al., 2011). A number of studies have estimated the production of NPs on global and national scales. Table 5 indicates some of the predicted values for NP production as a function of time. From Table 5, it can be seen that there is significant

variability in the estimates. The modeling effort presented here is an extension from the work completed by Hendren et al., (2011), and as such utilizes global estimates for NP production relative to US based predictions. In the case of Ag NPs, these global estimates by Keller et al., (2013) result in an order of magnitude difference in the influent concentration relative to estimates published for the US by Hendren et al., (2011). Hendren et al., 2011 predicted influent concentrations of Ag into WWTPs on the order of 0.00013 mg/L whereas the global estimates used indicate influent concentrations around 0.0012 mg/L. This difference was not observed, however when comparing influent estimates for TiO_2 NPs. Hendren et al., 2011 predicted concentrations of 0.26 mg/L while Keller et al., 2013 estimated about 0.29 mg/L of influent TiO_2 NPs. This indicates the inherent variability in estimating the production and waste stream release of NPs.

Table 5. Global and national production estimates for Ag, ZnO, and TiO_2 NPs.

NP	Global Production (tons/yr) Keller et al., 2012	Global Production Median (tons/yr) Piccinno et al., 2012	US Production (tons/yr) Hendren et al., 2011
Ag	452	55	2.8 - 20
ZnO	34,000	550	
TiO_2	88,000	3,000	7,800 – 38,000

Keller et al. (2013) employed market analysis and life-cycle considerations to explore the most common uses of a variety of NPs and the likely release from those applications to the environment. This estimate was obtained by assuming maximum production and release scenarios. A variability of 10% was applied in the model due to

lack of uncertainty on the estimate. Table 6 identifies the range of production volumes for the NPs to be evaluated in the present study and the amount predicted to be released to WWTPs based on the predominant applications into which the NPs are incorporated. The majority of ZnO NPs are incorporated in the medical field, cosmetics, electronics and optics, and coatings, paints, and pigments. The largest rates of emission during the use phase were observed to be from cosmetics, which are directly exposed to the waste stream (Keller et al., 2013). TiO_2 NPs were largely used in cosmetics and coatings, paints, and pigments; all being applications that can lead to WW release. Finally, Ag NPs were most commonly included in textiles, cosmetics, coatings, paints, and pigment, and medical applications, also allowing for NP introduction to the waste stream (Keller et al., 2013). The annual global production in Table 6 was converted to a volumetric loading by determining the global volume of wastewater treated. This conversion required the assumption that those places treating their wastewater were likely the only areas with access and readily using nano-enabled products. Recent work completed by Sato et al. (2013) indicated the annual volume of wastewater treated by North America, Latin America, Europe, Russia, the Middle East, Africa, Oceania, and Asia. The conclusion was approximately 181.3 km^3yr^{-1} of generated wastewater was properly treated in WWTPs. This volume of wastewater was used to obtain WWTP influent NP concentrations in mgL^{-1}.

Table 6. Global Production and loading on WWTPs of Ag, ZnO, and TiO_2 NPs.

NP	Global Production (tons/yr)	Global WWTP Loading (tons/yr)	Fraction to WWTP (unitless)	Reference
Ag	452	200	0.44	Keller et al., 2013
ZnO	34,000	11,700	0.34	
TiO_2	88,000	47,700	0.54	

4.3.4 Experimental Determination of the Distribution Coefficients

Time-dependent distribution coefficients (γ) were measured in batch experiments. Primary and secondary wastewater sludge was sampled from the wastewater influent and activated sludge basin of the North Durham County Water Reclamation Facility in Durham, NC. This facility was designed to treat approximately 20 MGD and utilizes biological nutrient removal to decrease phosphorous, biological oxygen demand (BOD), and ammonia. The average pH of the wastewater was measured to be 7.6 with a chemical oxygen demand that ranged between 350 and 550 mgL^{-1} (as measured by HACH test kits). The primary sludge had an average total suspended solids (TSS) content of 380 mgL^{-1} while the secondary sludge had a TSS of 3.81 gL^{-1}. Sludge was stored at 4 °C for less than one week prior to experimental completion (Hendren et al., 2013) and experiments were conducted at room temperature (~ 20 °C). In the batch tests, NPs were added at concentrations of 10 mgL^{-1} to the sludge suspension and mixing ensued for a programmed period of 1 hour after which the suspension was gravity separated for approximately 30 minutes. The supernatant was

decanted and acidified with 2% HNO_3 prior to analysis on the ICP-OES. The solid concentration was determined via mass balance for most samples and confirmed by solid digestion (US EPA 1994) on a subset of samples. This parameter was used to describe the affinity of the NP for association with the solid versus the liquid phase of sludge. The coefficient was observed to reach a maximum after 10 minutes of mixing and therefore the γ value determined at 1 hour was used to represent the distribution in the primary and secondary clarifiers where the hydraulic residence time is approximately 2 hours and 5.5 hours, respectively (Dissertation Chapter 2).

4.4 Results and Discussion

4.4.1 Estimation of the transformation rates

In this work, redox transformations of Ag and ZnO were assumed to be first order. The transformation magnitude of Ag NPs in aerobic and anaerobic systems was taken from work completed by Kaegi et al. (2011) and ZnO transformations were obtained from the study by Lombi et al. (2012). It had to be assumed here that NP size would negligibly impact the overall transformation rate for the Ag NPs studied because that data is currently unavailable. The transformation of Ag NPs into Ag_2S depends not only on the rate of sulfidation but also the rate of dissolution. It would, therefore be expected that size would play a role in the overall transformation of Ag NPs because of the observed differences in dissolution as a function of size (Ma et al., 2012). Thus, in this work, the overall transformation from the original NP was determined and utilized,

relative to the individual transformations that contribute to the overall. These determinations were obtained from literature batch experiments in aerated and non-aerated wastewater as illustrated in Table 7. While TiO_2 NPs are photocatalytic, they are highly insoluble and do not readily undergo redox transformations. Therefore it was assumed that the transformation rate coefficients in WWTPs for TiO_2 NPs would be negligible. Literature indicated a magnitude of transformation as a function of time, from which a rate coefficient was determined using the following method (Dale et al. 2013):

Equation 4.21

$$[NP] = [NP]_{initial} e^{-kt}$$

Equation 4.22

$$k = \frac{-ln\left(\frac{[NP]}{[NP]_{initial}}\right)}{t}$$

Table 7. Experimental results from literature used to determine the transformation rate coefficients for Ag and ZnO NPs.

NP	Aerobic Reaction Time	% NP Remaining	Anaerobic Reaction Time	% NP Remaining	Reference
Ag	2 hours	79	2 hours	10	Kaegi et al., 2011
ZnO	5.5 hours	0.1	3 hours	12	Lombi et al., 2012

The experimental data used indicated that the aerobic transformation of ZnO was higher than the anaerobic transformation, while the opposite was true for Ag NPs. Both aerobic and anaerobic rates of transformation for ZnO and Ag NPs were very high indicating transformation was kinetically favorable (Table 8). The key assumption

necessary due to limitations in data availability was that a single aerobic and anaerobic rate coefficient could describe any WWTP compartment based on whether the environment was typically aerobic or anaerobic. For example, the anaerobic rate coefficient was used to describe NP transformations in both the sewer system and anaerobic digestion, however it is possible that this is not realistic and that the kinetics of transformation differ depending on the WWTP compartment of residence. In addition, due to lacking or unclear data this work assumes that the transformations experienced by Ag and ZnO NPs in WWTPs are irreversible (Lowry et al., 2012). The high magnitude of transformation to a sulfidized phase observed in previous reports following exposure of ZnO and Ag NPs to wastewater justifies this assumption, although further research on this topic would further improve the accuracy of this simulation (Kaegi et al., 2011, Lombi et al., 2012). Error on these calculated rates of transformation was assumed to be the error on the XANES measurement of 10%.

Table 8. Estimated rates of aerobic and anaerobic transformation of Ag, ZnO and TiO_2 NPs.

NP	$k_{aerobic}$ (hr^{-1})	Standard Deviation	$k_{anaerobic}$ (hr^{-1})	Standard Deviation
Ag	0.118	10%	1.152	10%
ZnO	1.67	10%	0.707	10%
TiO_2	0	0	0	0

4.4.2 Distribution Coefficients

The experimentally determined γ values for the six important NPs are presented in Table 9. The distribution coefficient was determined by normalizing the solid associated NPs by the mass of solids and then dividing by the concentration of the NP remaining in the supernatant. In this way, the higher the γ value, the greater affinity of the NP for association with the solid phase. Primary γ values were normalized by a smaller mass of solids (due to lower TSS in primary wastewater) and therefore, corresponded to lower removals overall, on the order of 50%, despite having higher values. In agreement with previous research, the secondary γ values corresponded to high association of all NPs with the solid phase (> 75% removal in activated sludge) (Kiser et al., 2009, Hendren et al., 2013). These results indicated more efficient removal of NPs by sludge with higher TSS as is expected in secondary treatment relative to primary clarification. For the NPs studied, the primary γ values were all on the same order, which suggests that differential affinity for the solids was not as important in the primary clarifier. In secondary treatment, γ values differed more. It was observed that TiO_2 NPs had the highest affinity for association with the solids followed by ZnO, PVP-functionalized Ag, and GA-functionalized Ag.

Table 9. Experimentally determined primary and secondary distribution coefficients for Ag, ZnO, and TiO_2 NPs.

NP	Primary γ (Lmg^{-1})	Standard Deviation	Secondary γ (Lmg^{-1})	Standard Deviation
PVP – Ag 40 nm	0.0036	0.00081	0.0040	0.00086
PVP – Ag 8 nm	0.0026	0.00014	0.0035	0.00018
GA – Ag 25 nm	0.0014	0.00027	0.00064	0.00003
GA – Ag 6 nm	0.0011	0.00091	0.00058	0.00005
ZnO	0.0051	0.00028	0.0058	0.00010
TiO_2	0.0088	0.00017	0.0091	0.00011

4.4.3 Exposure Concentrations

The modeled exposure concentrations of the NPs and their transformation byproducts in wastewater effluent and biosolids can be found in Table 10. For the metal and metal-oxide NPs studied, > 95 % of the material was predicted to associate with the biosolids (95% for Ag NPs, 99% for ZnO NPs, and 99% for TiO_2 NPs). TiO_2 NPs do not undergo transformation in WWTPs and therefore there was no generation of transformation byproducts. In contrast, both Ag NPs and ZnO NPs can undergo sulfidation reactions (Lombi et al., 2012, Ma et al., 2011, Kaegi et al., 2011). Ag NPs, regardless of size and surface functionalization was predicted to result in 97% transformation within WWTPs. Previous work has identified the transformation of Ag NPs to be highly kinetically favorable and an oxysulfidation reaction into Ag_2S species in WWTPs (Kaegi et al., 2011). Similar concentrations of NPs and transformed products

in the effluent and biosolids for different Ag species indicate that minor differences in distribution do not greatly impact the fate and transport of the material, rather the high overall removal and rate of transformation is the more critical factor dictating exposure. Due to limited data however, the size dependence of this overall rate of transformation, which incorporates sulfidation and dissolution, cannot be completely accounted for. Further insight into the impact of size on the overall transformation of Ag would greatly improve the accuracy of the model predictions.

ZnO NPs were also predicted to undergo significant transformation with approximately 97% of influent NPs released from the plant in the transformed state. Previous research indicated that in aerobic conditions, the transformation of ZnO NPs was extremely fast and that the byproducts formed were a mixture of ZnS, $Zn_3(PO_4)_2$, and Zn associated with Fe oxy/hydroxides (Ma et al., submitted). In anaerobic digestion, the transformation of ZnO NPs was also significant but the majority of the transformation byproduct exists in the reduced ZnS state, which will be released from the plant in biosolids (Lombi et al., 2012). Following biosolid drying and composting at the plant, biosolids can be applied to agricultural lands where ZnO NPs speciation can be altered further (Lombi et al., 2012). It has been observed in composting that the ZnS byproducts, once exposed to the now aerobic conditions during drying, transform into mostly $Zn_3(PO_4)_2$ and Zn species associated with Fe oxy/hydroxides.

Previous modeling efforts have also provided estimates for NP concentrations leaving WWTPs (Hendren et al., 2013, Gottschalk et al., 2009, Blaser et al., 2005, Boxall, et al., 2007, Westerhoff et al., 2011). All of these studies determine the concentrations of NPs by either accounting for high distribution to the solid phase or by measuring influent and effluent concentrations. With respect to Ag NPs, estimates of WWTP released concentrations in this study were of the same order (1-5 mg/kg) as previously reported relative to the predicted influent concentrations (Gottschalk et al., 2009). Differences in final concentrations of NPs in biosolids and effluent stemmed mostly from differences in the predicted influent concentrations, which are highly uncertain and variable (Hendren et al., 2011). None of these former efforts, however, explored the concentrations of NPs and transformation byproducts. The results presented here for ZnO and Ag NPs illustrate the importance of transformation and also provide simulated concentrations of ZnS and Ag_2S leaving WWTPs. With respect to TiO_2 NPs, Westerhoff et al. (2011) measured influent and effluent concentrations of TiO_2 at a municipal WWTP. Again the predicted effluent and biosolids concentrations are on the same order indicating that these concentrations are environmentally relevant.

This work indicates the critical importance of accounting for transformations of NPs in the environment, which can greatly impact fate and transport. This study can also help prioritize future research efforts by identifying those major species that will be released from WWTPs in either effluent or biosolids such that the correct species

exposure can be investigated. Further improvement on input calculations will be important for providing the most environmentally relevant exposure model for NPs.

Table 10. Predicted exposure concentrations in effluent and biosolids for NPs of interest.

NP	Type	Influent Concentration (mgL^{-1})	Effluent Concentration (mgL^{-1})	Standard Deviation	Biosolids Concentration (mg NP g^{-1} solids)	Standard Deviation
PVP – Ag 40 nm	Nanoparticle	0.0012 ± 0.00016	1.69E-6	8.60E-7	2.87E-5	1.76E-5
	Transformation byproduct		4.54E-6	4.45E-6	0.0010	0.0002
PVP – Ag 8 nm	Nanoparticle		1.82E-6	8.64E-7	2.87E-5	1.71E-5
	Transformation byproduct		4.67E-6	4.41E-6	0.0010	0.0003
GA – Ag 25 nm	Nanoparticle		1.45E-6	8.12E-7	2.87E-5	1.71E-5
	Transformation byproduct		4.31E-6	4.56E-6	0.0010	0.0002
GA – Ag 6 nm	Nanoparticle		1.45E-6	8.15E-7	2.87E-5	1.71E-5
	Transformation byproduct		4.31E-6	4.56E-6	0.0010	0.0002
ZnO	Nanoparticle	0.072 ± 0.0103	5.09E-5	1.15E-5	0.0015	0.0007
	Transformation byproduct		0.0003	0.0001	0.0592	0.0144
TiO_2	Nanoparticle	0.293 ± 0.0423	0.0012	0.0006	0.2478	0.0561
	Transformation byproduct		0	0	0	0

4.4.4 Model Sensitivity to Input Parameters

The sensitivity of the model to the parameterization was investigated by varying the parameters within an expected range and subsequently observing the impact on final effluent and biosolid concentrations. As expected, the influent concentration of NPs released during the NP life cycle to the waste stream greatly influenced the ultimate concentrations of NPs in effluent and biosolids in agreement with previous sensitivity analyses on similar models (Hendren et al., 2011). Variations of two orders of magnitude in the distribution coefficient was not observed to impact the final NP

concentrations likely due to the high overall rates of removal. In addition, the total suspended solids (TSS) concentrations did not have an impact. The transformation rate coefficient was observed to impart a minor influence in final concentrations. Increasing this coefficient resulted in even smaller concentrations of the native NP and slightly higher concentrations of the transformation byproduct (for example 99% transformation overall for ZnO NPs). In contrast, decreasing the transformation rate coefficient by an order of magnitude resulted in 88% transformation overall relative to 97% for ZnO NPs. In total, high amounts of transformation were still observed. The final parameter investigated was residence time in the WWTP compartments. While this parameter could greatly impact the model outputs by order of magnitude variations, those variations would be unreasonable estimates of reality. Therefore, within realistic scenarios for WWTP residence times, the impact was minimal on the NP and transformation byproduct concentrations in the effluent and biosolids.

4.5 Conclusions

The three metal and metal-oxide NPs with different physicochemical behavior will accumulate extensively in the biosolids. Negligible concentrations of Ag NPs will be measured in the effluent of WWTPs due to high association with the solid phase where the majority will be transformed to Ag_2S (Ma et al., 2011). Similarly, ZnO and TiO_2 NPs will have a much higher concentrations in the solid phase. Due to higher influent concentrations to the WWTP of ZnO and TiO_2 NPs, a more significant fraction

will be measureable in the effluent. ZnO NPs will preferentially transform, likely to sulfide species before release from the plant in biosolids while TiO_2 NPs will remain in their native state (Lombi et al., 2012).

This work introduces an environmentally relevant, discretized Monte Carlo model that can predict concentrations of NPs and transformation byproducts released from WWTPs. In comparison to previous models where WWTPs were considered black box models, discretization does significantly enhance the overall model predictions. Thus, justification for the use of simplified modeling frameworks has been shown. Still this work highlights the necessity of accounting for both distribution and transformation of NPs in WWTPs. In addition, this study introduced functional assays that can provide critical information on the important WWTP processes that impact fate and transport. These functional assays in environmental matrices allow for experimental parameterization of the model, which improves the accuracy of simulations. Further research into the magnitude of NP production that can lead to release to the waste stream along with further study into environmental or NP characteristics that can impact distribution and transformation will continue to improve the relevance of these simulations. Finally, application of WWTP modeling methods, black box or discretized to other NPs can help to provide the same information concerning exposure concentrations.

5. Heteroaggregation, Transformation, and Fate of CeO_2 Nanoparticles (NPs) in Wastewater Treatment.

5.1 Abstract

Wastewater Treatment Plants (WWTPs) are considered a key pathway by which engineered nanomaterials (ENMs) may enter the environment following release from ENM-enabled products. ENMs present as nanoparticles (NPs) have already been identified by researchers in the head works of WWTPs, however limited information is available concerning NP transformation and removal within WWTPs.

This work considers the transformation of CeO_2 NPs in water treatment in a two step process of heteroaggregation with bacteria followed by the subsequent reduction of Ce(IV) to Ce(III). Measurements of NP association with solids in activated sludge were combined with estimates of oxidation/reduction rate constants for CeO_2 NPs obtained from bench scale studies in Monte Carlo simulations to estimate the concentrations and speciation of Ce in WWTP effluents and biosolids. Experiments indicated that the majority of the CeO_2 NPs will accumulate in biosolids where it will exist in a reduced Ce(III) phase. Surface functionalization was observed to impact both the distribution coefficient and the rates of transformation. The relative affinity of CeO_2 NPs for bacterial suspensions in the activated sludge appears to explain differences in the observed rates of Ce reduction for the two types of CeO_2 NPs studied. Still, the modeling results predicted that overall approximately 95% of CeO_2 NPs in the waste stream would preferentially associate with the solid phase where approximately 50% of the Ce would

be transformed to a Ce(III) phase, regardless of differences in surface composition. This phase would be predicted to be Ce_2S_3 in the final anaerobically digested solids.

5.2 Introduction

As use of engineered nanomaterials (ENMs) in commercial products continues to grow, the potential for environmental exposure to ENMs also increases (Wiesner et al., 2009). Unfortunately, limited information and predictive tools are available to evaluate the potential transport and effects of nanoparticles (NPs) in aquatic and terrestrial environments (Lowry and Casman 2009).

One important environmental exposure pathway by which some NPs may be released to the environment involves ENMs shed from commercial products that make their way into Wastewater Treatment Plants (WWTPs) (Blaser et al., 2008). The literature already includes several reports of NPs in the influents to WWTPs (e.g., Benn and Westerhoff, 2008, Westerhoff et al. 2011, Kim, et al., 2012). Various modeling approaches have been used to predict NP concentrations entering WWTPs as well as their removal during treatment. For example, Mueller and Nowack (2008) employed the principles of material flow analysis to define predicted environmental concentrations (PEC) for Ag NPs, TiO_2 NPs, and Carbon Nanotubes (CNTs). They modeled the amount of ENMs entering the environment following product use based on estimates of ENM production that was then routed by assumed fractions into WWTPs and waste incineration plants to arrive at concentrations in air, water and soil. Similarly,

Gottschalk et al., (2009, 2010, 2011) determined PEC values for Ag, TiO_2, and ZnO NPs using probabilistic material flow methods coupled with geographic and temporal data to arrive at higher resolution estimates of ENM release. Hendren et al., (2013) combined laboratory data on silver nanoparticle separation in wastewater with Monte Carlo simulations of wastewater treatment to provide probabilistic estimates of NPs in WWTP effluents and biosolids. Several previous studies have considered the role of size and surface structure on the behavior of metal and metal-oxide NPs in WWTPs (Kaegi et al., 2011 and 2013, Gomez-Rivera et al., 2012, Ma et al., 2013, Levard et al., 2012, Lombi et al., 2012). However, predictive methods for determining the fate of NPs during wastewater treatment remain in development with a particular lack of information on important transformations that may occur during treatment and the relative abundance of NP species in WWTP effluents and biosolids.

In this work, we combine two key measurements of ENM properties, describing the kinetics of both the phase distribution and redox transformations, in simulations to predict the fate of CeO_2 NPs during wastewater treatment. CeO_2 NPs may enter waste streams in significant amounts when used in coating, polishing and paint applications (Keller et al., 2013). The model incorporates probabilistic inputs to account for the inherent uncertainty due to limitations in available data and error encountered in experimental measurements and differences in environmental conditions.

5.3 Methods

5.3.1 Model Formulation

The Monte Carlo modeling effort used in this work builds on a previously developed model (Hendren et al., 2013) for aerobic wastewater treatment and nanoparticle removal in secondary clarifiers. Described in Chapter 4, the model presented by Hendren et al., (2013) was expanded to include simple descriptions of both aerobic and anaerobic treatment and redox transformations of NPs that may occur in the sewer system, primary treatment, secondary treatment, and anaerobic digestion. In the sewer system, the only critical process impacting NP fate was assumed to be transformation. Previous work with Ag NPs indicated that the flow in a sewer was enough to prevent deposition of the NPs onto the walls or any biofilms that typically form (Kaegi et al. 2013). Heteroaggregation and transformation were both considered in primary and secondary treatment while only further transformation was considered in digestion. The concentration of the native NPs in addition to the concentration of the transformation byproduct was predictively estimated in effluent and biosolids.

Model parameterization for heteroaggregation was accomplished using a functional assay for quantifying NP affinity for the surface of the background particles found in these systems. Nanoparticle transformation by bacteria is described as sequential processes of transport, attachment and reaction. Transport can be explained by the collision rate kernel, β, which describes nanoparticle transport to the vicinity of a

non-nano background particle (such as a bacterium in a suspension of activated sludge). Attachment reflects the relative affinity, α_{NB} of nanoparticles of concentration, n, for background particles of concentration, B. Under the assumption that CeO_2 NPs must first attach to bacteria to be reduced, the total rate constant for an observed apparent rate of the reduction reaction, k_T is related to the rates of heteroaggregation and the intrinsic reaction rate constant, k_{red} as:

Equation 5.1

$$\frac{1}{k_T} = \frac{1}{k_{red}} + \frac{1}{\alpha_{NB}\beta nB}$$

Rearranging, an expression (Equation 5.2) is obtained for the relationship between the apparent overall reaction rate constant and the intrinsic reaction rate constant as modified by a potentially rate-limiting step of heteroaggregation.

Equation 5.2

$$k_T = \frac{k_{red}\alpha_{NB}\beta nB}{k_{red} + \alpha_{NB}\beta nB}$$

Thus, by Equation 5.2 when heteroaggregation is not limiting, ($k_{red} << \alpha_{NB}\beta nB$), $k_T \cong k_{red}$. Conversely, when heteroaggregation is limiting, due for example to a small affinity between nanoparticles and bacteria, then $k_{red} \geq \alpha_{NB}\beta nB$ and the overall reaction rate constant, k_T, observed experimentally is predicted to be proportional to α_{NB}.

The aerobic transformation of CeO_2 nanoparticles suggested a reversible reaction due to the observation of a steady state amount of reduction for both pristine and citrate-functionalized NPs. For this to be accurately modeled, both the rate of reduction

and the rate of reoxidation must be included in the model equations where transformation is occurring under aerobic conditions. Equations 5.3 through 5.6 describe the mass balance in the primary clarifier on the liquid phase NP and NP transformation product along with the solid phase NP and NP transformation product, respectively.

Mass balances on the initial and reduced Ce species in primary clarification for CeO_2 are therefore written as:

Equation 5.3

$$V\frac{dC_{p1}}{dt} = QC_1 - Q_pC_{p1} - Q_{ps}C_{ps1} - k_{red}C_{p1}V + k_{ox}C_{p2}V$$

Equation 5.4

$$V\frac{dC_{p2}}{dt} = QC_2 - Q_pC_{p2} - Q_{ps}C_{ps2} + k_{red}C_{p1}V - k_{ox}C_{p2}V$$

Equation 5.5

$$V\frac{dC_{ps1}}{dt} = QC_1 - Q_pC_{p1} - Q_{ps}C_{ps1} - k_{red}C_{ps1}V + k_{ox}C_{ps2}V$$

Equation 5.6

$$V\frac{dC_{ps2}}{dt} = QC_2 - Q_pC_{p2} - Q_{ps}C_{ps2} + k_{red}C_{ps1}V - k_{ox}C_{ps2}V$$

The concentration of metals from nanomaterials in the sludge (C_{ps1} and C_{ps2}) are related to the concentration in the suspended material (C_{p1} and C_{p2}) by the distribution coefficient γ such that

Equation 5.7

$$\gamma = \frac{\left(\frac{M_S}{M_B}\right)}{C_L}$$

Similarly to Equations 5.3 through 5.6, mass balance equations in secondary treatment for CeO_2 reversible aerobic reaction are presented in Equations 5.8 through 5.11.

Equation 5.8

$$V\frac{dC_{s1}}{dt} = Q_p C_{p1} - Q_s C_{s1} - Q_{ss} C_{ss1} - k_{red} C_{s1} V + k_{ox} C_{s2} V$$

Equation 5.9

$$V\frac{dC_{s2}}{dt} = Q_p C_{p2} - Q_s C_{s2} - Q_{ss} C_{ss2} + k_{red} C_{s1} V - k_{ox} C_{s2} V$$

Equation 5.10

$$V\frac{dC_{ss1}}{dt} = Q_p C_{p1} - Q_s C_{s1} - Q_{ss} C_{ss1} - k_{red} C_{ss1} V + k_{ox} C_{ss2} V$$

Equation 5.11

$$V\frac{dC_{ss2}}{dt} = Q_p C_{p2} - Q_s C_{s2} - Q_{ss} C_{ss2} + k_{red} C_{ss1} V - k_{ox} C_{ss2} V$$

These equations were solved for the case of steady state in the mathematical modeling software, R.

5.3.2 Nanoparticles

Pristine and citrate-functionalized CeO_2 NPs were chosen due to their occurrence in consumer products and technologies that have the potential for release to the waste stream (Blaser et al. 2008, Keller et al., 2013). Pristine CeO_2 NPs and citrate

functionalized CeO_2 (Nanobyk®) were commercially available. They were both colloidally stable in their commercialized stock suspension with average hydrodynamic diameters centered around 8 nm. Titrations of the suspensions were performed to determine the iso-electric point (IEP) of the CeO_2 NPs (Auffan et al., 2014). Between pH 4 and 10, the electrophoretic mobility of the functionalized NPs remained strongly negative, attributed to the dissociation of the protons of the citrate at pH 3.1 (pKa_1), 4.8 (pKa_2) and 6.4 (pKa_3) (Martell and Smith, 1977). For the pristine CeO_2 NPs an IEP close to a value of pH 7 was obtained (Auffan et al., 2014).

5.3.3 Production Quantities

Production volumes for CeO_2 NPs were estimated to determine the amount of NPs that could be potentially released to wastewater streams. Previous estimates of US (Hendren et al., 2011) and global (Keller et al., 2013) production of CeO_2 NPs were examined to obtain an upper bound on production. Global production quantities entering wastewater were converted to influent concentrations by assuming that only those countries that treat municipal wastewater have open access to nano-enabled products allowing for an estimate of the global volume of wastewater treated of 181.3 km^3/yr (Sato et al., 2013). The influent value predicted using this method was then compared to previous methods for predicting the concentration of CeO_2 NPs likely to enter WWTPs.

5.3.4 Distribution Coefficients

Time-dependent distribution coefficients (γ) were measured in 25 mL batch experiments as described previously (Dissertation Chapter 3). Briefly this method involves mixing NPs for a prescribed period with background particles in the form of either primary or secondary sludge and then allowing for settling of the particles from suspension. Measurements of the NPs remaining in suspension as a function of mixing time and the associated values of the distribution coefficient, γ, describing the ratio of NP concentrations in the supernatant and the settled material, were used to estimate the quantity $\alpha_{nB}\beta nB$ (Dissertation Chapter 3). The measurement at 1 hour corresponded to a maximum amount of distribution of the NP between the liquid and solid phase and was therefore used to represent distribution in the primary and secondary clarifiers.

5.3.5 Transformation Rate Constants

Redox transformation of CeO_2 NPs in wastewater was monitored by following the Cerium L_3-edge XANES spectra collected on the XAFS bending magnet beamline (11.1) at the Elettra-Trieste Synchrotron light source (Italy) using a Si(111) monochromator. Samples were prepared as described previously with CeO_2 NP addition of 0.4 mg Ce / 30 mg sludge to optimize the $\Delta\mu$ during XANES analysis and mixing times between 30 minutes and 1 day (Dissertation Chapter 2). The Ce(IV) references included the initial NPs, pristine and citrate-functionalized along with Ce(III) oxalate and a micron-sized (> 5 μm grain size) CeO_2 sample. The spectra presented were

the summation of 3 to 5 scans and the energy was calibrated using a macroscopic (> 5 μm grain size) CeO_2 reference compound. XANES spectra were all pre-edge subtracted and normalized in the same manner using IFEFFIT software (Ravel and Newville, 2005). Least-squares optimization of Linear Combination Fitting (LCF) was also performed using IFEFFIT. The precision of LCF is estimated to be ± 10%. LCF results indicating the amount of Ce(III) versus Ce(IV) were used to determine the overall transformation rate constants by plotting log transformed data versus time and assuming a simultaneous reverse oxidation reaction in activated sludge.

5.4 Results and Discussion

5.4.1 Input Source of CeO_2 NPs

The upper bound of global production of CeO_2 NPs was estimated by Keller et al., 2013 using market study analysis to total 10,000 tons annually with approximately 1,100 tons entering the waste stream based on maximum production and emission rate scenarios. This results in a fraction to wastewater of 0.11. This fraction is significantly less than other metal and metal oxide NPs including Ag, ZnO, and TiO_2 NPs with fractions of 0.44, 0.34, and 0.54 respectively as determined by the same method (Keller et al., 2013). This lower fraction to wastewater reflects the assumption that a greater portion of products using CeO_2 NPs will result in direct release to the environment during use or contain the NP in an immobilized form within products that will lead to greater disposal in landfills rather than being transported through WWTPs. The most

significant portion of CeO_2 NPs released to the waste stream was predicted to occur from applications involving coatings, pigments and paints (Keller et al., 2013). These assumption lead to a maximum estimated influent concentration of 0.0067 mgL^{-1} CeO_2 NPs taking into account the amount of treated wastewater globally (Sato et al, 2013). A variability of 10% was placed on the influent calculation to allow for uncertainty in the data when absolute error was unavailable.

Hendren et al., 2011 estimated that the US production of CeO_2 NPs ranged between 35 and 700 tons/year. In Monte Carlo simulations, the authors allowed the fraction of US produced CeO_2 NPs entering wastewater to vary between 0 and 0.65, leading to an estimated influent concentration of 0.0042 ± 0.0036 mgL^{-1} relative to the 0.0067 ± 0.00098 mgL^{-1} that was determined in this study. These concentrations are of the same order and provide confidence in these production estimates that were determined independently at different scales.

5.4.2 Experimentally Determined Distribution Coefficients

Separation of NPs during wastewater treatment and the surface affinity of NPs for the background suspensions they are in contact with, was evaluated by determining the distribution coefficient, γ, over time according to Equation 5.7, where M_S is the mass of the NP associated with the solid phase at the end of the mixing and settling period, M_B is the mass of the wastewater solids initially present, and C_L is the concentration of the NP that remains in the liquid phase following settling. Values of the distribution

coefficient at small mixing times were used to obtain estimates of the surface affinity coefficients (Dissertation Chapter 3). The surface affinity of the citrate functionalized CeO_2 NPs was found to be less than that of pristine CeO_2 NPs (Table 11).

It was observed that after 10 minutes of mixing the distribution stabilized (Dissertation Chapter 3) and therefore measurements obtained after 1 hour of mixing would be a reasonable representation of what occurs in primary and secondary clarifiers where residence times are about 2 hours and 5.5 hours, respectively. The measured γ values (Table 11) differed slightly between pristine and citrate-functionalized NPs in the batch experiment with the pristine sample associating to a higher degree with the solid phase. This phenomenon of higher affinity of pristine CeO_2 for the solid phase becomes increasingly distinct, with larger differences in measured γ values, as concentrations of added NPs increase in the experiment (Dissertation Chapter 3). The increased stability of the citrate-functionalized CeO_2 was likely the result of a negative surface charge on the surface of the particles at the near-neutral pH of wastewater imparted by a negative zeta potential in the same pH conditions (Dissertation Chapter 3). The trend toward more functionalized NPs exhibiting more stability and therefore remaining in the supernatant has also been noted by other researchers (Kiser et al., 2009, Hendren et al., 2013). These experimentally determined distribution coefficients were normalized by the concentration of the background solids present in the experiment, which is a smaller number for primary sludge relative to secondary sludge. The corresponding percent

removals are approximately 52% and 48% in primary sludge and 92% and 90% in secondary sludge for the pristine and citrate-functionalized CeO_2 NPs, respectively. Consistent with trends predicted for heteroaggregation, these results show that the mass of sludge impacts the overall percent removal as secondary sludge with a higher TSS leads to higher amounts of NP association with the solid phase.

It is important to note that the characteristics of wastewater vary with geographic location, climate and input sources. Monte Carlo methods allow for one means of capturing this variability, although the standard deviations used in these simulations were derived from measurements using a single source of wastewater.

Table 11. Primary and secondary distribution coefficients and attachment efficiencies for pristine and citrate functionalized CeO_2 NPs (10mgL^{-1} CeO2).

NP	Primary γ (Lmg^{-1})	Standard Deviation	Secondary γ (Lmg^{-1})	Standard Deviation	α_{NB} (Barton et al., 2014)
Pristine CeO_2	0.003	0.0012	0.006	0.0017	0.0064
Citrate - coated CeO_2	0.001	0.00043	0.003	0.00067	0.0023

5.4.3 Transformation Rate Constants

XANES was used to determine the aerobic and anaerobic rates of transformation presented in Table 13. XANES spectra at the Ce L_3-edge from the aerobic and anaerobic experiments are shown in Figures 14 and 15 respectively. XANES spectra of Ce(III) compounds present a single absorption jump or white line (~ 5724 eV) corresponding to the $2p_{3/2} \rightarrow 4f^1 5d$ electronic transition (Takahashi et al., 2002), while CeO_2 crystallites

exhibit a double white line (~ 5728 eV and ~ 5735 eV) corresponding to the final state $2p4f^{1}5d^{1}L$ and $2p4f^{0}5d^{2}$ of Ce(IV) respectively (Dexpert et al., 1987, Finkelstein et al., 1992). The spectra of CeO_2 NPs in the aerobic and anaerobic sludge indicated the increasing presence of a Ce(III) phase over time. The LCF results of the aerobic and anaerobic reductive transformation of CeO_2 NPs are provided in Table 12. In aerobic sludge, the presence of the Ce(III) phase was not obvious until after 1 hour of incubation. The amount of reduction then continued until 1 day, at which point it was observed to reach a maximum amount of Ce(III) present corresponding to about 20 – 30 % reduction of the added NPs. This plateau could correspond to a reversible reduction/oxidation reaction. In contrast, a maximum was not seen in anaerobic sludge. Reduction to a Ce(III) phase was observed around 3 hours and increased linearly up to 1 day. The reduction of Ce(IV) was slower as a function of time in the anaerobic system. We hypothesize that this could be due to the slowed or different metabolism of anaerobic bacterial communities (Madigan et al., 2009) because it has been suggested that microbial metabolism is responsible for CeO_2 NP reduction (Thill et al., 2006, Zeyons et al., 2010, Dissertation Chapter 2). Another possibility that would result in slower kinetics of reduction in anaerobic sludge would be different surface affinities. Previous work identified the importance of surface interaction for reduction and if the surface affinities are different between the NPs and aerobic or anaerobic bacteria, the kinetics of transformation could be altered.

In activated sludge, the transformation was observed to reach a steady state amount of reduction between 8 hours and 1 day in the batch experiment. This trend would be indicative of a reaction with both a forward and a reverse reaction rate constant, in this case, a rate of reduction and a rate of reoxidation. As such, the rate of transformation was determined by fitting a reversible reaction. As seen in Figure 16, the linear portion of the plot of ln $[(Ce(IV)_0 - Ce(IV)_{ss}) / (Ce(IV)_t - Ce(IV)_{ss})]$ versus time yielded a slope with a standard error, which was equivalent to the sum of the forward and reverse reaction rate coefficients. From the LCF results, the ratio of Ce(IV) / Ce(III) at steady state could also be determined and this ratio was equivalent to the oxidation rate constant divided by the reduction rate constant. This allowed for the calculation of the two individual rate constants, which could be used to parameterize the model and are shown in Table 13. The standard deviation on the rate coefficients was determined using Matlab (Matlab R2010a, the MathWorks Inc., Natick, MA, USA) in order to account for the error on each data point and the error in linear regression.

Anaerobic transformation rate coefficients were assumed to be the result of a first order reaction and determined according to Equation 5.12 and plots of ln $(1 - Ce(III) / C_0)$ as a function of time as indicated in Figure 17. From the plots, the slope of the linear trend line used to fit the reaction was the negative rate coefficient. The R^2 values suggested acceptable fits to the data given the inherent error in the measurements from

XANES experiments of about 10%. Again, error on the rate constant was calculated using Matlab (Matlab R2010a, the MathWorks Inc., Natick, MA, USA).

Equation 5.12

$$\frac{Ce\ (III)}{C_0} = 1 - e^{-kt}$$

Direct contact between bacteria and CeO_2 NPs has been observed to favor reduction of Ce (Zeyons et al., 2009). Our modeling approach assumes that NP attachment during heteroaggregation between NPs and bacteria is therefore a critical first step in producing the overall observed rate of Ce reduction. Thus the aerobic rate of reduction of CeO_2 NPs should depend on the differences observed in their affinity for bacterial surfaces. Experimentally, the total rate of reduction was measured, which would be a function of the intrinsic rate of reduction and the rate of heteroaggregation as described by Equation 5.2. Under the assumption that differences in the overall rate of reduction observed for the CeO_2 NPs with different surface chemistries indicate that heteroaggregation is limiting, the overall reduction rate constant is predicted to be proportional to α_{NB} leading to the prediction that:

Equation 5.13

$$k_{red\ total\ citrate} = \frac{k_{red\ total\ pristine}}{\alpha_{pristine}} \alpha_{citrate}$$

Using the estimated values of α_{NB} (Table 11) for pristine CeO_2 NPs (α = 0.0064) and for citrate-functionalized CeO_2 NPs (α = 0.0023) the overall reduction rate constant for the citrate-functionalized NPs as calculated by Equation 5.13, is 0.0282 h^{-1}. This rate

constant compares well with the actual measured rate constant of 0.0216 ± 0.0071 h^{-1}. This analysis would suggest that the differences observed in reduction rate is due to different affinities for the surface of the bacteria as a result of surface functionalization or lack thereof on the CeO_2 NP samples.

The apparent aerobic rates of reduction for pristine and citrate-functionalized CeO_2 differed with respect to surface coating. The magnitude of pristine CeO_2 reduction was larger that of the citrate-functionalized, which are likely attributed to differences in affinity for bacteria or surface protection imparted by the citrate coating. The citrate-functionalized CeO_2 NPs have a higher stability and therefore do not associate to the same extent with the solid phase (Dissertation Chapter 2 and 3). In addition, surface coatings that prevent association of NPs and bacteria, have been shown to reduce the overall reduction (Zeyons et al., 2009). Calculated rates of oxidation (the reverse reaction), did not appear to present the same obvious surface functionalization dependence. This finding was logical as it would be expected that the exposed Ce(III) would reoxidize back to Ce(IV) at a similar rate.

In contrast to the aerobic rates, the anaerobic rates of transformation were not significantly different based on surface functionalization. Solids concentrations were much higher in the anaerobic system and it is likely that heteroaggregation was not limiting. Much slower rates of reduction may reflect greater sensitivity of bacterial communities in anaerobic sludge to CeO_2. We speculate that the slowed transformation

kinetics in anaerobic digestion were likely the result of slowed or changing metabolism of anaerobic bacterial communities.

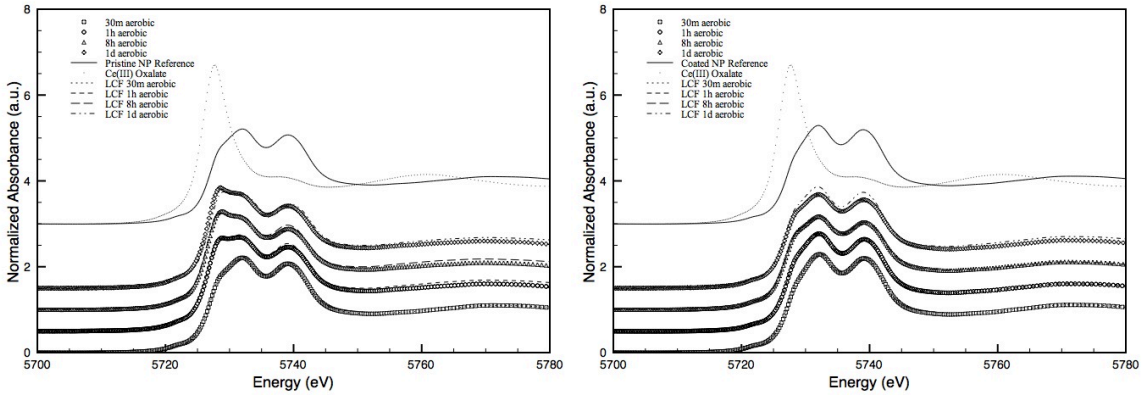

Figure 14. XANES results for pristine CeO_2 NPs (A) and citrate-functionalized CeO_2 NPs (B) associated with the solid phase of aerobic sludge.

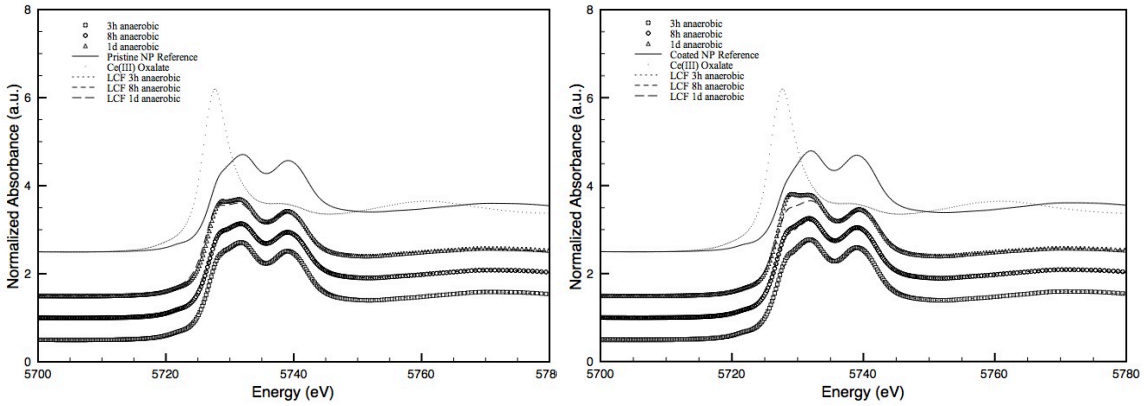

Figure 15. XANES results for pristine CeO_2 NPs (A) and citrate-functionalized CeO_2 NPs (B) associated with the solid phase of anaerobic sludge.

Table 12. Linear combination fitting results for CeO2 samples with aerobic and anaerobic sludge as a function of mixing time.

SAMPLE	Duration	% Ce(IV)	% Ce(III)	R	SAMPLE	Duration	% Ce(IV)	% Ce(III)	R
Pristine CeO_2 solid phase speciation in aerobic sludge	30 min	100	0	0.000483	Coated CeO_2 solid phase speciation in aerobic sludge	30 min	100	0	0.000510
	1 hour	87	5	0.000092		1 hour	98	2	0.000284
	8 hours	81	23	0.000332		8 hours	91	8	0.000568
	1 day	82	24	0.000369		1 day	91	7	0.000384
Pristine CeO_2 solid phase speciation in anaerobic sludge	3 hours	93	9	0.000184	Coated CeO_2 solid phase speciation in anaerobic sludge	3 hours	91	11	0.000339
	8 hours	89	11	0.000059		8 hours	88	14	0.003164
	1 day	84	18	0.000401		1 day	84	21	0.000487

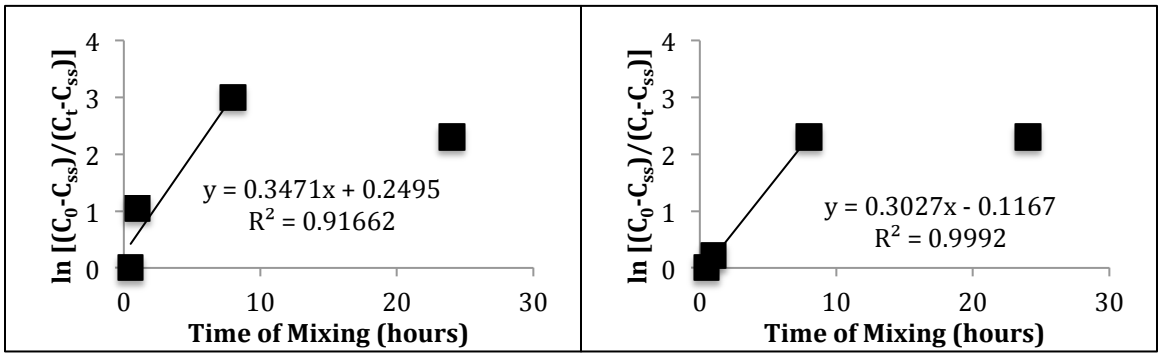

Figure 16. Increasing amount of a Ce(III) phase versus time for pristine CeO_2 NPs (A) and citrate-functionalized CeO_2 NPs (B) in aerobic sludge with the corresponding trend line for determination of the aerobic transformation rate coefficient.

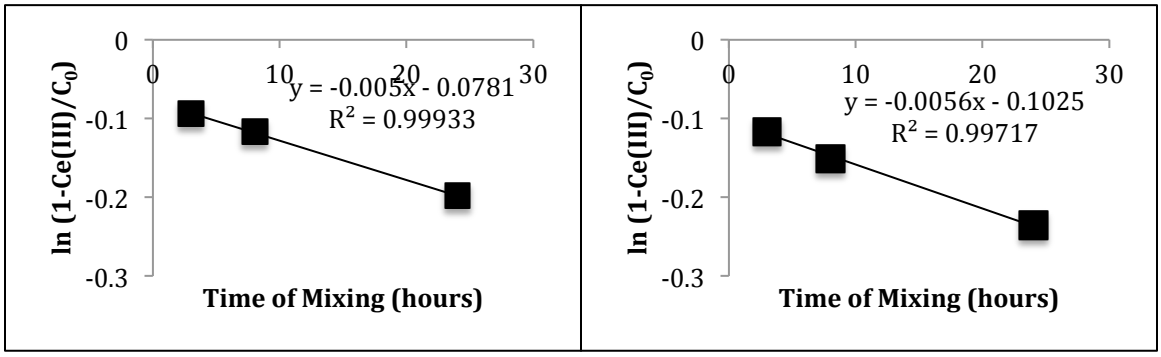

Figure 17. Increasing amount of a Ce(III) phase versus time for pristine CeO_2 NPs (A) and citrate-functionalized CeO_2 NPs (B) in anaerobic sludge with the corresponding trend line for determination of the aerobic transformation rate coefficient.

Table 13. Rate coefficients of transformation for CeO_2 NPs in aerobic and anaerobic sludge.

NP	$k_{aerobic}$ (hr^{-1}) reduction	Standard Deviation	$k_{aerobic}$ (hr^{-1}) oxidation	Standard Deviation	$k_{anaerobic}$ (hr^{-1})	Standard Deviation
Pristine CeO_2	0.0785	0.0306	0.2685	0.105	0.0050	0.00013
Citrate - coated CeO_2	0.0216	0.0071	0.2808	0.0086	0.0056	0.00029

5.4.4 Predicted Exposure Concentrations

The estimated concentrations of pristine and citrate-functionalized CeO_2 NPs discharged from WWTPs are presented in Table 14. The results indicate that in the case of pristine CeO_2, 3.4% of the added NPs remained in the liquid phase while that number was only slightly higher at 3.7% for citrate functionalized NPs. This suggests that between the primary clarifier and the secondary clarifier, almost all of the CeO_2 NPs (approximately 96% overall) introduced to the waste stream will preferentially associate with the solid phase and be transported to anaerobic digestion, due to high association with the solids, which are in great excess relative to the added NPs. As such, CeO_2, like

other metal and metal oxide NPs investigated in the same manner has the potential for high accumulation in biosolids that are typically disposed of either by land application, landfilling, or incineration. Thus those CeO_2 NPs that enter the waste stream will eventually be exposed to predominantly terrestrial environments.

With respect to predicted transformation, overall 54.9% of the added pristine NPs were transformed while 56.2% of the citrate coated NPs underwent reduction. These amounts of transformation agree well with previous bioreactor experiments, where complete transformation was not observed after 5 weeks of incubation. The surface functionalization was not observed to significantly impact the ultimate fate of CeO_2 NPs in WWTPs because the anaerobic rates of reduction for both samples were similar. From these results, it can be concluded that the kinetics of reduction in the anaerobic digester drive the total amount of transformation due to higher residence times and a continually increasing reduction. The effluent concentrations of CeO_2 NPs were estimated to be extremely low, less than 1 ppb and only significant accumulation of any species would be predicted to be observed in biosolids.

The concentrations of the NP species in the other flows within the WWTP are presented in Table 15. The results indicated that transformation in the sewer system could lead to approximately 1/3 reduction of the native CeO_2 species. Due to similar rates of anaerobic transformation, differences in the concentrations of NPs and transformation byproducts were not observed for different surface functionalization.

Concentrations present in primary effluent and solids indicated approximately 50% distribution to the solid phase, as expected. In this compartment aerobic transformation would be dominant and the rate of reoxidation was calculated to be much higher than reduction. Therefore, higher concentrations of the native NP were observed in both the effluent and solids. The same trend in higher concentrations of oxidized NP species was also observed in the secondary solids. In addition, more distribution to the solid phase was observed leading to very low effluent concentrations from secondary treatment (Table 14). This means that significant accumulation of reduced species would only be likely following anaerobic digestion where higher amounts of Ce(III) byproducts would be produced.

Determined rates of transformation, leading to approximately 50 – 60% reduction overall for CeO_2 NPs suggested the accumulation of a Ce(III) phase in the environment upon discharge from WWTPs in biosolids. The likely complexes leaving WWTPs were hypothesized to be Ce_2S_3, which would be stable in anaerobic digestion (Dissertation Chapter 2). It could be possible that further transformation would occur once the solids were no longer maintained under anaerobic conditions. In this case, the speciation of Ce would be expected to change and be governed by more dominant aerobic species including $Ce_2(SO_4)_3$-$8H_2O$ or $CePO_4$. Further analytical techniques must be employed to decipher those Ce species present in the environment in order to prioritize future research efforts with the most relevant, aged particles.

This model indicates the critical importance in understanding and predicting the processes that will affect the fate and transport of NPs in the environment. In order to most accurately continue to study those species that will be exposed to aquatic and terrestrial environments, future research must account for key transformations and the ultimate compartment in which these species will accumulate. This will allow for the most complete prediction of risk and impact of NPs that are released from products and technologies to the waste stream. In addition, this model justifies the consideration of WWTPs as black box models. Similar predictions for ultimate distribution were observed in previous modeling efforts (Hendren et al., 2011). While this more simplified black box system is therefore adequate for WWTPs, it must consider transformation in concurrence with distribution to predict the fate and transport of NPs.

Table 14. Predicted pristine and citrate-functionalized CeO_2 NP exposure concentrations in WWTP effluent and biosolids.

NP	Type	Influent Concentration (mgL^{-1})	Effluent Concentration (mgL^{-1})	Standard Deviation	Biosolids Concentration (mg NP g^{-1} solids)	Standard Deviation
Pristine CeO_2	Nanoparticle	0.0068 ± .00098	1.65E-5	7.53E-6	0.00253	0.00061
	Transformation byproduct		1.22E-5	5.46E-6	0.00318	0.00090
Citrate - coated CeO_2	Nanoparticle		1.69E-5	7.72E-6	0.00245	0.00072
	Transformation byproduct		1.19E-5	5.31E-6	0.00326	0.00120

Table 15. Predicted concentrations of pristine and citrate-functionalized CeO2 NPs in the sewer and primary effluent and the primary and secondary solids.

NP	Type	Sewer Effluent (mgL^{-1})	Standard Deviation	Primary Effluent (mgL^{-1})	Standard Deviation	Primary Solids (mgL^{-1})	Standard Deviation	Secondary Solids (mgL^{-1})	Standard Deviation
Pristine CeO_2	Nanoparticle	0.0043	0.0011	0.0013	0.00024	0.0032	0.00052	0.0015	0.00027
	Transformation byproduct	0.0024	0.0010	0.00094	0.00020	0.0013	0.00045	0.00072	7.1E-5
Citrate - coated CeO_2	Nanoparticle	0.0043	0.0011	0.0014	0.00025	0.0033	0.00054	0.0016	0.00029
	Transformation byproduct	0.0024	0.0010	0.00091	0.00020	0.0012	0.00045	0.00070	6.9E-5

5.5 Conclusions

This study has provided an estimate of the environmentally relevant concentrations of pristine and citrate functionalized CeO_2 NPs leaving WWTPs in effluent discharge and biosolids. Surface functionality appears to play virtually no role in determining the ultimate redox speciation of CeO_2 NPs leaving the WWTP as most of these NPs are removed to sludge and subsequently treated anaerobically where heteroaggregation is not limiting and bacteria may potentially digest organic moieties on NP surfaces. As in previous studies, estimates of the concentrations of ENM-based material released from WWTPs are highly sensitive to the assumptions made regarding production quantities and NP concentrations entering the WWTP. As researchers continue to improve the estimates for influent concentrations in wastewater, the aforementioned determined percentages of distribution and transformation can be applied to understand the magnitude of transformation and the compartment in which NPs and transformation byproducts preferentially associate. From this work, future research efforts can be prioritized as the more critical species and environmentally

relevant concentrations are elucidated for NPs that enter the waste stream following release from nano-enabled applications or other points in the life cycle.

6. Implications for Land Application Resulting in Removal of NPs from WWTPs.

6.1 Abstract

Increased use of engineered nanoparticles (NPs) in consumer products and technologies has resulted in release of NPs to the waste stream during all life cycle stages of the material. NPs that enter the waste stream can undergo changes in the technical compartments of a wastewater treatment plant (WWTP) and then be discharged to the environment in surface water effluent, recycled through land application of biosolids, or disposed of in biosolids that are incinerated or landfilled. Research has indicated that most metal and metal-oxide NPs that are liberated from products to the waste system accumulate in the biosolids with implications for land application.

This work aimed to provide a simplified tool to predict the ultimate steady state concentrations of NPs in land application units (LAUs) following biosolid introduction as sustainable fertilizers. This model incorporated important fate and transport processes including loss through water erosion and runoff, leaching and plant uptake. In addition, scenarios assessed the impacts of different biosolids loading and different NP core and solubility.

The results of this study indicated that the solid phase concentrations of ZnO and TiO_2 NPs would be on the order of 0.4 mg/kg at steady state and 300 mg/kg after two hours, respectively. These concentrations are orders of magnitude lower than estimated

background level soil concentrations of 150 mg/kg Zn and 4,700 mg/kg for Ti but accumulation overtime could lead to more significant concentrations closer to the background. The processes of leaching and uptake were observed to impact NP fate although leaching was experimentally determined to be low. In contrast, rain erosion did not impact overall steady state concentrations of the NP in soil. Further insight into actual plant uptake and differences between applied NP species and background metals will improve our understanding of the actual risks associated with land application of biosolids that have accumulated NP species in wastewater treatment.

6.2 Introduction

The increasing use of engineered nanoparticles (NPs) in novel products and technologies has resulted in release to the environment (Gottschalk and Nowack 2011, Benn and Westerhoff 2008). Release of NPs during all stages of the life cycle from production through use and disposal can result in direct environmental exposure or accumulation of NPs in the waste stream (Blaser et al., 2008, Westerhoff et al., 2011). A number of NP applications result in large releases to wastewater treatment plants (WWTPs) where the NPs can undergo various processes that impact their fate and transport (Kaegi et al., 2011). Due to the critical need, recently a number of experimental studies and modeling efforts have been completed that explore the unique behavior of NPs in the environmental matrix of wastewater to determine the key processes that will

drive NP exposure (Kaegi et al., 2011, 2013, Ma et al., 2013, Lombi et al., 2012, Levard et al., 2012, Gomez-Rivera et al., 2012, Hendren et al., 2013, Dissertation Chapter 2 and 3).

Previous work presented a WWTP model for metal and metal oxide NPs released from products to the waste stream that accounted for key transformations and distribution of the NPs between the liquid and solid phase to predict exposure (Dissertation Chapter 4 and 5). The results of the study indicated that a majority of these NPs released to WWTPs accumulated in biosolids, including Ag, ZnO, TiO_2, and CeO_2 NPs. In addition, it was observed that the NPs underwent very fast redox reactions within the aerobic and anaerobic compartments with the exception of TiO_2 NPs. This has ultimate implications for disposal or recycling of these biosolids that are laden with NPs and NP transformation byproducts either by land application, landfilling, or incineration.

Land application of biosolids was originally thought to be a sustainable practice, where nutrient rich wastes following wastewater treatment were reused to improve farming land. Approximately 50% of the generated biosolids are used in land application scenarios but this only results in biosolid application to approximately 1% of all farmland in the United States (USDA, 2011). Still, due to the increasing prevalence of NPs released to the waste stream that will likely accumulate in biosolids, it is critical to understand and have tools to predict the fate of NPs in such terrestrial systems.

Currently there are studies being conducted exploring the interactions of NPs accumulated in biosolids with agricultural land environments (CEINT and TINE). Pilot scale WWTP experiments were conducted with ZnO and Ag NPs where the transformations of both NPs were analyzed within the plant and then following biosolid composting, a process of drying biosolids prior to land application (Lombi et al., 2012, Ma et al., 2013). The results identified the transformation of both ZnO and Ag to be sulfidation within the WWTP. Following digestion and composting, there was a change in speciation observed for the ZnO NPs. While the Ag_2S remained, the ZnO further transformed to three species; some ZnS remained but also present was $Zn_3(PO_4)_2$ and Zn-FeOOH. This experimentation illustrates the critical importance of understanding the transformation potential of NPs in different environmental conditions. In addition, this work highlights the importance of tracking the NP transformations to understand the predominant species being exposed. For example, studying pristine NPs in land application units (LAUs) is not as environmentally relevant as studying NPs that have been aged in biosolids.

The work presented here aims to provide a modeling framework by which experimental efforts can be prioritized for the parameterization of a LAU exposure model. The input to the LAU model would be the NP, if still present as is the case with TiO_2 NPs, and the transformation byproduct, which in many cases, will be the most important species with the highest concentration. The crux of the model involves the

determination of the processes that will most critically impact the fate and transport of the NP in the LAU. Once those processes have been elucidated, it will be key to design functional assay type experiments in environmental media to measure the rates.

It has been shown that metal and metal-oxide NPs associate to a great degree with the solids in wastewater treatment plants and accumulation in biosolids is likely. The motivation for this work is to understand the fate and impacts of NPs in contaminated biosolids during prolonged application onto agricultural land. This exposure model was developed to provide a simplified tool that can provide an estimation of the concentrations that will exist in terrestrial compartments following release of NPs from WWTPs over the duration of land application.

6.3 Methods

6.3.1 Model Formulation

Figure 18 illustrates the conceptual model of the land application unit with the potential important processes impacting NP fate and transport highlighted. The model assumes a mass loading of NPs associated with biosolids as predicted from the WWTP model would be applied to a till depth and undergo various processes that could impact exposure through the unit. The goal of this model is to generate a time dependent mass balance relationship that provides realistic estimates of the mass concentration of NPs that remain associated with the solid phase. The key environmental fate processes that could occur in this system include uptake into plants and bacteria, mobilization from the

solid phase and subsequent leaching, runoff of particulates containing NPs, and further transformation of aged NP species.

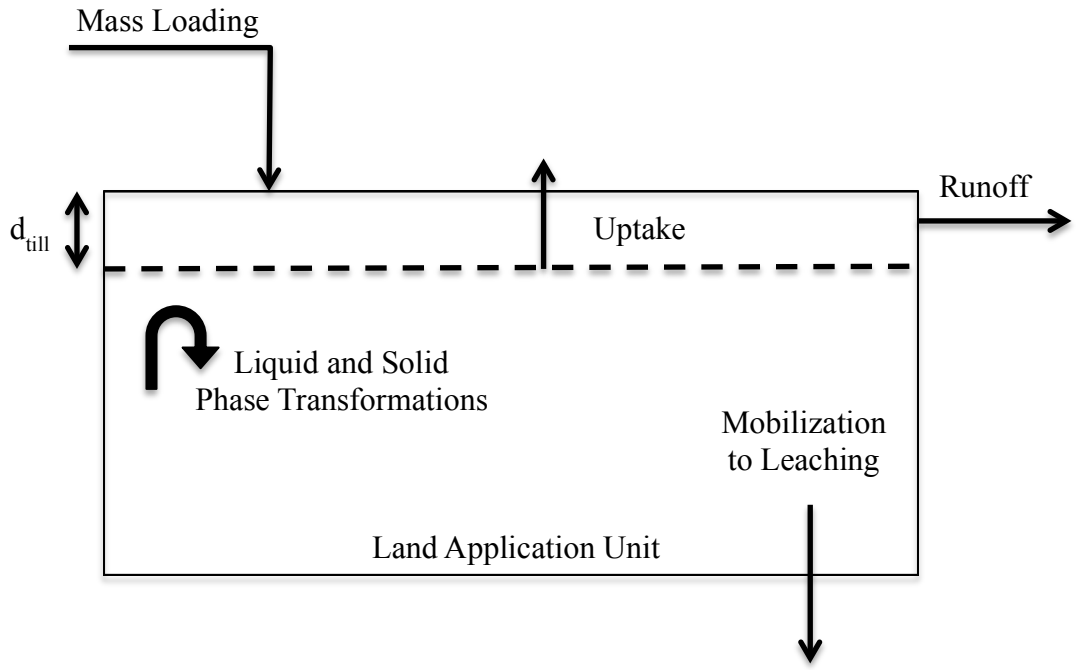

18. Conceptual Model of a Land Application Unit (LAU) where NP fate is impacted by processes of runoff, uptake, leaching and transformation.

The generalized mass balance differential equation to describe the fate and transport of aged NPs when they are land applied as biosolids following wastewater treatment is illustrated in Equation 6.1. Table 16 describes the parameters used in the model with associated units and method of determination. Parameter inputs were assumed to possess an associated uncertainty. As such, parameterization was stochastic where applicable and described by normal distributions with an average and standard deviation.

Equation 6.1

$$\mathrm{V}\frac{d[q_s(1-\varepsilon)]}{dt} = W\mathrm{L}w - f_{er}Rq_s(1-\varepsilon)Lw - R_I k_I q_s(1-\varepsilon)\mathrm{L}w - P_{uptake}q_s(1-\varepsilon)\mathrm{L}w - k_t q_s(1-\varepsilon)\mathrm{V}$$

Table 16. Parameters with associated descriptions, units, variable type, and values used in the exposure LAU model.

Parameter	Description	Units	Variable Type	Value
L	Length of land application	L	Assigned	8.46E9 cm
A	Area of land applied area = w*d_{till}	L^2	Calculated	1.69E10 cm^2
d_{till}	Depth of till	L	Assigned	25 cm
w	Width of land applied area	L	Assigned	8.46E9 cm
q_s	NP associated with solid phase	M/M	Simulated	Simulated
1- ε	Mass of solid per volume of field	M/L^3	Assigned	1.6 g/cm^3
W	Areal Mass Loading	M/TL^2	Estimated from WWTP Model	NP Dependent
f_{er}	Fraction of soil available for erosion by runoff = d_{er}/d_{till}	unitless	Calculated	0.1
R	Average Rainfall	L/T	Calculated	0.003 - 0.02 cm/hr
P_{uptake}	Plant uptake mass transfer coefficient	L/T	Experimental	Variable (on order of leaching)
k_t	Transformation rate coefficient	/T	Experimental	0 (current assumption)
f_I	Fraction of NPs available for leaching	unitless	Experimental	Mobile NP / Total NP
R_I	Fluid available for infiltration	L/T	Experimental	Slope of leaching experiment
d_{er}	Depth available for erosion by runoff	L	Assigned	2.5 cm

The time dependent solution to Equation 6.1 for the concentration of the NP species associated with the solid phase is described in Equations 6.2 through 6.4.

Equation 6.2

$$\frac{d[q_s(1-\varepsilon)]}{dt} = \frac{W}{d_{till}} - \frac{f_{er}R}{d_{till}}q_s(1-\varepsilon) - \frac{R_I f_I}{d_{till}}q_s(1-\varepsilon) - \frac{P_{uptake}}{d_{till}}q_s(1-\varepsilon) - k_t q_s(1-\varepsilon)$$

Equation 6.3

$$\frac{d[q_s]}{dt} = \frac{W}{d_{till}(1-\varepsilon)} - \frac{f_{er}R}{d_{till}}q_s - \frac{R_I f_I}{d_{till}}q_s - \frac{P_{uptake}}{d_{till}}q_s - k_t q_s$$

Equation 6.4

$$q_s = q_{s0}e^{-\left[\frac{f_{er}R}{d_{till}}+\frac{R_I f_I}{d_{till}}+\frac{P_{uptake}}{d_{till}}+k_t\right]t} + \frac{\left(\frac{W}{d_{till}(1-\varepsilon)}\right)}{\frac{f_{er}R}{d_{till}}+\frac{R_I f_I}{d_{till}}+\frac{P_{uptake}}{d_{till}}+k_t}\left[1-e^{-\left[\frac{f_{er}R}{d_{till}}+\frac{R_I f_I}{d_{till}}+\frac{P_{uptake}}{d_{till}}+k_t\right]t}\right]$$

Alternatively, if steady state is assumed, q_s can be simulated according to Equation 6.5.

Equation 6.5

$$q_s = \frac{\left(\frac{W}{d_{till}(1-\varepsilon)}\right)}{\frac{f_{er}R}{d_{till}}+\frac{R_I f_I}{d_{till}}+\frac{P_{uptake}}{d_{till}}+k_t}$$

6.3.2 Model Parameterization

6.3.2.1 Nanoparticles

The metal and metal oxide NPs investigated in this work were chosen due to their prevalence in consumer products and technologies (Blaser et al. 2008). The ZnO and TiO_2 NPs employed were outlined in the Transatlantic Initiative for Nanotechnology and the Environment (TINE) to be critical materials to study further. The ZnO NPs (Nanosun P99/30) were donated by Micronisers (Dandenong, Australia)

and the TiO_2 NPs were purchased from Evonik Industries (Essen, Germany), neither possessed surface macromolecule functionalization.

6.3.2.2 Land Application Unit Parameters

The parameters used to describe a typical land application unit were obtained from literature. For this work, the LAU consisted of an average size US farm of 418 acres (USDA, 2011). An average tillage depth was assumed at 25 cm, with 10% of that depth available to erosion by runoff (Raper et al., 2000). Average soil density was used for typical soil types that are present in farmland. As such, a density of 1.6 g/cm^3 was chosen to describe the unit (Mays, 2011). Another important parameter that was assigned but allowed to vary was the rainfall on the LAU. Average annual rainfall amounts were obtained for states in the US. A high value for annual rainfall was observed to be 63 in/year while a low value was 9.5 in/year (Mays, 2011). An error of 10% on these values was assumed due to lack of information on the true standard deviation of these values.

6.3.2.3 Areal Mass Loading

The mass loading of NPs on the land application unit per time was obtained from previous modeling efforts that simulated the amount of NPs released from WWTPs. The output of the Monte Carlo model that followed the fate and transport of NPs through WWTPs was a mass concentration of NPs in biosolids in mass of NP/mass of solid. This mass concentration was converted to an areal mass loading by assuming

two types of land application, a high loading scenario and a low loading scenario with 1 ton/acre*yr and 20 tons/acre*year, respectively (US EPA, 1994).

6.3.2.4 Leaching

Leaching experiments were conducted in outdoor lysimeters with ZnO NPs according to the experimental setup illustrated in Figure 19. Three treatments were used, one as a control with soil and sludge, one with the bulk metal in sludge and soil, and one with the NP in sludge and soil. There were 8 replicate lysimeter tubes used leading to 24 samples overall. Each lysimeter contained 900 grams dry weight of the soil/sludge mixture. The sludge was mixed with Woburn soil at a ratio of 42:58, which yielded a total NP concentrations of 1400 ppm ZnO. Leaching was quantified using naturally occurring rain events over a five-month period of time. The concentrations of the NPs in the leachate were measured as a function of time such that a rate constant for leaching could be determined for parameterization of the model. A plot of the natural log of the leached concentration of NPs versus time yielded a linear relationship where the slope of the linear regression is equivalent to the negative of R_{ff}/d_{till}.

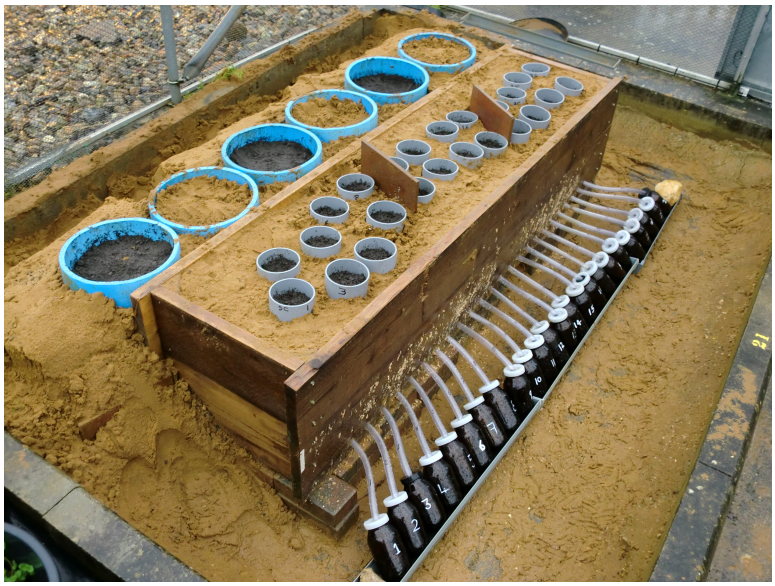

Figure 19. Experimental set-up of outdoor lysimeters to quantify the NP leaching through simulated land application.

6.3.2.5 Uptake

Plant uptake studies are currently being conducted with Medicago Truncatula and wheat to determine the concentrations of NPs that are removed from soil into important agricultural plants. Knowledge of the driving factors that lead to plant uptake of NPs in soil is very limited. However, it is anticipated that this processes will not be kinetically fast and that rates of uptake will likely be low. As such, in this work, plant uptake rates were assumed to be relatively small and on the order of leaching, but were varied to observe the impact of changing uptake on the amount of NP in the solid phase.

6.3.2.6 Transformation

The predicted concentrations of NPs and transformation byproducts released from WWTPs indicated that the predominant species in biosolids would be the transformation product, except in the case of TiO_2. For the purposes of this work, further transformation into other species was not considered. While it is possible that further transformations in a terrestrial environment could occur, the goal of this initial work was just to understand the concentration of the NP species that remained in the soil compartment allowing for loss to leaching, runoff and uptake.

6.4 Results and Discussion

6.4.1 Model Parameterization

Model parameters obtained from literature were provided in Table 16. Experimental parameters were either determined in the case of mobilization to leaching (only available for ZnO) or varied with respect to plant uptake. Due to limited information, only ZnO and TiO_2 NPs were simulated, but these methods could be applied with experimentation or theory to other metal or metal-oxide NP.

For the NPs available for loss to leaching, determination was obtained by fitting the curve of ln ($C_{NP\text{-}leached}$) versus time, which provided a linear relationship (Figure 20). A trend line was used to fit the data and the slope of this line provided the negative value for R_{ifl}/d_{till}. From this value (~ 0.01 d^{-1}), rate constants of a similar order were assumed for plant uptake.

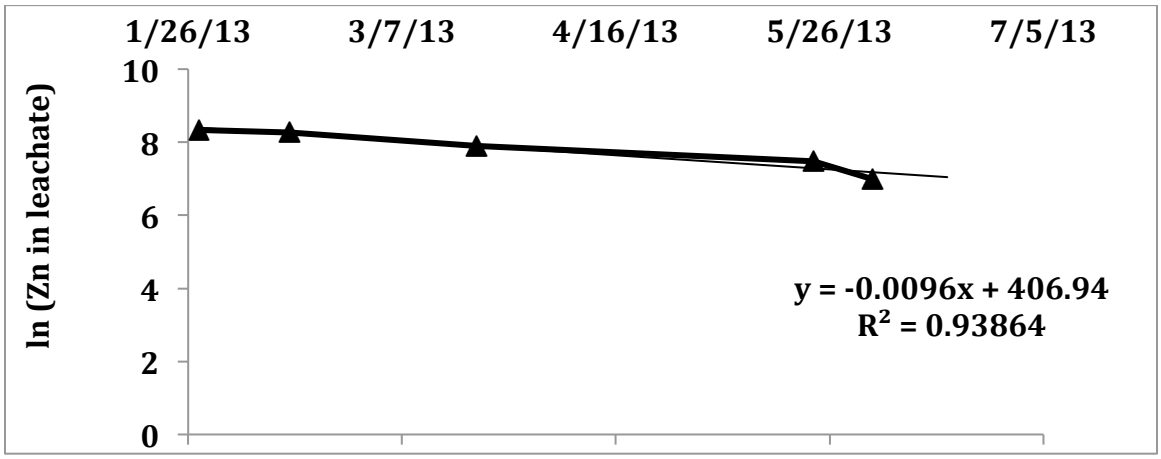

Figure 20. Rate constant determined for the leaching of ZnO NPs applied to soil (preliminary results completed by Mark Durenkamp, Rothamsted Research, United Kingdom).

6.4.2 Scenario Development for ZnO and TiO_2 NPs

The goal for this work was to determine the important processes that would dictate the fate and transport of the NPs through the LAU. The impacts of changing the rate of rainfall, loading, uptake, leaching, and NP solubility (ZnO versus TiO_2) were assessed. For the simulations, model parameterization was completed probabilistically to account for some of the inherent uncertainty in the data for NPs in LAUs. Error in the estimates of NPs and transformation byproducts were included as determined from the WWTP Monte Carlo exposure model. Where error was unavailable or lacking, error of 10% was employed as a first estimate due to known variability in the parameters. The time dependent concentrations of ZnO and TiO_2 NPs were evaluated.

6.4.3 Impact of Rainfall

The impact of rainfall was investigated by calculating the time dependent solid phase mass concentration of nano-ZnO species using the lowest and highest average annual rainfall values for states in the US. The low end for annual rainfall was found to be approximately 10 in/yr while the high was 63 in/yr. From Figure 21, it can be seen that changing the amount of rainfall observed annually did not impact the overall concentration of the ZnO NPs associated with the solid phase. With both rainfall rates, the simulation predicts a steady state concentration of 0.4 mg of NP per kg of soil. This concentration is a few orders of magnitude less than the average background concentration of Zn metal in soils (~ 150 mg/kg), however speciation of the applied ZnO species is likely different and potentially more available to transport processes (Kearney, 1996). Steady state concentrations due to annual loading and removal through transport processes were achieved around 100 days of operation. In Equation 6.4, the amount of rainfall is divided by the depth of till in the LAU, which effectively means that shorter till depths could lead to more significant transport of NPs in soil erosion by rainfall. In sum, differences in annual average rainfall among US states did not significantly impact the magnitude of the steady concentration of the NP or the time required by the system to achieve steady state.

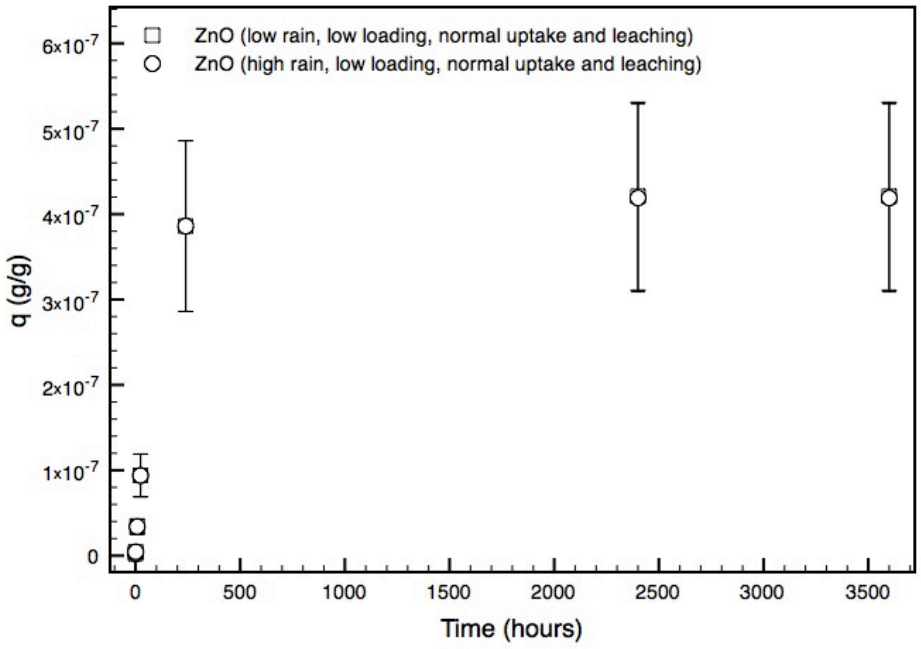

Figure 21. Impact of changing annual rainfall from ~10 in/yr to 63 in/yr on the overall mass concentration of ZnO NPs or transformation byproducts remaining in the soil.

6.4.4 Impact of Areal Mass Loading

The areal mass loading was determined by transforming the mass concentration of NPs predicted to accumulate in biosolids by a Monte Carlo WWTP model (Dissertation Chapter 4) into a loading assuming two scenarios for biosolids application. Typical applications of biosolids range from 1 – 20 tons per acre per year (US EPA, 1994). A low end of 1 and a high end of 20 was therefore employed to obtain a low and high loading of NPs. The WWTP model indicated greater than 95% association of Ag, ZnO, and TiO_2 NPs with biosolids. Ag NPs were predicted to have the smallest global production and thus have the smallest loading in biosolids at 0.003 μg/kg on the low estimate and 0.052 μg/kg as a high estimate. ZnO NPs have a higher estimated

production volume and therefore have a higher biosolids mass concentration. Low ZnO NP loading was calculated to be 0.18 μg/kg and the high loading was determined to be 3.01 μg/kg. TiO_2 is one of the most produced NPs globally and has a low biosolids loading of 0.74 μg/kg and a high loading of 12.6 μg/kg.

Due to limited data on leaching for Ag and TiO_2, the impact of loading was assessed for ZnO NPs with the results presented in Figure 22. It was observed that, as expected, loading leads to different steady state concentrations of the NP. With low ZnO loading, the steady concentration in a LAU is approximately 0.42 ± 0.11 mg/kg while high loading leads to a steady state concentration of less than 7.2 ± 1.9 mg/kg. This leads to approximately the same difference in final concentration as is observed in loading. While the final mass concentration is different, loading does not appear to impact the time to steady state when all other processes remain the same between the simulations.

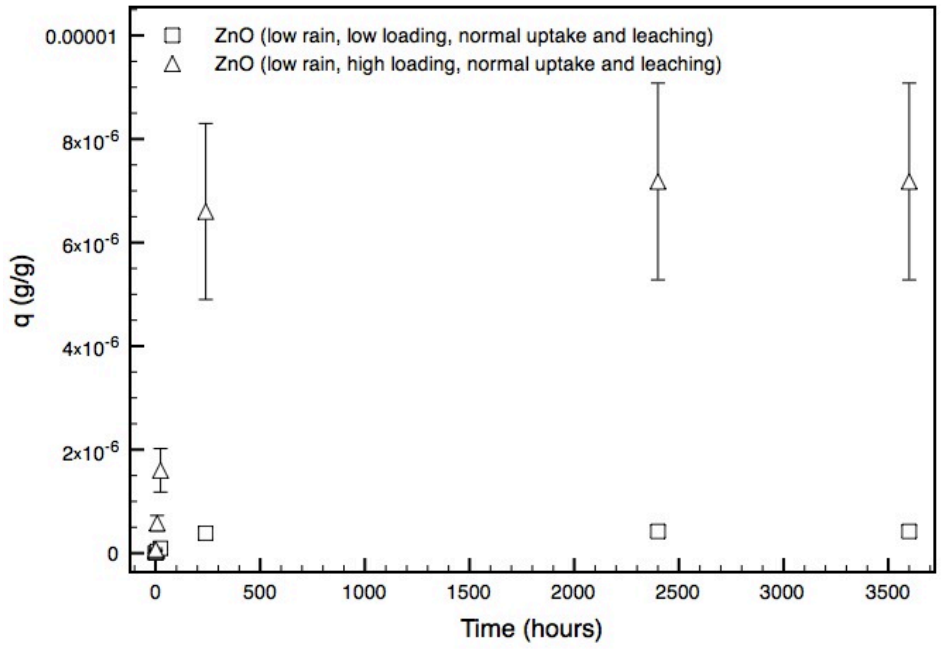

Figure 22. Impact of changing biosolids loading from 1 to 20 tons/acre*yr on the overall mass concentration of ZnO NPs or transformation byproducts remaining in the soil.

6.4.5 Impact of Transport Processes

The two main transport processes in addition to surface runoff, which was observed to be limited, were leaching and plant uptake (as further transformations were deemed unnecessary in this initial simulation where the goal was to determine the mass concentration of any remaining nano species). Leaching of the NPs would require liberation (likely in the form of dissolution) from the soil particles into pore water and subsequent transport of that water out of the till depth zone, further into the soil. Experimental evaluation of leaching indicated that a very minimal portion < 1%, of the NPs would actually be available for leaching. Due to the lack of information on plausible rates of plant uptake, rates similar to leaching were assumed. In Figure 23, the

normal leaching rate constant was assumed to be low at 0.0005 hr^{-1} and the plant uptake rate was assigned an assumed low value of 0.0125 cm/hr. In addition, the scenario with no leaching or uptake was investigated along with the scenario where leaching and uptake rates were an order of magnitude higher. The assumption for similar rates of leaching and uptake was made because it would be expected with increased mobilization of the NPs into pore water (leaching), availability of those NPs for plant uptake would also increase. In the same way, low leaching would correspond to low uptake. In the case where both processes are considered normal, the concentration of the ZnO NP species associated with the solid phase increases linearly with time up to a value of 0.42 ± 0.11 mg ZnO NPs per kg of soil. In contrast, when the transport processes are more active and all other parameters equal, the concentration of ZnO NPs associated with the soil appears to achieve a maximum concentration of only 0.042 ± 0.01 mg ZnO NPs per kg of soil (an order of magnitude less). This suggests that these transport processes could play an important role in mitigating the concentrations of NPs in the soil, but this could lead to implications for plants or ground water, the compartments into which the NPs are entering.

In addition, although this is likely not the case for ZnO NPs, which have a relatively high solubility, the situation where uptake and leaching were not active was also investigated. From Figure 23, it can be seen that when the key transport processes of leaching and uptake are no longer present; the system does not achieve steady state

concentrations of ZnO NP species associated with the solid phase over two years. This suggests that rainfall-generated runoff is not a sufficient enough removal process to allow for the system to achieve steady state in less than two years. This also supports the importance of other transport processes like leaching and uptake as determiners of fate of NP species in LAUs.

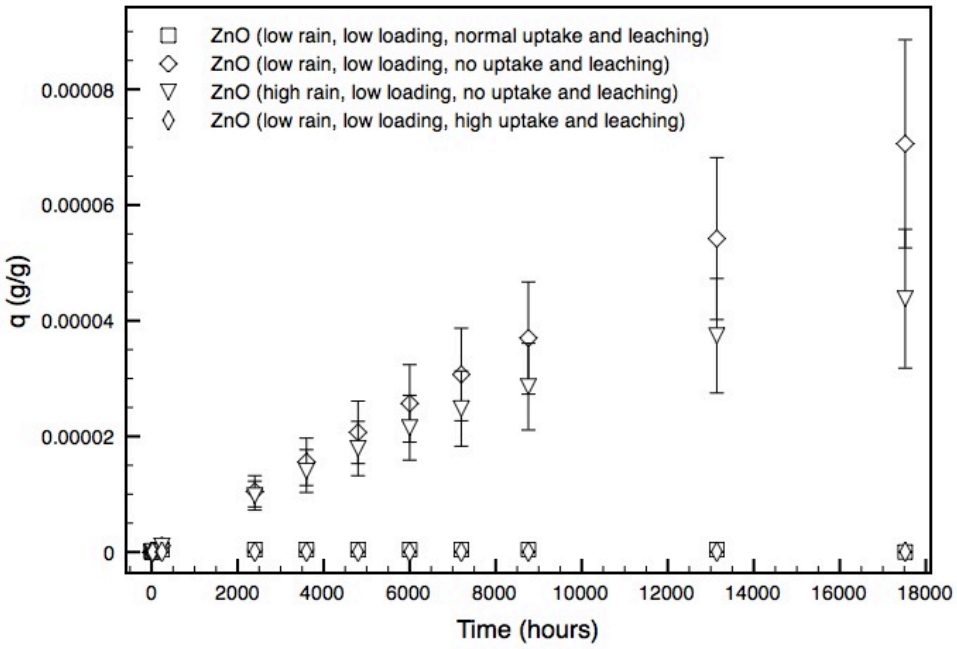

Figure 23. Impact of changing the transport processes of leaching and uptake on the overall mass concentration of ZnO NPs and transformation byproducts remaining in the soil.

6.4.6 Comparing ZnO and TiO_2 NPs: Impact of Solubility

The process of leaching that will alter the fate of NPs in LAUs will likely be impacted by the solubility of the aged NP species. For example, ZnO NPs that have transformed in $Zn_3(PO_4)_2$ and Zn-FeOOH and Ag that exists as Ag_2S following wastewater treatment will have a higher propensity for dissolution into the pore water

than TiO_2 NPs that are relatively insoluble. Figure 24 indicates the NP species for ZnO and TiO_2 associated with the solids in the LAU as a function of time. The parameters that vary between these two simulations are the leaching rate constant and the areal mass loading, which was predicted to be different for the two NP samples due to different production volumes. For ZnO NPs, the measured leaching rate constant of 0.01 d^{-1} was used, in addition to a rate constant of 0 for comparison and a leaching rate constant of 0 was applied for TiO_2 due to insolubility and little leaching likely. With respect to mass loading, TiO_2 NPs are produced to a higher degree than ZnO. The results of this simulation indicate that a higher concentration of TiO_2 NPs will exist in LAUs. This will be the result of higher loading values and the lack of loss to leaching. The curves also suggest that without the presence of leaching or uptake, steady state for TiO_2 NPs will not be achieved within two years. The concentration of TiO_2 NPs in the LAU was predicted to be 290 ± 73 mg/kg soil after two years. This is also observed for ZnO NPs under the situation where uptake and leaching are ignored, however this is likely not realistic and only provided for comparison. In this scenario, the concentration of ZnO NP species is lower than TiO_2 after two years because less ZnO NPs are produced and assimilated into consumer products and technologies. However, under realistic conditions for ZnO NP species, the system would be expected to reach steady state around 100 days.

Overall the maximum estimates of ZnO NPs in LAU soils at steady state were predicted to be a few orders of magnitude less than the background level concentrations for Zn, similar to the concentration of TiO_2 NPs after two years, which was a couple of orders of magnitude lower than background Ti in typical soils. The average concentration of Zn in soils is 150 mg/kg with a maximum of 250 mg/kg and a minimum of 10 mg/kg (Kearney, 1996). The average concentration of Ti is higher at 4,700 mg/kg with a maximum of 12,000 mg/kg and a minimum of 2,000 mg/kg (Kearney, 1996). This suggests that the actual mass loading of the Ti and Zn metal may be insignificant relative to the background levels of Ti and Zn present in high degree in soils. Still, it is possible that the unique characteristics of the NP species could render their behavior different than natural counterparts. Further research must address the differences in natural metals and applied NP species to understand if the NP impacts will actually be different.

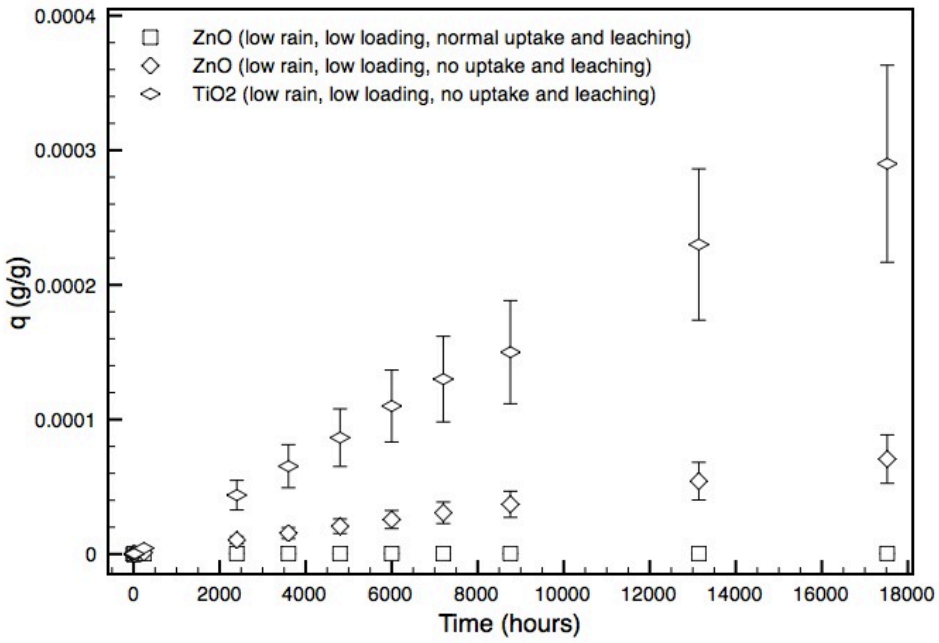

Figure 24. Impact of different production quantities and solubility of NPs on the overall mass concentrations in the soil as a function of time.

6.5 Conclusions

This work provides an initial assessment of the important processes that will impact the overall fate and transport of NPs in LAUs. The results indicate that the predicted concentrations of NPs in LAUs will be low, on the order of 0.4 mg/kg for ZnO NPs at steady state and 290 mg/kg for TiO_2 NPs after two years. These estimates at least an order of magnitude lower than background level concentrations for Zn and Ti in typical soils. This indicates that increased accumulation of metals may not impact the terrestrial environment, however it could still be possible that NP unique properties may result in different behavior of the applied species relative to the natural counterparts. Further investigation of the differences between the nano-scale species of

ZnO and TiO_2 and natural species, will allow for a better understanding of how to assess the exposure of NP contaminated biosolids in LAUs.

From this study, it can be seen that transport processes including leaching and uptake along with biosolids loading will all impact NP fate. When leaching and uptake were active, steady state was observed in approximately 100 days. Leaching was observed experimentally to be minimal with < 1% of added NPs leaching through the soil, however the model suggests that this process in addition to minimal uptake is still necessary for achievement of overall steady state concentrations. This could have implications for crop plant and microbial uptake, which will require further research and discretization between the two processes. The kinetics and mechanism of microbial uptake relative to plants is likely very different and complex. Elucidation of these distinct uptake processes will improve this modeling effort. In sum, further knowledge about the nature of the NPs in biosolids that are land applied and the associated bioavailability and mechanism of plant and microbial interaction of those species will be key to understanding the potential for exposure and uptake of NPs.

In addition, certain agricultural fields are treated with a no tillage process. This could dramatically change the processes dictating overall transport in the LAU. It would be expected that a lack of tillage would lead to more significant loss of NPs by water erosion and overland surface flow. Consequently, minimal loss to plant uptake and leaching would be expected when tilling is not employed. Further insight into the

most used processes and their overall impacts will be critical for prediction of NP fate in all types of LAUs.

7. Dissertation Synthesis and Conclusions

7.1 Summary of Objectives

The main objective of this doctoral work was the development of a nano-specific exposure model with experimental parameterization to predict environmentally relevant concentrations of NPs and NP transformation byproducts released from WWTPs. Much of the previous research on NP exposure assessment have indicated insurmountable challenges with respect to providing concentration estimates due to the large gaps in data and characterization of NPs in environmental media. However, the need for such models is pressing as NPs are already entering aquatic and terrestrial environments. As the prevalence of NPs in consumer products and technologies grows, so does the need for predictive methods to indicate the important environmental compartments of accumulation, NP species present in those compartments and the associated impacts. While the most inclusive means of exposure forecasting would involve the comprehensive environment assessment described in Figure 3, using this method would be impossible for NPs due to the infancy and therefore limited data in the field of nanotechnology. Still, using results from the few studies completed on NPs in the environment, simplified models can provide a relative understanding of NP behavior in complex media for prioritization of future research efforts.

The doctoral research presented here provides a simplified modeling approach for NPs released from the different stages in the life cycle to the waste stream, which will

undergo treatment in a WWTP and possible exposure in effluent discharge and biosolids. In addition, a framework for the inclusion of results from functional assay experiments to improve the environmental relevance of the model was outlined in this dissertation. In this way, the initial objectives were accomplished and this work has provided a simplified tool that has universal applicability and can be continually improved as new data and information becomes available about NP contaminants and their environmental interactions.

7.2 Interpretation of Results

The ultimate goal of this work was to provide estimates on the concentrations of metal and metal-oxide NPs in different environmental compartments following transport through WWTPs. In doing so, this research aimed to identify if discretization rather than black box modeling efforts provided significant enhancement of model results. Investigation into the processes that impact the fate of metal and metal-oxide NPs in WWTPs was conducted in an effort to parameterize a WWTP model. In congruence with this work, a LAU model was also constructed to understand the exposure of NPs that accumulate in biosolids.

The results of this dissertation indicated that the two most important processes for consideration in WWTP exposure assessment of NPs were distribution between the solid and liquid phase and transformation. Functional assay and bioreactor experiments were devised to explore these two processes and generate distribution coefficients and

transformation rate coefficients for four important metal and metal-oxide NPs, Ag, ZnO, TiO_2, and CeO_2, used often in products and research. It was observed that the majority of the NPs studied preferentially associated with the solid phase in WWTPs and would therefore accumulate in biosolids. Minor differences were observed in the distribution coefficient as a function of the NP core and surface functionalization; however, the modeling exercise indicated that those differences did not greatly impact the overall distribution of the NPs. Modeling results suggested that over 90% of Ag, TiO_2, CeO_2, and ZnO NPs would associate with biosolids. These results agree with pilot scale studies and other experimental work with metallic NP distribution and justify the use of a single distribution coefficient completed with secondary wastewater to describe overall distribution of the NPs in WWTPs. A novel approach to further the application of the distribution coefficient was to determine α, or the attachment efficiency between the NPs and the background wastewater solids. Currently, α, an important, fundamental NP property in specific environmental systems, has only been defined in pristine systems and determination is difficult. The mathematical relationship connecting the distribution coefficient to a relative α, allows for this parameter to be more easily determined in complex media.

In addition to exploring distribution, this work identified the major transformation of CeO_2 NPs in WWTPs. Previous work has indicated that Ag and ZnO NPs undergo redox transformations to Ag_2S and ZnS in WWTPs, although these

transformations have not been accounted for in previous modeling efforts. Similar experimentation was conducted with CeO_2 NPs, which exist initially in the Ce(IV) oxidation state. Significant reduction of CeO_2 NPs to a Ce(III) phase, likely Ce_2S_3 was observed. Transformation rate coefficients were calculated for model parameterization. This dissertation work also illustrated the connection between transport, attachment, and then subsequent transformation in the case of CeO_2 NPs. Using the work that explored the distribution coefficient and attachment efficiency for CeO_2 NPs in congruence with the measured rates of transformation, an intimate relationship was shown between these processes, which is in agreement with previous experimental work where it was observed that interaction with bacteria was necessary for transformation. In sum, this work indicated that differences in rates of transformation could be accounted for due to differences in affinity and heteroaggregation.

The ultimate conclusions from this dissertation suggest that for the metal and metal-oxide NPs studied, significant accumulation in biosolids would be expected. Furthermore, the predominant species present in the biosolids will no longer be the initial NP but rather the transformation byproduct. Comparing this discretized modeling effort to those computational works that treat WWTPs as black box model, this work provides justification for the use of black box modeling. By accounting for high distribution and transformation, discretization of the WWTP compartments appears to provide negligible improvements especially when considering the inherent

uncertainty. However, it is critical to note that transformation must be considered when assessing NP fate and impacts.

This work suggests that terrestrial exposure to NPs from WWTPs through LAUs or landfills will be more significant that aquatic exposure and that studying the native NP will not provide environmentally relevant information as the critical species will be the redox product. Further transport and transformation are inevitable in a LAU, where 50% of generated biosolids are applied in addition to other terrestrial environments. The results of the simplified computational effort presented indicate that ZnO NP loading and steady state concentrations and TiO2 concentrations after two years will be orders of magnitude lower than background metal levels. However, the speciation and availability of the NP species are likely different from natural analogs and could still impact the terrestrial environment. The concentrations of the NP species were observed to be impacted by the processes of uptake and leaching while increasing average rainfall played little role in ultimate concentrations. This preliminary work necessitates further experimental research into the behavior of NP species that are applied to fields through contamination in biosolids.

7.3 Future Directions

This work provides a method for predicting environmental exposures of NP contaminants with very limited data on the behavior of such material in different environmental systems. The large gaps in knowledge concerning the impacts of NP

induced novel physicochemical properties on environmental interactions render large uncertainties in predictive modeling. A myriad of assumptions are necessary in order to complete this type of assessment from error in experimental parameters to estimations of input values based on data interpolation. Therefore, future research perspectives would include improved approximation of model parameters.

One source of experimental uncertainty that was propagated through the model determinations was introduced by the assumption that classes of environmental systems would all possess similar composition. For example, in the majority of this work, a single type of wastewater was used from a municipal plant in the US. Using environmental media was critical to maintain relevance in parameter determination but the inherent complexity among the same media from different sources was something that was not accounted for. It was assumed that the single source of wastewater in the US was sufficiently similar to other wastewaters that the experimental parameters would be applicable to all wastewater samples. However, it is known that wastewater can vary significantly depending on the geographic location, climate, and typical source waters (municipal and industrial). Therefore, further research into identifying the main differences in wastewater and using reference systems on either end of the spectrum could elucidate the impact of wastewater constituents on the distribution and transformations of the NPs. In an effort to account for some of this error, the model parameters were provided as probabilistic inputs with associated distributions. While

wastewater complexity is high, it is encouraging to note that the same types of transformations were observed for different sampling locations. For example, reduction of CeO_2 NPs was observed in wastewater from the US and also sludge sampled from a municipal plant in Aix-en-Provence, France. Furthermore, many researchers across the globe have observed the sulfidation of Ag and ZnO NPs in wastewater. This suggests that the type of transformation likely remains the same among all wastewaters but differences could arise in the kinetics of those transformations.

Another critical source of uncertainty that would improve many research efforts in the field of nanotechnology is production volumes of NPs. Production volumes and release during this life cycle phase are typically either held as proprietary information or currently unknown. A number of researchers have attempted various methods for the estimation of the total production volumes of various NPs but without proper reporting from manufacturing companies about total production and the different types of functionalization present, complete accuracy will be impossible. In addition to understanding overall production of NPs it will also be of critical importance to understand the product types into which all produced NPs are incorporated. NP release from products will vary based on the matrix that the NP modification exists in and this will impact the leaching of the NP from the product. Furthermore, the use and disposal of the product will dictate the environmental compartment into which released NPs will accumulate whether it be the waste stream, landfills, or direct exposure to air, water, or

soil. In sum, there would be a great decrease in uncertainties across the field if total production volume of NPs and associated product incorporation, release potential from products during use and disposal, and probable environmental exposure pathways upon release were known.

This work highlights other future research needs by illustrating the importance of transformation byproducts. The results of this research indicate that NPs will undergo fast transformations upon entering the environment, which suggests that the NP species of focus in environmental studies may actually need to be the aged products instead of the native NP. While transformation byproducts may still exist in the nano scale, it will be important to understand their unique physicochemical properties relative to the initial NP that could impact fate and transport. These transformed species may be the most environmentally relevant to concentrate future research efforts on.

Another critical perspective for future research is enhancing the scientific community's ability to study NP contaminants in environmental matrices. This work employed analytical tools to track metal concentration with the assumption that it would all result from the added nanoparticles. Increased detection and size characterization methods would improve our understanding of the mechanisms behind NP behavior in the environment in addition to providing a more clear indication of the type of species exposed for improved toxicology studies.

7.4 Expected Significance and Societal Impacts

The ultimate importance of this research is the introduction of a model that accounts for nano-specific processes to predict exposure concentrations of metal and metal-oxide NPs leaving WWTPs. This work provided a simplified modeling tool based on experimental parameterization that can be applied to any number of NPs that are exposed to wastewater treatment. It incorporates the key processes that impact the fate of NPs in this system, namely distribution and transformation in the case of WWTPs, and experimental methods for determining their associated model parameters. In addition to tracking the concentration of the native NPs released during the material life cycle, this method also calculates the concentrations of transformation byproducts. As such, this work can help inform and prioritize future research efforts by indicating the environmental compartments that are most affected by NPs released to the waste stream and the likely species present in those compartments following NP transformation in WWTPs. Finally, the models developed in this study were designed to allow for easy introduction of more environmental and nano-specific complexities as they become available in an effort to maintain the most accurate description of NP environmental exposure through wastewater.

Appendix A

This appendix includes the supporting information section that is available online in support of the manuscript submitted by Barton et al., 2014 to Environmental Science and Technology, "The Transformation of Pristine and Citrate-Functionalized CeO2 Nanoparticles in a Laboratory Scale Activated Sludge Reactor."

A1. TEM Images of CeO_2 Nanoparticles

A 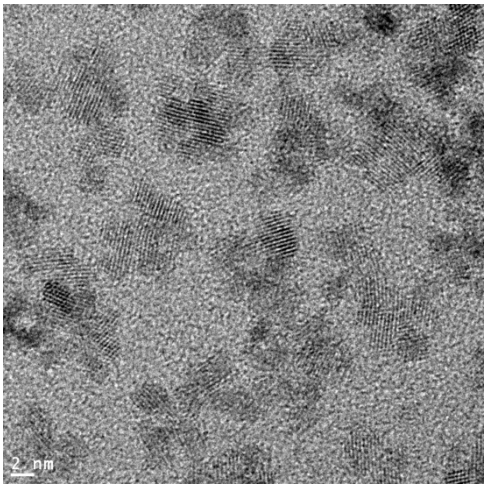

B 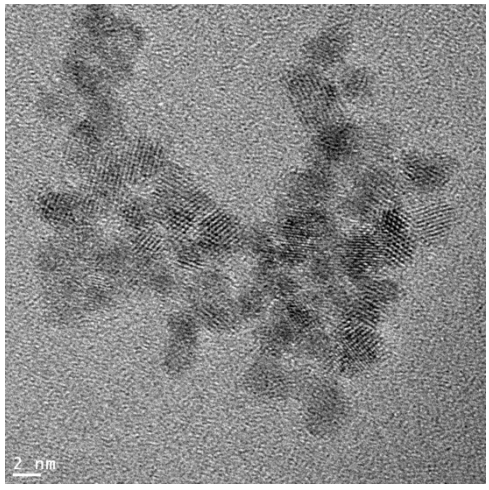

TEM images of (A) Pristine CeO_2 Nanoparticles and (B) Citrate-functionalized CeO_2 Nanoparticles with 3-4 nm diameter crystallites of cerianite are observed. Scale bar: 2 nm.

A2. Chemical and Mineral Components of Wastewater Treatment Plant Sludge.

Major Chemical Components of Sludge (μXRF) % by weight			Major Mineral Phases (XRD)	
	Reactor 1 (prior pristine CeO_2 addition)	**Reactor 2 (prior functionalized CeO_2 addition)**	**Reactor 1 (prior pristine CeO_2 addition)**	**Reactor 2 (prior functionalized CeO_2 addition)**
Carbon (C)*	32		Quartz	Quartz
Oxygen (O)*	29		Calcite	Calcite
Hydrogen (H)*	5		Halite	Halite
Nitrogen (N)*	5			
Sulfur (S)*	1			
Phosphorous (P)	0.7	0.8		
Calcium (Ca)	2	2.5		
Iron (Fe)	4	6		
Silicon (Si)	0.4	0.2		
Potassium (K)	0.5	0.5		
Chlorine (Cl)	10	9		

Data was collected using XRF and XRD of dried sewage sludge. Major chemical analysis was adapted from Hernandez et al. 2011 (*) and confirmed with additional semi-quantitative XRF analyses of sludge from both bioreactors presented here in relative percentages by weight.

A3. ^{13}C NMR Spectra of Initial EPS

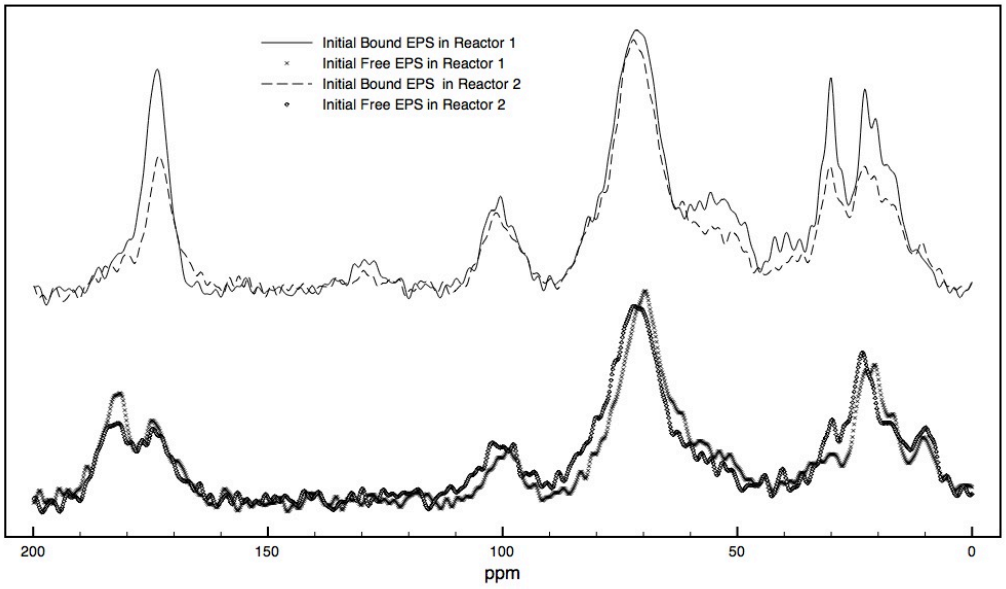

Initial ^{13}C NMR spectra of bacterially associated EPS (bound) and free suspended EPS (free) for Reactors 1 (prior pristine CeO_2 NPs addition) and 2 (prior citrate-functionalized CeO_2 NPs addition).

A4. Chemical Shift Assignments for ^{13}C Spectra for Major Constituents of EPS.

Chemical Shift (ppm)	Structural Group	Corresponding Compound	Approximate Position in Bound EPS (ppm)	Approximate Position in Free EPS (ppm)
160 – 200	Amides, carboxyl groups	protein, peptidoglycan, fatty acids	170	185 170
110 – 160	Aromatic, olefinic C	protein and nucleic acid		
90 – 110	Anomeric C	carbohydrate	100	100
65 – 90	O-alkyl C	carbohydrate	70	70
45 – 65	αC of amino acids	protein		
0 – 45	Aliphatic C	protein and fatty acid	30 22	22 10

Adapted from Metzger et al., 2009.

A5. Diversity Indices of Bioreactors Prior to NP Addition.

Reactor eventually spiked with	Richness	Shannon-Wiener	Bray-Curtis dissimilarity
Reactor 1 (prior pristine CeO_2 addition)	769 ± 5	7.77 ± 0.03	0.32
Reactor 2 (prior citrate-functionalized CeO_2 addition)	883 ± 5	7.82 ± 0.03	

Appendix B

This appendix includes the supporting information section that is available online in support of the manuscript submitted by Barton et al., 2014 to Environmental Engineering Science, "Theory and Methodology for Determining Nanoparticle Affinity for Heteroaggregation in Environmental Matrices Using Batch Measurements."

B1. Distribution Coefficients Measured at the Programmed Times and NP Concentrations.

NP	d_p	ϱ_p	C_p	Time	γ
	(nm)	(g/mL)	(mg/L)	(sec)	L/mg)
GA Ag	25	10.50	10	1	0.00040
				60	0.00043
				300	0.00049
				600	0.00051
				1800	0.00054
				3600	0.00060
			50	0	0.00039
				60	0.00046
				300	0.00050
				600	0.00054
				1800	0.00059
				3600	0.00064
	6	10.50	10	0	0.00044
				60	0.00047
				300	0.00050
				600	0.00053
				1800	0.00060
				3600	0.00066
			50	0	0.00040
				60	0.00041
				300	0.00043

				600	0.00049
				1800	0.00052
				3600	0.00058
PVP Ag	40	10.50	10	0	0.00130
				60	0.00189
				300	0.00264
				600	0.00313
				1800	0.00445
				3600	0.00478
			50	0	0.00125
				60	0.00168
				300	0.00231
				600	0.00293
				1800	0.00351
				3600	0.00399
	8	10.50	10	0	0.00105
				60	0.00134
				300	0.00186
				600	0.00216
				1800	0.00258
				3600	0.00281
			50	0	0.00106
				60	0.00130
				300	0.00182
				600	0.00224
				1800	0.00280
				3600	0.00352
Pristine CeO_2	8	7.22	10	0	0.00147
				60	0.00176
				300	0.00302
				600	0.00427
				1800	0.00552
				3600	0.00593
			50	0	0.00649
				60	0.01067
				300	0.01686
				600	0.02190
				1800	0.02256

				3600	0.02375
Citrate CeO_2	10	7.22	10	0	0.00133
				60	0.00159
				300	0.00195
				600	0.00249
				1800	0.00313
				3600	0.00382
			50	0	0.00149
				60	0.00164
				300	0.00190
				600	0.00243
				1800	0.00267
				3600	0.00291
TiO_2	20	4.23	10	0	0.00200
				60	0.00216
				300	0.00354
				600	0.00527
				1800	0.00550
				3600	0.00598
			50	0	0.00230
				60	0.00290
				300	0.00470
				600	0.00750
				1800	0.00840
				3600	0.00910
ZnO	30	5.61	10	0	0.00270
				60	0.00321
				300	0.00404
				600	0.00578
				1800	0.00552
				3600	0.00578
			50	0	0.00240
				60	0.00295
				300	0.00396
				600	0.00528
				1800	0.00509
				3600	0.00576

B2. Parameterization Description and Units for Relationship between Distribution Coefficient and Attachment Efficiency.

Symbol	Description	Units
α_{homo}	Attachment efficiency between two NPs	Unitless
α_{hetero}	Attachment efficiency between a NP and a background particle	Unitless
r_h	Hydrodynamic radius	Length
d_c	Diameter of the background collectors	Length
ε	Porosity of the packed bed	Unitless
L	Length of the column	Length
C	Final mass concentration of NPs	Mass/Volume
C_0	Initial mass concentration of NPs	Mass/Volume
η_0	Single collector efficiency	Unitless
γ	Distribution coefficient	Volume/Mass
M_S	Mass of the NP associated with the solid phase (background)	Mass
M_B	Mass of solids background	Mass
C_L	Mass concentration of NPs in the liquid phase	Mass/Volume
n	Final number concentration of NPs	Number/Volume
n_0	Initial number concentration of NPs	Number/Volume
β	Collision frequency	Volume/Time*Number
B	Number concentration of background particles	Number/Volume
k_b	Break-up rate coefficient	/Time
C_B	Mass concentration of background particles	Mass/Volume
f	Fraction of NPs in an aggregate	Unitless
r(t)	Removal	Unitless

Appendix C

This appendix includes the supporting information section that is available online in support of the manuscript submitted by Barton et al., 2014 to Science of the Total Environment, "Probabilistic Exposure Assessment for Ag, TiO_2, and ZnO Nanoparticles (NPs) Released to Wastewater Treatment Plants (WWTPs)."

C1. Parameters for WWTP Exposure Model.

Parameter	Description	Units	Value	Variable Type
C_{in}	Influent concentration to sewer system	mgL^{-1}	Table 2	Uniform
C_1	NP concentration to primary clarifier	mgL^{-1}	Calculated	Calculated
C_2	Transformation byproduct concentration to primary clarifier	mgL^{-1}	Calculated	Calculated
C_{p1}	NP concentration to secondary treatment	mgL^{-1}	Calculated	Calculated
C_{ps1}	NP concentration in solids from primary treatment to anaerobic digestion	mgL^{-1}	Calculated	Calculated
C_{p2}	Transformation byproduct concentration to secondary treatment	mgL^{-1}	Calculated	Calculated
C_{ps2}	Transformation byproduct concentration in solids from primary treatment to anaerobic digestion	mgL^{-1}	Calculated	Calculated
C_{s1}	NP concentration discharged in effluent	mgL^{-1}	Calculated	Calculated
C_{ss1}	NP concentration in solids from secondary treatment to anaerobic digestion	mgL^{-1}	Calculated	Calculated
C_{s2}	Transformation byproduct concentration discharged in effluent	mgL^{-1}	Calculated	Calculated
C_{ss2}	Transformation byproduct concentration in solids from secondary treatment to anaerobic digestion	mgL^{-1}	Calculated	Calculated
C_{b1}	NP concentration in biosolids	mgL^{-1}	Calculated	Calculated
C_{b2}	Transformation byproduct concentration in biosolids	mgL^{-1}	Calculated	Calculated
$k_{anaerobic}$	First order anaerobic transformation rate coefficient	d^{-1}	Experimental	Lognormal
$k_{aerobic}$	First order aerobic transformation rate coefficient	d^{-1}	Experimental	Lognormal
θ_{sewer}	Hydraulic Residence Time in sewers	d	0.002 – 0.05	Uniform
θ_p	Hydraulic Residence Time in primary treatment	d	0.0625 – 0.1042	Triangular
θ_s	Hydraulic Residence Time in secondary treatment	d	0.229 ± 0.078	Lognormal
θ_x	Solids Residence Time in secondary treatment	d	3 – 15	Triangular
θ_d	Solids Residence Time in anaerobic digestion	d	15 – 60	Triangular
f_p	Fraction of flow from primary treatment to anaerobic digestion	unitless	0.6 ± 0.1	Normal
ρ_{sludge}	Density of sludge	mgL^{-1}	1210 ± 190	Lognormal
γ_1	Primary distribution coefficient	Lmg^{-1}	Experimental	Lognormal
γ_2	Secondary distribution coefficient	Lmg^{-1}	Experimental	Lognormal
X_{s1}	Concentration of primary suspended solids	mgL^{-1}	380 ± 45	Lognormal
X_{s2}	Concentration of secondary suspended solids	mgL^{-1}	3810 ± 450	Lognormal

References

Abbott, L. and A.D Maynard *Exposure assessment approaches for engineered nanomaterials*. Risk Analysis, 2010. **30**(11): p. 1634-1644.

Akkache, S., et al., *Effect of exo polysaccharide concentration in the rheological properties and settling ability of activated sludge*. Environmental Technology, 2013, p. 1-9.

Arvidsson, R., et al.,*Challenges in exposure modeling of nanoparticles in aquatic environments*. Human and Ecological Risk Assessment, 2011. **17**(1): p. 245-262.

Auffan, M., et al., *Towards a definition of inorganic nanoparticles from an environmental, health and safety perspective.* Nature Nanotechnology, 2009. **4**: p. 634-641.

Auffan, M., et al., *Relation between the redox state of iron-based nanoparticles and their cytotoxicity toward Escherichia coli.* Environmental Science and Technology, 2008. **42**: p. 6730-6735.

Auffan, M., et al., *Inorganic manufactured nanoparticles: how their physicochemical properties influence their biological effects in aqueous environments*. Nanomedicine, 2010. **5**(6): p. 999-1007.

Benn, T. and P. Westerhoff, *Nanoparticle silver released into water from commercially available sock fabrics.* Environmental Science and Technology, 2008. **42**(11): p. 4133-4139.

Blaser, S.A., et al., *Estimation of cumulative aquatic exposure and risk due to silver: Contribution of nano-functionalized plastics and textiles.* Science of the Total Environment, 2008. **390**: p. 396-409.

Bottero, J.Y. and M.R. Wiesner *Considerations in evaluating the physicochemical properties and transformations of inorganic nanoparticles in water*. Nanomedicine, 2010. **5.6**: p. 1009.

Boxall, A.B.A., et al., *Current and future predicted environmental exposure to engineered nanoparticles.* 2007, Central Science Laboratory: Sand Hutton, UK.

Brar, S. K., et al., *Engineered nanoparticles in wastewater and wastewater sludge - Evidence and impacts*. Waste Management, 2010. **30**(3): p. 504-520.

Cadoret, A., et al., *Availability of low and high molecular weight substrates to extracellular enzymes in whole and dispersed activated sludges*. Enzyme Microbiology Techmology, 2002. 31(1-2): p. 179-186.

Chen, K.L. and M. Elimelech *Interaction of fullerene (C_{60}) nanoparticles with humic acid and alginate coated silica surfaces: measurements, mechanisms, and environmental implications*. Environmental Science and Technology, 2008. **42**(20): p. 7607-7614.

Christian, P., et al., *Nanoparticles: structure, properties, preparation, and behavior in environmental media*. Ecotoxicology, 2008. **17**(5): p. 326-343.

Consumer Products Inventory, in *The Project on Emerging Nanotechnologies*. 2013, Woodrow Wilson International Center for Scholars.

Cornelis, G., et al., *A method for determination of retention of silver and cerium oxide manufactured nanoparticles in soils*. Environmental Chemistry, 2010. **7**: p. 298-308.

Cornelis, G., et al., *Solubility and batch retention of CeO_2 nanoparticles in soil*. Environmental Science and Technology, 2011. 45: p. 2777-2782.

Dale, A.L., et al., *Modeling nanosilver transformations in freshwater sediments*. Environmental Science and Technology, 2013. **47**(22): p. 12920-12928.

Diot, M.A. *Etude du vieillissement et de l'alteraion de nanocomposites de la vie courante*. PhD Dissertation. Universite Paul Cezanne d'Aix-Marseille. Aix-en-Provence, France, 2012.

Doolette, C. L., et al., *Transformation of PVP coated silver nanoparticles in simulated wastewater treatment processes and the effect on microbial communities*. Chemistry Central Journal, 2013. **7**(46): p. 2-18.

Dowd, S. E., et al., *Survey of fungi and yeast in polymicrobial infections in chronic wounds*. Journal of Wound Care, 2011. **20**(1): p. 40-47.

Espinasse, B., et al., *Transport and retention of colloidal aggregates of C_{60} in porous media: effects of organic macromolecules, ionic composition, and preparation method*. Environmental Science and Technology, 2007. **41**(21): p. 7396-7402.

Essington, M. E. and S. V. Mattigod *Lanthanide Solid Phase Speciation*. Soil Science Society of America Journal, 1985. **49**: p. 1387-1393.

Ganesh, R., et al., *Evaluation of nanocopper removal and toxicity in municipal wastewaters*. Environmental Science and Technology, 2010. **44**(20): p. 7808-7813.

Gilks, W.R., et al., *Markov Chain Monte Carlo in Practice: Interdisciplinary Statistics*. 1996: Chaptman & Hall/CRC. 481.

Gomez-Rivera, F., et al., 2012. *Fate of cerium dioxide (CeO_2) nanoparticles in municipal wastewater during activated sludge treatment*. Bioresource Technology, 2012. **108**: p. 300-304.

Gottschalk, F., et al., *Possibilities and Limitations of Modeling Environmental Exposure to Engineered Nanomaterials by Probabilistic Material Flow Analysis.* Environmental Toxicology and Chemistry, 2010. **29**(5): p. 1036-1048.

Gottschalk, F., et al., *Probabilistic Material Flow Modeling for Assessing the Environmental Exposure to Compounds: Methodology and an Application to Engineered nano-TiO_2 Particles.* Environmental Modelling and Software, 2010. **25**: p. 320-332.

Gottschalk, F., et al., *Modeled environmental concentrations of engineered nanomaterials (TiO2, ZnO, Ag, CNT, Fullerenes) for different regions.* Environmental Science and Technology, 2009. **43**: p. 9216-9222.

Gottschalk, F. and B. Nowack *The release of engineered nanomaterials to the environment*. Journal of Environmental Monitoring, 2011. **13**(5): p. 1145-1155.

Grieger, K., et al., *Redefining Risk Research Priorities for Nanomaterials*. Journal of Nanoparticle Research, 2010. **2**(2): p. 383-392.

Grieger, K.D. *Environmental risk analysis for nanomaterials: review and evaluation of frameworks*. Nanotoxicology, 2011. **6**(2): p. 196-212.

Grieger, K.D., et al., *The known unknowns of nanomaterials: Describing and characterizing uncertainty within environmental, health and safety risks*. Nanotoxicology, 2009. **3**(3): 1-12.

Hannah, W. and P.B. Thompson *Nanotechnology, risk and the environment: a review*. Journal of Environmental Monitoring, 2008. **10**(3): p. 291-300.

Hendren, C.O., *Framing and Assessing Environmental Risks of Nanomaterials*. PhD Dissertation. Duke University. Durham, NC, 2010.

Hendren, C.O., et al., *Modeling nanomaterial fate in wastewater treatment: monte carlo simulation of silver nanoparticles (nano-Ag)*. Science of the Total Environment, 2013. **449**: p. 418-425.

Hendren, C.O., et al., *Estimating production data for five engineered nanomaterials as a basis for exposure assessment*. Environmental Science and Technology, 2011. **45**(7): p. 2562-2569.

Hu, M., et al., *Microbial community structures in different wastewater treatment plants as revealed by 454-pyrosequencing analysis*. Bioresource Technology, 2012. **117**: p. 72-79.

Jorand, F., et al., *Chemical and structural (2D) linkage between bacteria within activated sludge flocs*. Water Research, 1995. **29**(7): p. 1639-1647.

Kaegi, R., et al., *Behavior of metallic silver nanoparticles in a pilot wastewater treatment plant*. Environmental Science and Technology, 2011. **45**(9): p. 3902-3908.

Kaegi, R., et al., *Fate and transformation of silver nanoparticles in urban wastewater systems*. Water Research, 2013. **47**: p. 3866-3877.

Kearney Foundation of Soil Science, *Background concentration of trace and major elements in california soils*. Kearney Foundation Special Report, 1996. UCLA.

Keller, A.A., et al., *Global life cycle releases of engineered nanomaterials*. Journal of Nanoparticle Research, 2013. **15**: p. 1692-1709.

Kiser, M.A. *Fate of engineered nanomaterials in wastewater treatment plants.* PhD Dissertation. Arizona State University. Tempe, AZ, 2011.

Kiser, M.A., et al., *Biosorption of nanoparticles to heterotrophic wastewater biomass*. Water Research, 2010. **44**(14): p. 4105-4114.

Kim, B., et al., *Characterization and environmental implications of nano- and larger TiO_2 particles in sewage sludge and soils amended with sewage sludge*. Journal of Environmental Monitoring, 2012. **14**(4): p. 1129-1137.

Kim, B., et al., *Discovery and characterization of silver sulfide nanoparticles in final sewage sludge products.* Environmental Science and Technology, 2010. **44**(19): p. 7509-7514.

Law, N., et al., *The formation of nano-scale elemental silver particles via enzymatic reduction by Geobacter sulfurreducens*. Applied Environmental Microbiology, 2008. **74**: p. 7090–7093.

Lecoanet, H.F., et al., *Laboratory assessment of the mobility of nanomaterials in porous media*. Environmental Science and Technology, 2004. **38**: p. 5164–5169.

Levard, C., et al., *Sulfidation processes of PVP-coated silver nanoparticles in aqueous solution: Impact on dissolution rate*. Environmental Science and Technology 2011. **45**: p. 5260-5266.

Levard, C., et al., *Environmental transformations of silver nanoparticles: Impact on stability and toxicity*. Environmental Science and Technology, 2012. **46**: p. 6900-6914.

Li, B. and P.L. Bishop *Oxidation-reduction potential changes in aeration tanks and microprofiles of activated sludge floc in medium- and low-strength wastewaters*. Water Environmental Research, 2004. **76**(5): p. 394-403.

Limbach, L.K., et al., *Removal of oxide nanoparticles in a model wastewater treatment plant: influence of agglomeration and surfactants on clearing efficiency*. Environmental Science and Technology, 2008. **42**(15): p. 5828-5833.

Lin, S., et al., *Deposition of silver nanoparticles in geochemically heterogeneous porous media: Predicting affinity from surface composition analysis.* Environmental Science and Technology, 2011. **45**(12): p. 5209–5215.

Lin, S., et al., *Polymeric coatings on silver nanoparticles hinder autoaggregation but enhance attachment to uncoated surfaces*. Langmuir, 2012. **28**(9): p. 4178-4186.

Lipton, J., et al., *Short communication: selecting input distributions for use in Monte Carlo simulations.* Regulatory Toxicology and Pharmacology, 1995. **21:** p. 192-198.

Liu, G., et al., *Effect of ZnO particles on activated sludge: role of particle dissolution*. Science of the Total Environment, 2011. **409**(14): p. 2852-2857.

Lombi, E., et al., *Fate of zinc oxide nanoparticles during anaerobic digestion of wastewater and post-treatment processing of sewage sludge*. Environmental Science and Technology, 2012. **46**(16): p. 9089-9096.

Lowry, G.V. and E.A. Casman *Nanomaterial transport, transformation, and fate in the environment: A risk-based perspective on research needs*. Nanomaterials: Risks and Benefits, 2009. **2**: p. 125-137.

Lowry, G.V., et al., *Transformations of nanomaterials in the environment.* Environmental Science and Technology, 2012. **46**(13): p. 6893-6899.

Ma, R., et al., *Fate of zinc oxide and silver nanoparticles in a pilot wastewater treatment plant and in processed biosolids*. Environmental Science and Technology, 2013.

Ma, R., et al., *Size controlled dissolution of organic-coated silver nanoparticles*. Environmental Science and Technology, 2012. **46**: p. 752-759.

Mackay, D., et al., *Assessing the fate of new and existing chemicals: a five-stage process.* Environmental Toxicology and Chemistry, 1996. **15**(9): p. 1618-1626.

Martin-Cereceda, M., et al., *Characterization of extracellular polymeric substances in rotating biological contactors and activated sludge flocs*. Environmental Technology, 2001. **22**(8): p. 951-959.

Maynard, A.D. *Nanotechnology: Assessing the risks*. Nano Today, 2006. **1**(2): p. 22-33.

Mays, L. *Water Resources Engineering*. 2nd Edition. 2011: John Wiley & Sons.

Metcalf and Eddy, *Wastewater Engineering: Treatment, Disposal and Reuse*. Vol. Third. 2003: McGraw-Hill, Inc.

Metzger, U. *The concentration of polysaccharides and proteins in EPS of Pseudomonas putida and Aureobasidum pullulans are revealed by ^{13}C CPMAS NMR spectroscopy*. Applied Microbiology Biotechnology, 2009. **85**: p. 197-206.

Morgan, K. *Development of a Preliminary Framework for Informing the Risk Analysis and Risk Management of Nanoparticles.* Risk Analysis, 2005. **25**(6): p. 1621-1635.

Mueller, N.C. and B. Nowack *Exposure modeling of engineered nanoparticles in the environment.* Environ. Sci. Technol., 2008. **42**(12): p. 4447-4453.

Musee, N. *Simulated environmental risk estimation of engineered nanomaterials: a case of cosmetics in Johannesburg City*. Human and Experimental Toxicology, 2010. **30**(9): p. 1181-1195.

Napper, D. and A. Netschey *Studies of the steric stabilization of colloidal particles*. Journal of Colloid Interface Science, 1971. **37**(3): p. 528–535.

Navrotsky, A. *Energetics of nanoparticle oxides: interplay between surface energy and polymorphism*. Geochemical Transformations, 2003. 4(6): p. 34-37.

Nowack, B. and T.D. Bucheli *Occurrence, behavior and effects of nanoparticles in the environment*. Environmental Pollution, 2007. **150**(1): p. 5-22.

Nowack, B., et al., *Potential scenarios for nanomaterial release and subsequent alteration in the environment*. Environmental Toxicology and Chemistry, 2012. **31**(1): p. 50-59.

Park, B., et al., *Hazard and risk assessment of a nanoparticulate cerium-oxide based diesel fuel additive - a case study.* Inhalation Toxicology, 2008. **20**(6): p. 547-566.

Pelletier, D.A., et al., *Effects of engineered cerium oxide nanoparticles on bacterial growth and viability*. Applied and Environmental Microbiology, 2010. **76**(24): p. 7981-7988.

Petosa, A.R., et al., *Aggregation and deposition of engineered nanomaterials in aquatic environments: role of physicochemical interactions*. Environmental Science and Technology, 2010. **44**(17): p. 6532-6549.

Phenrat, T., et al., *Aggregation and sedimentation of aqueous nanoscale zerovalent iron dispersions*. Environmental Science and Technology, 2007. 41: p. 284-290.

Piccinno, F., et al., *Industrial production quantities and uses of ten engineered nanomaterials in Europe and the world*. Journal of Nanoparticle Research, 2012. 14(1109): p. 1-11.

Praetorius, A., et al., *Development of environmental fate models for engineered nanoparticles – a case study of TiO_2 nanoparticles in the rhine river*. Environmental Science and Technology, 2012. **46**(12): p. 6705-6713.

R Development Core Team, *R: A language and environment for statistical computing. R Foundation for Statistical Computing*. Vienna, Austria, 2008. ISBN 3-900051-07-0, URL http://www.R-project.org.

Raper, R. et al., *Tillage depth, tillage timing, and cover crop effects on cotton yield, soil strength, and tillage energy requirements*. Applied Engineering in Agriculture, 2000. **16**(4): p. 379-385.

Ravel, B. and M. Newville *ATHENA, ARTEMIS, HEPHAESTUS: data analysis for X-ray absorption spectroscopy using IFEFFIT*. Journal of Synchrtron Radiation, 2005. **12**: p. 537-541.

Rottman, J., et al., *Interactions of inorganic oxide nanoparticles with sewage biosolids*. Water Science and Technology, 2012. **66**(9): p. 1821-1827.

Sato, T., et al., *Global, regional, and country level need for data on wastewater generation, treatment, and use*. Agricultural Water Management, 2013. **130**: p. 1-13.

Sears, K., et al., *Density and activity characterization of activated sludg flocs*. Journal of Environmental Engineering, 2006. **132**: p. 1235-1242.

Schmid, M., et al., *Characterization of activated sludge flocs by confocal laser scanning microscopy and image analysis*. Water Research, 2003. **37**: p. 2043-2052.

Shatkin, J.A. and B.E. Barry *Approaching risk assessment of nanoscale materials*. in *2006 Nano Science and Technology Institute Nanotechnology Conference and Trade Show*. 2006. Cambridge, MA: Nano Science and Technology Institute (NSTI).

Smoluchowski, von, M. Z Physical Chemistry, 1917. **92**(129).

Snidaro, D., et al., *Characterization of activated sludge flocs structure*. Water Science Technology, 1997. **36**(4): p. 313-320.

Theis, T.L., et al., *A life cycle framework for the investigation of environmentally benign nanoparticles and products*. Physica Status Solidi – Rapid Research Letters, 2011. **5**(9): p. 312-317.

Thill, A., et al., *Flocs restructuring during aggregation: experimental evidence and numerical simulation*. Journal of Colloid and Interface Science, 2001. **243**(1): p. 171-182.

Thill, A., et al., *Cytotoxicity of CeO_2 nanoparticles for Escherichia coli. Physico-chemical insight of the cytotoxicity mechanism*. Environmental Science and Technology, 2006. **40**(19): p. 6151-6156.

Tiede, K., et al., *Considerations for environmental fate and ecotoxicity testing to support environmental risk assessments for engineered nanoparticles.* Journal of Chromatography A, 2009. **1216**(3): p. 503-509.

United States Department of Agriculture. *Farms, land in farms, and livestock operations: 2010 summary*. National Agricultural Statistics Service, 2011.

United States Environmental Protection Agency. *EMMC Version: Determination of metals and trace elements in water and wastes by inductively coupled plasma – atomic emission spectroscopy*. Method 200.7, Revision 4.4, 1994.

United States Environmental Protection Agency. *Land application of sewage sludge: A guide for land appliers on the requirements of the federal standards for the use or disposal of sewage sludge, 40 CFR Part 503*. Office of Enforcement and Compliance Assurance, 1994.

Veerapaneni, S. and Wiesner, M.R. *Particle deposition on an infinitely permeable surface: Dependence of deposit morphology on particle size*. Journal of Colloid and Interface Science, 1994. 162(1): p. 110-122.

Wania, F. *Multi-compartmental models of contaminant fate in the environment.* Biotherapy, 1998. **11**: p. 65-68.

Westerhoff, P.K., et al., *Occurrence and removal of titanium at full scale wastewater treatment plants: implications for TiO_2 nanomaterials*. Journal of Environmental Monitoring, 2011. **13**(5): p. 1195-1203.

Wiesner, M.R. *Kinetics of aggregate formation in rapid mix*. Water Research, 1992. **26**(3): p. 379-387.

Wiesner, M.R., et al., *Decreasing uncertainties in assessing environmental exposure, risk, and ecological implications of nanomaterials.* Environmental Science and Technology, 2009. **43**(17): p. 6458-6462.

Wiesner, M.R., et al., *Assessing the risks of manufactured nanomaterials.* Environmental Science and Technology, 2006. **40**(14): p. 4336-4345.

Xiao, Y. and M.R. Wiesner *Transport and retention of selected engineered nanoparticles by porous media in the presence of a biofilm*. Environmental Science and Technology, 2013. **47**: p. 2246-2253.

Zeyons, O., et al., *Direct and indirect CeO_2 nanoparticles toxicity for Escherichia coli and Synechocystis*. Nanotoxicology, 2009. **3**(4): p. 284-295.

Biography

Lauren Elizabeth Barton was born on March 23, 1987 in Lansing, Michigan. In January of 2009, she completed her undergraduate studies at The University of Notre Dame in Notre Dame, Indiana with a B.S. in Biochemistry. Following her B.S., she continued her studies at the University of Notre Dame, where she earned her M.S. in Civil Engineering and Geological Sciences in August of 2010. Her thesis focused on the "Size-dependent Structure and Reactivity of Nanohematite." That same August she began her doctoral career at Duke University in Durham, North Carolina in the Department of Civil and Environmental Engineering with a dissertation focused on the "Fate and Transformations of Metal-(Oxide) Nanoparticles in Wastewater Treatment." In her Masters, she published two peer-reviewed articles and co-authored another. In her doctorate work, she will have published five peer-reviewed articles and co-authored one. Concurrent with her doctoral degree, she worked as an intern at Research Triangle Institute International in Research Triangle Park, North Carolina, where she worked on model improvement and assisted with proposal development.

She was awarded the Chateaubriand Fellowship from the French Embassy in May of 2011, which allowed her to enroll in a dual degree between Duke University and the University of Aix-Marseille in Aix-en-Provence, France. She also received the Jeffery B. Taub Environmental Engineering Graduate Student award from the Department of Civil and Environmental Engineering in 2013.